Rockefeller University
Digital Commons @ RU

Student Theses and Dissertations

2010

Synaptic Specificity in the Zebrafish Lateral Line

Aaron Nagiel

Follow this and additional works at: http://digitalcommons.rockefeller.edu/student_theses_and_dissertations

 Part of the Life Sciences Commons

Recommended Citation
Nagiel, Aaron, "Synaptic Specificity in the Zebrafish Lateral Line" (2010). *Student Theses and Dissertations.* Paper 66.

This Thesis is brought to you for free and open access by Digital Commons @ RU. It has been accepted for inclusion in Student Theses and Dissertations by an authorized administrator of Digital Commons @ RU. For more information, please contact mcsweej@mail.rockefeller.edu.

SYNAPTIC SPECIFICITY IN THE ZEBRAFISH LATERAL LINE

A Thesis Presented to the Faculty of

The Rockefeller University

in Partial Fulfillment of the Requirements for

the degree of Doctor of Philosophy

by

Aaron Nagiel

June 2010

© Copyright by Aaron Nagiel, 2010

SYNAPTIC SPECIFICITY IN THE ZEBRAFISH LATERAL LINE

Aaron Nagiel, Ph.D.
The Rockefeller University 2010

The proper wiring of the vertebrate brain represents an extraordinary developmental challenge, requiring billions of neurons to select their appropriate synaptic targets. In view of this complexity, simple vertebrate systems provide necessary models for understanding how synaptic specificity arises. The posterior lateral-line organ of larval zebrafish consists of polarized hair cells organized in discrete clusters known as neuromasts. Here I show that each afferent neuron of the posterior lateral line establishes specific contacts with hair cells of the same hair-bundle polarity. I quantify this specificity by modeling the neuron as a biased selector of hair-cell polarity and find evidence for bias from as early as 2.5 days post-fertilization. More than half of the neurons form contacts on multiple neuromasts, but the innervated organs are spatially consecutive and the polarity preference is consistent. Using a novel reagent for correlative electron microscopy, HRP-mCherry, I show that these contacts are indeed afferent synapses bearing vesicle-loaded synaptic ribbons. Moreover, afferent neurons reassume their biased innervation pattern after hair-cell ablation and regeneration. By documenting specificity in the pattern of neuronal connectivity during development and in the context of organ regeneration, these results establish the posterior lateral-line organ as a vertebrate system for the *in vivo* study of synaptic specificity.

In order to shed light on the mechanism for this specificity, I investigated whether afferent neurons distinguish hair-cell polarities by analyzing differences

in the synaptic signaling between oppositely polarized hair cells. By examining two mutant zebrafish lines with defects in mechanoelectrical transduction, I found that afferent neurons can form specific synapses in the absence of stimulus-evoked patterns of synaptic release. Asking next whether this specificity could arise through intrinsically generated patterns of synaptic release, I found that the polarity preference persisted in two mutant lines lacking essential synaptic proteins. These results indicate that lateral-line afferent neurons do not utilize synaptic activity to distinguish hair-cell polarities and suggest that molecular markers of hair-cell polarity guide prepatterned afferents to form the appropriate synapses.

ACKNOWLEDGMENTS

I would never have reached this point without the support and encouragement of my family. I wish to thank: my parents, Moises and Ruth, for dedicating their lives to the care of my siblings and me, spoiling us with a peaceful and nurturing home environment; Isaac and Belanie, my siblings, who although younger than me, continue to impress me through their hard work and enthusiastic pursuit of success; my grandparents, Zeide and Bube, for providing the kind of encouragement and support only grandparents can give; my uncle, Abraham Rothman, who for as long as I can remember instilled in me a sense of curiosity and passion for knowledge that persists to this day; the rest of my family, who facilitated my academic pursuits through unwavering support.

Special thanks goes to those who led me into the MD-PhD track and then guided me during my time here. Thomas Michel, my incredibly supportive undergraduate thesis advisor, wisely persuaded me to seek out PhD training to supplement medical school. The director of the program, Olaf Andersen, has been an unstinting provider of valuable career advice to me. The MD-PhD office—Ruthie, Elaine, Renee, and Irma—and the Dean's Office at Rockefeller have done an incredible job making my time here go as smoothly as possible.

I am very fortunate to have worked with a marvelous group of people in the Hudspeth Laboratory. I am indebted to Hernán Lopez-Schier, a former post-doctoral fellow, for developing experimental tools and deepening our understanding of the zebrafish lateral line so that I could delve into my research from the moment I joined the lab. Michelle Gleason, another post-doctoral

fellow, held my hand through my first baby steps of molecular cloning and continued to provide me this level of experimental guidance throughout my time in the lab. Daniel Andor, a crackerjack physicist and math whiz, developed powerful statistical tools to analyze my data and taught me a lot about the significance (and insignificance) of *p*-values. Amalia Pasolli in the Fuchs laboratory trained me on the transmission electron microscope and was extraordinarily generous with reagents. I owe much to the helpful conversations I had regarding my work with Revathy Chottekalapanda, Lukasz Kowalik, Taeryn Kim, Jason Schwarz, and Aaron Steiner, all of whom have become good friends. And of course, a huge debt of gratitude goes to Deji Afolalu, who took great care of our fish colony and ensured effortless weekly breedings. Finally, a thank you is required for all those who helped me out with the small and medium-sized stuff: Yaneth Castellanos, Masha Vologodskaia, Serhiy Pylawka, Aleks Stefanovic, Erica Keen, Jonathan Fisher, Suchit Patel, and last but certainly not least, Beth Dougherty.

I am very grateful to the members of my faculty advisory committee—Tim Ryan, Elaine Fuchs, and Cori Bargmann—for providing me with insightful comments and questions, and I appreciate their enthusiasm for my project. I especially want to thank Lisa Goodrich for traveling from Harvard Medical School to serve as my external examiner on the committee.

It's hard to acknowledge in words the contribution of my thesis advisor, Jim Hudspeth, to this body of work and to my development as a scientist and member of society. From the beginning, he roused my curiosities and hunger for knowledge simply by example, of which I know no better. His enthusiasm for science and everything beyond is contagious, and I was certainly infected. I am

grateful to have had the opportunity to cultivate my scientific interests under his tutelage.

Finally, I owe a deep and heartfelt debt of gratitude to my wife, Svetlana, for supporting and encouraging my success in the laboratory, by being understanding of my need to go to the lab at odd hours but also by yanking me out of the lab so I wouldn't burn out.

TABLE OF CONTENTS

LIST OF FIGURES

LIST OF ABBREVIATIONS

4-Di-2-ASP	4-(4-(diethylamino)styryl)-N-methylpyridinium iodide
ALL	anterior lateral line
cDNA	complementary DNA
DAB	3,3-diaminobenzidine
DNA	deoxyribonucleic acid
dpf	days post-fertilization
FACS	fluorescence-activated cell sorter
FM 1-43	*N*-(3-triethylammoniumpropyl)-4-(4-(dibutylamino)styryl)pyridinium dibromide
FM 4-64	*N*-(3-triethylammoniumpropyl)4-(6-(4-(diethylamino)phenyl)hexatrienyl)pyridinium dibromide
GFP	green-fluorescent protein
hpf	hours post-fertilization
HRP	horseradish peroxidase
mRNA	messenger RNA
PBS	phosphate-buffered saline
PBST	phosphate-buffered saline containing Tween 20
PCR	polymerase chain reaction
PLL	posterior lateral line
RNA	ribonucleic acid
TTX	tetrodotoxin
Tween 20	polyoxyethylenesorbitan monolaurate

CHAPTER ONE

Introduction

The human brain is a marvel of engineering that we are only beginning to understand. Some of its most basic functions, such as visual perception, spatial navigation, and complex motor tasks, are taken for granted as they are executed seamlessly in highly complicated environments. These functions have been difficult to reproduce in robots and computers. What is more astounding perhaps is that this functionality is not exceptional, in the sense that every member of the species, with rare exceptions, develops these capabilities with ease. How can an entity so complex be faithfully reproduced in every individual? Any plausible explanation must address the developmental patterning mechanisms that consistently give rise to the brain's network of neuronal connectivity. In other words, the magic of the brain must stem from its cellular architecture.

Each of the brain's estimated 10^{11} neurons may form thousands of synapses with other neurons (Jessell and Kandel, 1993). These sites of communication between neurons permit neural signals in the form of action potentials to course from cell to cell without direct electrical conduction. Instead, an action potential in one cell triggers the release of chemical neurotransmitter, which diffuses across the acellular space between the cells, known as the synaptic cleft. Receptor molecules on the post-synaptic neuron bind the neurotransmitter, precipitating an influx of cations and eliciting an action

potential anew (Unwin, 1993). This process of synaptic transmission can be excitatory or inhibitory and highly regulated, but there is not nearly enough versatility to account for the extent of neural function. Rather, the 10^{15} synapses of the human brain must elicit functionality through a specific pattern of neuronal connectivity, which results in the computational processing of inputs and outputs. How does such a complex network of cells develop and what molecular processes ensure its reproducibility? The following work describes the emergence of a new experimental system for studying this question.

Wiring the vertebrate nervous system

An essential feature of neural development is the establishment of specific synaptic connections. Over one hundred years ago, using only a basic light microscope and slides bearing stained neuronal processes, the Spanish neuroanatomist Santiago Ramón y Cajal inferred that nervous tissue is composed of cellular units, neurons, that are connected in predictable, stereotyped ways to form circuits (1911). He made remarkable insights into neural function by examining thousands of specimens of nervous tissue and illustrating the enormous diversity and complexity of neuronal morphology and subcellular structure. His inference that neural signals can propagate in a unidirectional fashion across a synaptic cleft allows one to view the brain as a set of interconnected circuits with distinct functions. This stood in stark contrast to the competing view at the time, voiced by Camillo Golgi, of the brain as a nebulous network of electrically coupled neurons with no reproducible blueprint (Mazzarello, 2007). The advent of transmission electron microscopy and *in vivo*

fluorescent imaging provided a wealth of evidence to support Cajal's extraordinary claims (Palay, 1956; Livet et al., 2007; Dhawale and Bhalla, 2008). Further, the application of electrophysiological manipulations and molecular biological techniques permitted a highly detailed analysis of neural circuit formation, from axon guidance to target recognition to the final step of synaptogenesis.

The experimental analysis of neuronal connectivity in vertebrate animals identified two general mechanisms by which neurons locate and synapse with their correct targets: those that require electrical activity, in the form of action potentials and neurotransmitter release, and those that do not. As will be described in the following sections, activity-independent mechanisms predominate during the initial steps of axon guidance and target recognition. During the subsequent step of synapse formation, however, work in several vertebrate systems has demonstrated a reliance on precise patterns of neuronal activity.

Axon guidance

In order to form the appropriate synapses, each growing axon must respond to guidance cues, find its target region, and then establish synapses with specific target cells (Goodman and Shatz, 1993; Benson et al., 2001). The first two of these steps—axonal guidance and target recognition—rely predominantly on molecular signposts that attract or repulse growth cones in a manner independent of neuronal activity. In a brilliant study performed in the 1930s, Victor Twitty and his colleagues utilized a species of California newt bearing

tetrodotoxin, a potent blocker of neuronal sodium channels. Although its neurons remain unaffected by the toxin and can fire action potentials, related urodele species experience complete neuronal activity blockade in the presence of the toxin. Twitty grafted body parts of the tetrodotoxin-bearing newt embryos onto susceptible newt embryos and observed their development. As expected, the chimeric larvae were completely paralyzed throughout embryonic development owing to the effect of the toxin. Once the toxin wore off, however, the larvae exhibited completely normal behavior. This remarkable result demonstrated that sensory and motor neuron pathfinding could occur in the absence of neuronal activity (Twitty and Johson, 1934).

More recently, forward genetic screens and *in vitro* assays have confirmed the existence of large families of cell surface and secreted proteins that orchestrate axonal pathfinding (Tessier-Lavigne and Goodman, 1996; Dickson, 2002). These axon guidance cues, which include the netrins, slits, semaphorins, and ephrins, mediate growth cone guidance through chemoattraction and chemorepulsion in a highly dynamic and flexible fashion. The particular response of a growth cone to any given ligand depends on its repertoire of receptors, its intracellular signaling apparatus, and the influence of modulatory proteins. In the case of vertebrate commissural axons, an individual axon is initially attracted towards the ventral midline of the spinal cord through midline expression of netrin (Kennedy et al., 1994; Serafini et al., 1994). Once the axon has crossed the midline, it becomes insensitive to netrins and is now repulsed by it (to prevent recrossing) through the action of midline slit and semaphorin (Shirasaki et al., 1998; Zou et al., 2000). As exemplified by commissural axons, these types of receptor-ligand interactions can push and pull growth cones over

long distances towards their target regions. Although some studies suggest a role for spontaneous neuronal activity in the guidance of axons (Hanson and Landmesser, 2004; Nicol et al., 2007), for the most part these events rely on spatially and temporally restricted expression of guidance cues in a manner independent of neuronal activity.

Target selection

In the 1950s, Roger Sperry developed our understanding of axonal target selection through a series of landmark studies on optic nerve regeneration in amphibians. Sperry and colleagues found that retinal ganglion cells innervate the optic tectum in a highly precise fashion, such that ganglion cells from a particular portion of the retina faithfully project to certain target areas in the optic tectum. On the basis of these findings, he formulated the chemoaffinity hypothesis, the idea that neuronal processes find their way to specific locations in the brain through molecular labels and gradients (Sperry, 1963). Sperry's hypothesis was borne out to a certain extent decades later through the discovery of a biochemical basis for retinotectal patterning (Walter et al., 1987; Baier and Bonhoeffer, 1992). Gradients of ephrins along the anteroposterior and dorsoventral axes of the tectum sort incoming retinal ganglion cell axons bearing particular Eph receptors corresponding to their retinal site of origin (Nakamoto et al., 1996; Feldheim et al., 2000; Mann et al., 2002).

In other settings, target areas secrete distinct neurotrophic factors which cause growing axons to invade the area and elaborate synapses. In the vertebrate inner ear, for example, neurotrophin 3 and brain-derived neurotrophic factor are

expressed in a complex spatiotemporal pattern that guides cochlear and vestibular sensory neurons to their targets (Tessarollo et al., 2004). Another instance of target-derived neurotrophin expression can be found in the innervation of the rodent whisker pad, which expresses several neurotrophins to recruit and maintain trigeminal sensory neurons (Ibanez et al., 1993).

Target-derived neurotrophins and tectal ephrin gradients represent two ways that growing axons reach the vicinity of their synaptic targets. Once there, however, complex neuronal targets such as the optic tectum utilize specific patterns of spontaneous and experience-evoked activity to implement the appropriate synaptic connections.

Synaptic specificity

How neurons decide to form stable synapses with particular target cells is incompletely understood, and the mechanisms in play often differ between species (Sanes, 2009). The vertebrate visual system is one of the best-studied examples of how coarse-grained axonal arborizations can become refined through neuronal activity. As described previously, the crude retinotectal map results from a mixture of axon guidance cues and ephrin-mediated targeting. Following optic nerve crush injury, retinal ganglion cells in the goldfish regenerate their axons and reestablish a fine-grained retinotopic map in the optic tectum. Treatment with tetrotodotoxin, however, leads to a marked expansion of retinal ganglion cell arbors and a loss of finely tuned synaptic connectivity (Meyer, 1983; Schmidt and Edwards, 1983). Although these experiments established the need for activity in tectal arbor refinement, they did not address

whether the pattern of activity needs to be meaningful and specific. To answer this question, goldfish were raised in the dark or with stroboscopic illumination. Dark rearing allows for spontaneous activity but no experience-evoked activity, whereas stroboscopic illumination imposes a global, unstructured pattern of activity. Fish raised in both conditions had markedly expanded tectal arbors compared to controls, indicative of the need for meaningful sensory experience in the refinement of retinotopy (Schmidt and Eisele, 1985; Eisele and Schmidt, 1988). The activity-dependent refinement of synaptic contacts seen in the tectum of lower vertebrates also features prominently in other settings, such as the establishment of ocular dominance columns in the mammalian visual cortex (Katz and Shatz, 1996).

This reliance on experience-dependent patterns of activity, however, could not explain how much of the refinement in the retinotopic map occurred prior to the onset of sensory experience. This discrepancy was resolved by the discovery that waves of spontaneous activity sweep across the retina, resulting in correlated firing of nearby retinal ganglion cells (Maffei and Galli-Resta, 1990; Meister et al., 1991). These patterns of spontaneous activity are highly structured and presumably mimic the effects of natural visual experience (Huberman et al., 2008).

How spontaneous and evoked activity achieve this remarkable effect has been the subject of much debate, but the work of the psychologist Donald O. Hebb has provided a conceptual framework for thinking about the question. Hebb postulated that correlated electrical activity between presynaptic and postsynaptic neurons led to a strengthening of synaptic transmission (Hebb, 1949; Stent, 1973). Although it was originally formulated in a very general

sense, Hebb's neurophysiological postulate has often been equated with the mantra, "neurons that fire together wire together." The correlated firing of nearby retinal ganglion cells in the case of visual experience or by patterned spontaneous discharges represents a good example of how activity can strengthen correlated inputs while eliminating uncorrelated inputs (Bi and Poo, 2001; Cang et al., 2008).

Substantial evidence for activity-dependent refinement of synaptic contacts, however, must be reconciled with data suggesting that normal cortical architecture can form in the absence of synaptic transmission (Verhage et al., 2000; Varoqueaux et al., 2002). Even the delicate layering of synaptic inputs to the zebrafish retina and optic tectum appears to occur in the absence of neuronal activity (Nevin et al., 2008). The degree of reliance on activity may to a certain extent depend on species-specific differences. However, even within the same species, the development of long-range sensory projections such as thalamocortical tracts might rely more on activity than the formation of local circuits, which could utilize cellular recognition to make the appropriate connections among neighboring neurons (Jontes and Phillips, 2006). In this case, synaptic specificity could derive from a combinatorial code of cell-surface molecules such as cadherins (Shapiro and Colman, 1999) or members of the immunoglobulin superfamily (Biederer et al., 2002; Yamagata and Sanes, 2008). In the chick retina, for instance, four immunoglobulin superfamily members—Dscam, DscamL, Sidekick 1 and Sidekick 2—are expressed in distinct subsets of retinal cells and are thought to guide lamina-specific arborization through homophilic molecular interactions (Yamagata et al., 2002; Yamagata and Sanes, 2008).

In spite of these seemingly clear-cut examples, it is most likely that activity-dependent and -independent pathways converge and dynamically influence each other (Cline, 2003). For example, membrane depolarization can elicit the transcription of hundreds of genes (Flavell and Greenberg, 2008), including regulators of synaptic strength and number such as MEF2, Otx2, and Npas4 (Flavell et al., 2006; Lin et al., 2008; Sugiyama et al., 2008). The neurotrophin BDNF is another activity-regulated gene that is not only transcribed but also secreted in an activity-dependent manner (Balkowiec and Katz, 2000; Hong et al., 2008). Clearly, our knowledge of the molecular mechanisms controlling synapse specificity in vertebrates is still limited, highlighting the need for *in vivo* studies in an experimentally tractable vertebrate system.

Development of the lateral-line organ in zebrafish

The lateral-line organ of larval zebrafish features a number of qualities that facilitate the study of synaptic connectivity. Lateral lines confer upon certain aquatic vertebrates the ability to sense water currents and thus aid in prey capture, predator avoidance, rheotaxis, and shoaling (Montgomery et al., 1997). The functional unit of the lateral line is the neuromast, which consists of superficial hair cells ensheathed by supporting cells, surrounded by mantle cells, and innervated by afferent and efferent neurons (Metcalfe et al., 1985). The bilaterally symmetrical lateral-line system of a larval zebrafish has two components: an anterior lateral line (ALL) covering the head and a posterior lateral line (PLL) along the tail, each containing about ten neuromasts at one

week of age (**Figure 1.1** ***A***) (Metcalfe et al., 1985; Raible and Kruse, 2000). The larval PLL is derived from a cranial neurogenic placode that gives rise to two migrating primordia composed of precursor cells (Metcalfe, 1985). The first primordium migrates caudally at 20 hours post fertilization (hpf) and deposits 7-9 pro-neuromasts along the horizontal myoseptum before reaching the tail fin at 42 hpf (Gompel et al., 2001b; David et al., 2002; Li et al., 2004). While the cell bodies coalesce into a post-otic ganglion and send axonal inputs to the hindbrain (**Figure 1.1** ***B***), the growth cones of the PLL nerve trail behind this primordium (Metcalfe, 1985; Gilmour et al., 2004). One to two days later, a second primordium migrates along the same trajectory, depositing a few pro-neuromasts along the trunk (Ledent, 2002). All these pro-neuromasts eventually develop into sensory organs containing mature hair cells innervated from below by afferent neurons (Dambly-Chaudière et al., 2003; Ghysen and Dambly-Chaudière, 2004).

The zebrafish features several characteristics that make it an attractive model organism. These include the fecundity, optical transparency, external development, and amenability to transgenic manipulations (Fetcho and Liu, 1998). The experimental study of PLL development in particular, however, highlights how these characteristics can be utilized towards experimental ends. First, large number of embryos can be quickly injected with a variety of DNA or RNA constructs, such as those encoding fluorescent proteins, for the expression of genes in a spatially and temporally restricted manner. Second, the superficial nature of the hair cells and neurons, which lie less than 20 μm below the body surface, permits the use of confocal imaging techniques for optical sectioning of fluorescently labeled cells. Third, the neuromast as an entity containing hair

cells, supporting cells, and innervating neurons is present on certain parts of the fish as early as 1.5 dpf. Furthermore, the rapidly developing embryo can be immobilized and imaged for long periods of time, up to 24 hours, without any nutrient requirements. These features of PLL development make it ideal not only for the study of synaptic specificity, but also for hair-cell regeneration, planar cell polarity, and collective cell migration.

The mechanosensory hair cell

The hair cell is responsible for detecting and transmitting mechanical stimuli to the nervous system. In the lateral line, as in all hair cell-containing sensory organs, the function of a hair cell incorporates two distinct processes: mechanoelectrical transduction and electrochemical transduction. Each of these transduction processes is mediated by highly specialized organelles.

The hair bundle on the apical surface of hair cells transduces mechanical deflections into membrane depolarizations (Hudspeth, 1989). It comprises a staircase-like arrangement of actin-filled stereocilia and a true cilium, the kinocilium, which stands at the tall edge. The stereocilia are linked at their tips by a proteinaceous tip link which gates a mechanotransduction channel. Mechanical deflections of the hair bundle toward the kinocilium cause the stereocilia to shear, raising the tension on the tip link, and increasing the open probability of the transduction channels. Channel opening permits cations to flow into the cell, thus depolarizing it. Deflections away from the kinocilium, on the other hand, result in a decreased open probability of the channels and therefore hyperpolarize the cell (Shotwell et al., 1981).

The second transduction process carried out by hair cells is electrochemical in nature. Membrane depolarizations trigger the release of neurotransmitter from the cell's base at presynaptic specializations known as synaptic ribbons (Keen and Hudspeth, 2006). L-type voltage-gated calcium channels positioned in the basolateral membrane mediate the influx of Ca^{2+} during membrane depolarizations (Sidi et al., 2004). The propinquity of these channels to the sites of vesicle fusion facilitates the Ca^{2+}-dependent release of the neurotransmitter glutamate into the synaptic cleft (Brandt et al., 2005). Postsynaptic glutamate receptors on afferent neurons bind the glutamate and depolarize the neurons for transmission to the brain.

Hair cell function is thus critically dependent on two subcellular specializations: the hair bundle and the ribbon synapse. The hair bundle is notable for its exquisite sensitivity to mechanical stimuli, which it translates into membrane depolarizations. The ribbon synapse bears the onerous task of continuously broadcasting the membrane voltage in a temporally precise fashion through the release of glutamate onto postsynaptic afferent neurons.

Hair-cell polarity in the lateral line

A striking feature of the lateral line is the planar polarization of hair cells within a neuromast (Flock and Wersäll, 1962), which is manifested in two ways. The first is the aforementioned hair-bundle polarity, which emerges as a consequence of an eccentrically placed kinocilium and the increasing height of the stereocilia as they near the kinocilium. This polarity defines the vector of mechanosensitivity and is intrinsic to each hair cell. The second manifestation of

polarity, which is governed by the planar-cell-polarity pathway, arises from the coordinated orientation of polarized hair bundles with respect to the bodily axes.

These two levels of hair-cell polarization are thought to arise through a three-step process which translates global, tissue-level positional cues into cytoskeletal changes that orient individual hair bundles (Kelly and Chen, 2007). In the first step, a long-range gradient of a signaling molecule or neighbor-to-neighbor propagation of a polarity cue lays down a polarity axis in the plane of the epithelium. Second, a group of core planar polarity proteins establish polarized complexes in the apical membrane along this axis. Finally, these asymmetric planar polarity complexes guide cytoskeletal rearrangements that result in an eccentrically placed kinocilium and stereociliary bundle. What little we understand about this process comes largely from research in *Drosophila*; work in vertebrates lags significantly behind. In neither case do we have a clear picture of how planar polarity unfolds from beginning to end (Zallen, 2007; Goodrich, 2008).

Despite these uncertainties, several planar-polarity genes have been identified and appear to have conserved roles from *Drosophila* to mammals. A notable example is that of *vangl2*, which is required for the proper orientation of hair bundles in the mouse cochlea and is asymmetrically localized within hair cells along the axis of planar polarity (Montcouquiol et al., 2003; Montcouquiol et al., 2006). The zebrafish *vangl2* (*trilobite*) mutant similarly shows defective orientation of neuromast hair cells with respect to the bodily axes (Lopez-Schier and Hudspeth, 2006). Despite losing their collective tissue-wide orientation pattern, individual hair cells in both cases nevertheless acquire polarized hair

bundles, suggesting that global cues simply guide an otherwise autonomous, cell-intrinsic polarization mechanism.

Lateral-line neuromasts contain two sets of hair cells, each with opposite hair-bundle polarity such that they obey a plane of mirror symmetry (**Figure 1.2**). This arrangement stems from the fact that hair-cell precursors consistently divide across this plane, producing a mirror-symmetric pair of daughter cells. As their hair bundles mature, these daughter cells acquire opposite hair-bundle polarizations, with their kinocilia abutting each other along the plane of symmetry. The development of hair-cell polarity in neuromasts thus results from a two-step process: first, precursors divide along the axis of mechanical sensitivity to produce two daughter cells; second, the hair bundles of these cells become oppositely oriented along this axis (Lopez-Schier and Hudspeth, 2006).

In neuromasts derived from the first primordium the axis of mechanosensitivity is oriented anteroposteriorly, whereas in those from the second primordium it is oriented dorsoventrally (**Figure 1.1** ***B***) (Lopez-Schier et al., 2004). The acquisition of orthogonal hair-cell polarizations may stem from the direction of migration of their respective primordia. The first primordium travels posteriorly along the horizontal myoseptum as it deposits its neuromast precursor cells. The second primordium also migrates posteriorly, but the deposited precursor cells veer ventrally before maturing into neuromasts. The resulting axis of mechanosensitivity in each case matches the direction of final precursor-cell migration. How the "memory" of migratory path is maintained through cycles of hair-cell death and regeneration and how it is manifested through planar polarity signaling remain unclear.

Afferent innervation of hair cells

Because fish can estimate the velocity and acceleration of water currents (Montgomery et al., 1997; Engelmann et al., 2000), the central nervous system must bear an internal map of hair-cell position and polarity. In order for this map to be established, afferent neurons must not only make the appropriate synaptic connections with hair cells in the periphery, but also establish precise contacts in the hindbrain, specifically the nascent medial octavolateral nucleus (Fame et al., 2006).

Somatotopy, the mapping of sensory inputs to corresponding positions in the brain, has been demonstrated in the central projection of the lateral-line nerve of larval zebrafish. Compared with anterior lateral-line neurons, PLL neurons project to a more dorsal position in the hindbrain (Alexandre and Ghysen, 1999). Even within the PLL, afferents innervating the most posterior neuromasts send their central projections dorsomedially when compared to those innervating more anteriorly located neuromasts. How this segregation of PLL nerve inputs is achieved during development remains unknown, but it appears to occur without somatotopic cues from the periphery. A PLL neuron extends its central axon prior to neuromast innervation, and the position of the target neuromast can be predicted from the morphology of the growth cone (Gompel et al., 2001a). Interestingly, auditory neurons in the mouse cochlear ganglion also assume stereotyped morphologies and axonal trajectories without input from the hair cells that they innervate (Koundakjian et al., 2007).

In addition to localizing stimuli, the lateral line represents stimulus directionality by keeping track of hair-cell polarity. Prior to the present work, it

remained unclear how afferent neurons collect information about stimulus orientation from neuromast hair cells. Extracellular recordings in the frog demonstrated that two afferents innervate each neuromast and that one afferent carries inputs from hair cells of one polarity and the other from hair cells of the opposite polarity (Görner, 1963). More recently, intracellular recordings from PLL neurons in larval zebrafish indicated that each afferent receives inputs from similarly oriented hair cells (Obholzer et al., 2008). The degree of specificity and the receptive field structure of single afferents, however, had not been explored at the level of single synapses. In this work, I investigated whether afferent neurons distinguish hair-cell polarities as they innervate lateral-line neuromasts during normal development and following regeneration. Next, I sought to determine the mechanism by which afferent neurons make this distinction.

Neuronal connectivity and human disease

An understanding of afferent connectivity in a simple model system like the zebrafish lateral line has the potential to provide insights into how specific patterns of neuronal connectivity are established and maintained in vertebrates. Because specific neuronal connections are essential for the function of neural circuits, aberrations in this process are likely to cause neurological and psychiatric disease. For example, certain synaptic cell-adhesion proteins, such as neurexins, neuroligins, and the scaffolding protein Shank3, have recently been implicated in the etiology of autism-spectrum disorders (Südhof, 2008). Although many questions linger regarding their role in synaptic physiology and social development, these examples may represent the tip of the iceberg.

A detailed understanding of the mechanisms that promote the proper wiring of the nervous system will undoubtedly augment our understanding and treatment of mental illnesses such as epilepsy, autism, and schizophrenia, as well as our capacity to harness normal developmental processes toward the recovery of brain function following stroke and traumatic injury.

Figure 1.1

Structure and innervation of the lateral line in a larval zebrafish

A, Labeling of hair cells in a living 6-dpf larva with 4-Di-2-ASP reveals more than ten neuromasts in the ALL and eleven neuromasts in the PLL on the animal's left side. The neuromasts on the right side of the transparent larva appear out of focus. Scale bar, 1 mm. ***B***, A schematic diagram (courtesy of A. James Hudspeth) of a zebrafish larva at 4 dpf depicts seven anteroposterior neuromasts (blue) and two dorsoventral neuromasts (green) of the PLL. Additional neuromasts, which are not shown, adorn the animal's head. The soma of a single afferent neuron (red) lies in the PLL ganglion immediately caudal to the developing ear. In this example, its peripheral axon runs in the PLL nerve and contacts hair cells in two neuromasts. The central axon bifurcates and synapses in the nascent octavolateralis nucleus along the length of the hindbrain. The diameters of the neuromasts, neuronal soma, and axons are exaggerated.

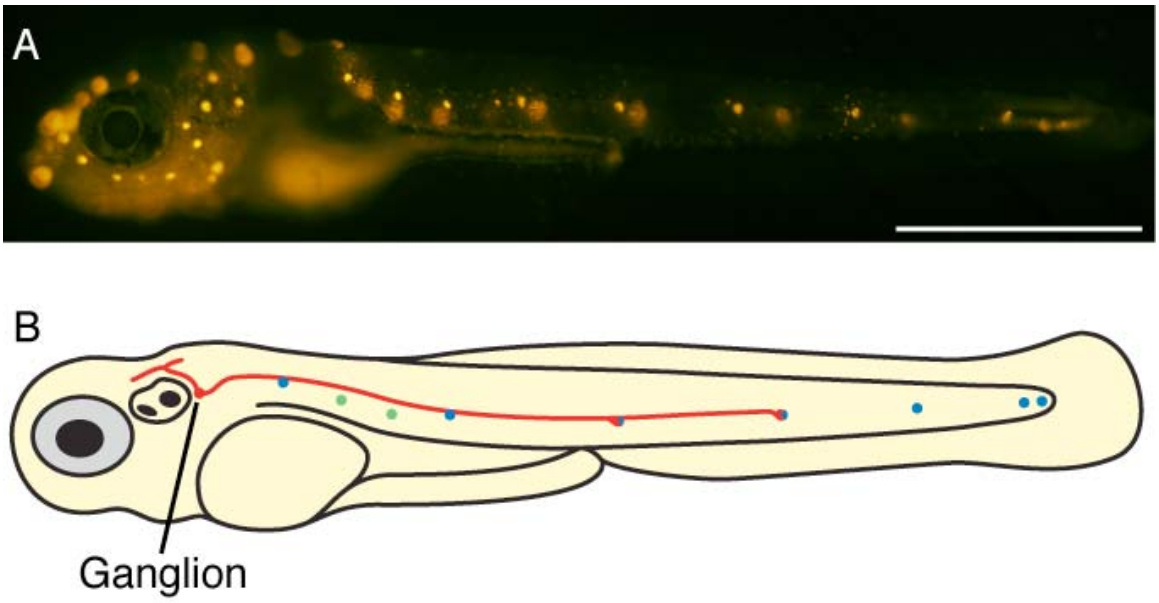
A
B
Ganglion

Figure 1.2

Hair-cell polarity in lateral-line neuromasts

A, Four hair cells occur at the center of a schematic depiction (courtesy of A. James Hudspeth) of a section through a single anteroposterior neuromast. Displacement of the gelatinous cupula by a hydraulic stimulus, in this instance directed toward the animal's posterior (red arrow), deflects the long kinocilia of the hair cells. When communicated to the stereocilia of the hair bundles, this movement depolarizes the posteriorly polarized hair cells (red) and hyperpolarizes the anteriorly polarized cells (blue). Supporting cells separate the hair cells; mantle cells outline the neuromast and contact the periderm cells of the larva's integument. The neuromast's innervation is not shown. The parallel dashed lines depict the plane of the parasagittal optical section shown in the following panel. ***B***, A light micrograph of a neuromast's apical surface reveals the staining of filamentous actin by fluorescent phalloidin. The 20-30 stereocilia in each hair bundle form a crescent in whose concavity stands the unlabeled kinocilium. The dashed lines delineate the horizontal plane of section depicted in the preceding panel. The two hair cells produced by an earlier mitosis remain immature: their hair bundles have yet to exhibit the polarization characteristic of mature hair cells.

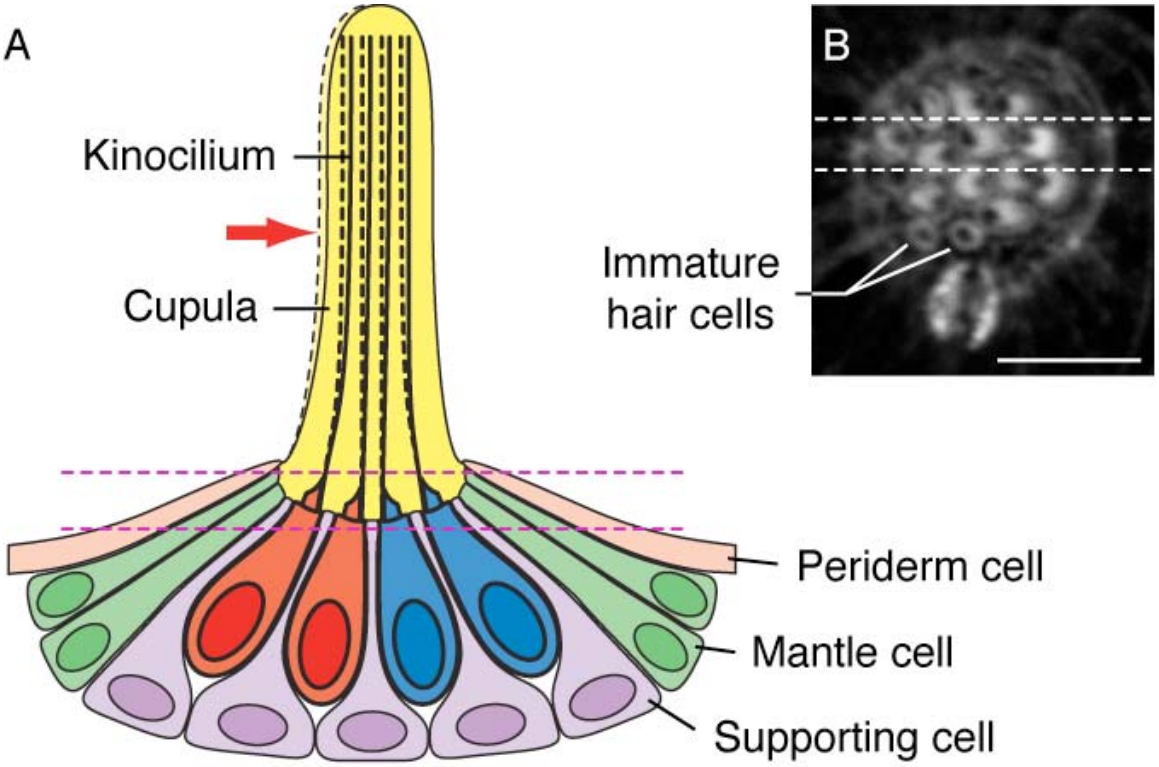
A
Kinocilium
Cupula
B
Immature
hair cells
Periderm cell
Mantle cell
Supporting cell

CHAPTER TWO

Materials and Methods

Fish strains and husbandry

Zebrafish were maintained in aquaria (Aquatic Habitats, Beverly, MA) at densities of no more than 15 larvae or two adult fish per liter of water containing 75 mg/ml Instant Ocean (Aquarium Systems, Mentor, OH) and 100 mg/ml $CaSO_4$. The water was monitored at daily intervals for conductivity (~400 μS), temperature (28.5°C), and pH (7.0). Naturally spawned eggs were collected, cleaned, staged (Kimmel et al., 1995), and maintained in system water supplemented with 1 μg/ml methylene blue to prevent fungal and bacterial growth and 200 μM 1-phenyl-2-thiourea at 1 day post-fertilization (dpf) to inhibit pigment formation. Embryos were kept at a density of 50 per 100-mm-diameter Petri dish. The wild-type strain used was *Tübingen Long Fin* (TL). The relevant transgenic strains and their respective transgenic insertions included: *HuC:GFP*, *Tg(elavl3:EGFP)*^{zf8}; *islet1:GFP*, *Tg(isl1:GFP)*^{rw01}; *ET4*, *Et(krt4:GFP)*^{sqet4}; *Pou4f3:gap43-GFP*, *Tg(Pou4f3:gap43-mGFP)*^{356t}; *neurogenin1*, *ngn1*^{hi1059Tg}; *tmie*, *tmie*^{ru1000}; *protocadherin 15a, pcdh15a*^{th263b}; *vlgut3*, *slc17a8*^{vo1}; and *cav1.3a*, *cacna1d*^{tc323d}.

Plasmid DNA construction

To create *HuC:mCherry*, *HuC:GFP* DNA (Park et al., 2000) was digested with XhoI and XbaI to remove the GFP-polyA sequence. The *HuC* promoter-containing

backbone was then gel-purified and ligated to an mCherry-polyA fragment that had been PCR-amplified with the following primers:

F: TGCTCGAGTGCCACCATGGTGAGCAAGGGCGAGG

R: GTCATTCTAGAGTCGCTTACAATTTACGCCTTAAG

To create *HuC:gap43-mCherry*, the *HuC:mCherry* plasmid was digested with XhoI and ligated to annealed oligonucleotides containing a Kozak sequence and the first 20 codons of the *gap43* cDNA:

F: TCGACTGCCACCATGCTGTGCTGCATCAGAAGAACTAAACCGG
TTGAGAAGAATGAAGAGGCCGATCAGGAG

R: TCGACTCCTGATCGGCCTCTTCATTCTTCTCAACCGGTTTAGTTC
TTCTGATGCAGCACAGCATGGTGGCAG

To create the *HuC:HRP-mCherry* plasmid, the NotI site of *HuC-mCherry* was destroyed by blunt-end ligation and the XhoI site was changed to a NotI-AgeI site with annealed oligonucleotides. The *HRP-C* cDNA was PCR-amplified with a forward primer containing a 5′ EcoRI site and a reverse primer containing a 5′ BamHI site:

F: CTGAATTCATGCAGTTAACCCCTACATTC

R: GAGGATCCAGAGTTGCTGTTGACCACTCTGC

This amplified segment of DNA was ligated into pBluescript SK+, which was subsequently digested with BamHI and NotI. Synthesized, annealed, 5′-phosphorylated oligonucleotides encoding the transmembrane region of cadherin2 (Cdh2) followed by an AgeI site were ligated into the BamHI/NotI-digested Bluescript plasmid.

F: GATCCGCAGCCGGGCTGGGCACCGGAGCCATCATCGCCATAC
TTATCTGCATCATCATTCTGCTGGTGCTGGTGTTGATGTTTG
TGATGTGGATGAAGAGACGGGATAAAGAGAGACAGACCG
GTGC

R: GGCCGCACCGGTCTGTCTCTCTTTATCCCGTCTCTTCATCCACA
TCACAAACATCAACACCAGCACCAGCAGAATGATGATGC
AGATAAGTATGGCGATGATGGCTCCGGTGCCCAGCCCGGC
TGCG

This plasmid was subsequently digested with HindIII and EcoRI and ligated to annealed, 5′-phosphorylated oligonucleotides comprising the signal sequence of *cdh2* with a NotI site and Kozak sequence upstream:

F: AGCTTGCGGCCGCCACCATGTACCCCTCCGGAGGCGTGATGCTG
GGGCTTCTCGCCGCTCTGCAGGTGGCGGTCCAGGGCACAGG
GGCGG

R: AATTCCGCCCCTGTGCCCTGGACCGCCACCTGCAGAGCGGCGA
GAAGCCCCAGCATCACGCCTCCGGAGGGGTACATGGTGGC
GGCCGCA

Finally, this plasmid was digested with NotI and AgeI, liberating the signal sequence-HRP-transmembrane domain construct, and ligated into the NotI-AgeI sites created on the *HuC:mCherry* plasmid.

DNA injection and screening of transgenic fish

One- and two-cell embryos were pressure-injected with supercoiled plasmid DNA at a concentration of 50 ng/μl. Animals were screened at 1.5-2 dpf for mCherry expression in the PLL nerve with a Zeiss Axioplan 2 wide-field fluorescence microscope. After selection of candidate fish with a 5X objective, definitive expression in the PLL nerve was ascertained using a 60X water-immersion objective.

Vital labeling of hair cells

Larvae were immersed in a 200 μM solution of 4-(4-(diethylamino)styryl)-*N*-methylpyridinium iodide (4-Di-2-ASP; Invitrogen) or in a 100 μM solution of *N*-(3-triethylammoniumpropyl)4-(6-(4-(diethylamino)phenyl)hexatrienyl)pyridinium dibromide (FM 4-64; Invitrogen) for 2 min at room temperature in the dark. The larvae were subsequently washed thrice in system water.

Live imaging of larvae

For imaging of 4-Di-2-ASP labeling, larvae were anesthetized in 625 μM 3-aminobenzoic acid ethyl ester methanesulfonate and imaged with a Zeiss Axioplan2 microscope using a 5X objective lens and a CCD camera (Olympus).

For confocal imaging, specimens were embedded under anesthesia in 1% low-melting-point agarose on a glass coverslip. Images were acquired with an Ultramer Perkin-Elmer spinning-disk system on a Zeiss Axiovert 200M microscope equipped with a 63X, 1.4 NA PlanApochromat objective, a Hamamatsu Orca-ER cooled CCD camera, and MetaMorph software for acquisition and analysis (Molecular Devices/MDS). Z-stacks were acquired at 1 μm intervals, imaging GFP (488 nm excitation, 500-550 nm emission) and mCherry or FM 4-64 (568 nm excitation, 590-650 nm emission). After imaging, the larvae were excised from the agarose and returned to individually marked dishes.

Mutant genotyping

Larvae were genotyped to confirm their status as mutants. After removal from the agarose, larvae were decapitated and their tails fixed for subsequent fluorescent-phalloidin staining. Their heads were individually digested overnight at 52°C in 2 mg/ml proteinase K in 1X Tris-EDTA buffer containing 1 mM EDTA and 10 mM tris(hydroxymethyl)aminomethane. The proteinase K was inactivated for 15 min at 95°C and 1 μl used in a standard PCR reaction using the following primers, designed to amplify the mutation-containing segment of the genomic DNA:

tmie

Ex1F2: AGCGCCTGGCGTCCTCAGAGCAG

Ex1R: TAAAAACCCGCCATCACCAGTC

pcdh15a

F1: GGCACACCTTCTACGTACCC

R1: CTCTGCCTTAATGACGAGAGAGA

cav1.3a

F7: CACTGAGGACAGCGCTCGCATTTCC

R7: CTGGAAGGATTTGATAAAGGTCC

vglut3

F3: TGTGACCGAAGAGGACAACA

R6: GTCACCAGTTAAAAATCCCTTTGG

Hair-cell ablation

Three-day-old larvae were treated for 1 hr with 10 μM $CuSO_4$ (Sigma) in system water, rinsed, and then returned to system water. The time course of recovery began when fish were removed from the $CuSO_4$ solution.

Immunofluorescence and phalloidin staining and imaging

Fish were fixed overnight at 4°C in phosphate-buffered saline (PBS) containing 1% Tween 20 (PBST) and 4% paraformaldehyde. Larvae were washed thrice in 1% PBST for 1 hr and then incubated in primary antibody or in fluorescent phalloidin. For whole-mount immunofluorescence labeling, fish were immersed overnight at 4°C in a 1:1000 dilution of mouse anti-acetylated α-tubulin primary

antibody (clone 6-11B-1; Sigma, St. Louis, MO), washed several times in 0.2% PBST, and then incubated in a 1:200 dilution of Alexa Fluor 488-conjugated secondary antibody (Invitrogen) overnight at 4°C. The fish were washed twice for four hours and stained with a 1:20 dilution of Alexa Fluor 568 phalloidin (Invitrogen) in 0.2% PBST overnight at 4°C. They were next washed twice for 4 hr and mounted in Vectashield (Vector Laboratories). Samples were imaged on an Olympus FV1000 laser-scanning confocal microscope with a 60X, 1.42 NA PlanApochromat objective lens at a scan rate of 8 μs per pixel with Kalman averaging.

Transmission electron microscopy

Larvae were fixed at 4°C overnight in 400 mM formaldehyde, 200 mM glutaraldehyde, 20 mM sucrose, 1 mM $CaCl_2$, and 90 mM sodium cacodylate at pH 7.2. The specimens were then washed in the same solution lacking the fixatives. *HuC:HRP-mCherry*-expressing fish were exposed to wash solution containing 1.4 mM 3,3-diaminobenzidine (Electron Microscopy Sciences) and 1% DMSO for 5 min at room temperature, followed by the addition of 0.0042% H_2O_2 for 5 min. After a series of washes, specimens were postfixed in 50 mM OsO_4, 20 mM sucrose, 1 mM $CaCl_2$, and 90 mM sodium cacodylate at pH 7.2 for 1.5 hr at 4°C. Several washes in distilled water were followed by dehydration through a series of ethanol concentrations to 95% ethanol.

Additional electron density was conferred by treatment with 0.4% uranyl acetate in 95% ethanol for 1 hr at room temperature. The tissue was dehydrated by immersion for 2 hr each in 100% ethanol and propylene oxide. Each specimen

was impregnated with an epoxy-resin mixture (Embed-812; Electron Microscopy Sciences), placed between two nonsticking plastic coverslips (Unbreakable Cover Slips; Fisher), and heated under vacuum for 48 hr at 50°C to cure the plastic.

Specimens were sectioned at a thickness of 70 nm with a diamond knife (Ultra 45°; Diatome, Biel, Switzerland) on an ultramicrotome (Ultracut-E; Leica). Serial sections were collected on formvar- and carbon-coated grids (Electron Microscopy Sciences) and stained for 2 min with 50% saturated aqueous uranyl acetate in 50% acetone and for 1.5 min with lead citrate. Micrographs were acquired with a transmission electron microscope (G2-12 Biotwin; Tecnai FEI, Hillsboro, OR) equipped with a CCD camera (Hamamatsu).

Image processing

Images were analyzed and adjusted for brightness and contrast with ImageJ (NIH). For the mosaic illustration in Fig. 1 *D*, individual images were merged using Adobe Photoshop (Adobe, San Jose, Ca.). Figures were assembled with Adobe Illustrator (Adobe).

Statistical analysis

Although the statistical analysis of polarity bias was developed and performed entirely by Daniel Andor-Ardó, the methods and results are included in this work because they are essential to the interpretation of my data.

To analyze innervation bias, hair cells were scored for membrane contact with labeled neurons. When possible, hair-cell polarity was inferred at 2.5 dpf and 3.5 dpf from the arrangement of hair cells; at 4.5 dpf and 5.5 dpf, hair-cell

polarity was ascertained definitively by fluorescent-phalloidin staining. Neuromasts innervated by more than one labeled fiber were excluded from the analysis. The weight of evidence was calculated in favor of a statistical model in which neurons are biased in their innervation of hair cells. When reported in decibans, which are analogous to decibels in acoustics, $W = 10 \cdot \log_{10}[P(\text{data} \mid M_B)/P(\text{data} \mid M_U)]$. The ratio $P(\text{data} \mid M_B)/P(\text{data} \mid M_U)$ is the Bayes factor, which indicates the support of the data for the hypothesis in which the neuron is biased, M_B, *versus* unbiased, M_U. $P(\text{data} \mid M)$ is the marginal likelihood, or evidence, for hypothesis M. To model the data from such a biased neuron, Fisher's noncentral hypergeometric distribution was utilized, with the probability of selecting one orientation of hair cell over another given by the parameter ω in the range 0 to 1. For the calculation of W, we marginalized over ω, that is, integrated over all possible values. A vague prior distributed as Beta(1,1) was used because it is uniform and therefore convenient for computation (Fog, 2008). When more typically non-informative priors, such as the proper Beta(1/2,1/2), were employed, W grew by 10%-20%; the persuasiveness of the result increased. The calculations were repeated using Wallenius's noncentral distribution, but the change in results was barely noticeable and the qualitative answers were in agreement. The unbiased model (M_U) is a special case of both these biased models for $\omega = 0.5$. In this instance no marginalization is necessary. Because we believe that it corresponds more closely to a physiological model of neuronal activity, I report the results from Fisher's distribution.

CHAPTER THREE

The specificity of afferent synapses onto plane-polarized hair cells

Electrophysiological work by others previously indicated that afferent neurons are responsive to stimuli in one particular orientation. This suggests that afferent neurons are somehow able to distinguish between oppositely polarized hair cells and form synaptic contacts with hair cells of the same polarity. In order to investigate this phenomenon at single-synapse resolution, it was essential to develop *in vivo* methods for the fluorescent labeling of single PLL afferent neurons as they contact fluorescently labeled hair cells. This chapter describes the implementation of this experimental approach towards a detailed description of afferent synaptogenesis with plane-polarized hair cells during normal development and during regeneration following hair-cell extirpation. This chapter also describes the development and utilization of a novel reagent for correlative transmission electron microscopy that confirmed that fluorescently labeled contacts observed *in vivo* bore the electron-microscopic features of functional ribbon synapses.

RESULTS

Afferent and efferent innervation of lateral-line hair cells

Because I wished to analyze the afferent innervation in particular, I first characterized the morphology of efferent neurons so that I could reliably exclude

them from the analysis. I examined efferent neurons labeled with GFP under the control of the *islet1* promoter (Higashijima et al., 2000) and then stained hair cells at 3 dpf with the fluorophore FM 4-64, which enters hair cells selectively through their mechanotransduction channels. The efferent axons appeared thin and featured bulbous terminals (**Figure 3.1** ***A, B***).

To visualize afferent neurons, I examined the most caudal neuromasts of *HuC:GFP* transgenic zebrafish, which express green-fluorescent protein (GFP) in all neurons early in development (Park et al., 2000). By studying these terminal neuromasts prior to 2 dpf, I could restrict the analysis to afferents inasmuch as efferent neurons do not reach this location until several hours later (Sapède et al., 2005). I found that the afferent fibers beneath each neuromast formed a dense, interlacing web that impeded the identification of fibers and of individual contacts (**Figure 3.1** ***C, D***).

The inability to resolve individual afferents in a stable transgenic line necessitated the labeling of single PLL neurons by transient-expression methods in which an arbitrary subset of neurons express a fluorescent protein. I injected wild-type embryos with the *HuC:GFP* plasmid and screened for larvae expressing GFP in the PLL nerve. Whereas lateral-line efferents have cell bodies in diencephalic and rhombencephalic nuclei (Metcalfe et al., 1985; Bricaud et al., 2001), GFP-labeled afferents possess somata in the PLL ganglion and send bifurcated axons into the hindbrain (**Figure 3.1** ***E***). At 1.5 dpf, the neurons also feature migratory growth cones destined to innervate a subset of PLL neuromasts (**Figure 3.1** ***F***).

Afferent and efferent PLL neurons therefore display clear morphological differences that are discernable not only by the anatomical location of cellular

structures but also by their distinct contacts with hair cells. These preliminary results also validated a technique for the labeling of single PLL afferents that requires neither surgical manipulation nor dye application.

Long-term monitoring of afferent innervation

I hypothesized that afferent fibers form stable synapses with hair cells of only one orientation, for such an arrangement would permit the encoding of four directions of mechanical stimulation at the first synapse of this sensory system. To test this hypothesis, I simultaneously visualized hair cells and the associated afferents *in vivo* by injecting the *HuC:mCherry* expression plasmid into embryos of the strain ET4, an enhancer-trap line in which hair cells express GFP (Parinov et al., 2004).

During early larval development or hair-cell regeneration, the highly stereotyped division of a hair-cell progenitor reliably produces a pair of hair cells of opposite polarity (Lopez-Schier and Hudspeth, 2006). When a neuromast displays mirror symmetry, it is possible to infer each hair cell's polarity based solely on its location and relationship to the other hair cells. Taking advantage of this regular pattern, I found that a single afferent neuron preferentially contacts hair cells of only one orientation. As early as 2.5 dpf, in a neuromast containing two mature hair cells, a labeled afferent fiber displayed a prominent bouton on the posteriorly polarized hair cell and a more limited contact onto the anteriorly polarized hair cell (**Figure 3.2** ***A, B***). One day later, the same neuromast had grown to encompass three pairs of hair cells. The three posteriorly polarized hair cells received voluminous contacts from the labeled fiber, whereas the anteriorly

polarized hair cells lay near finer neurites that lacked this robust morphology (**Figure 3.2** ***C-E***). By 4.5 dpf, when the neuromast had grown to six hair-cell pairs, the labeled neuron innervated a commensurately greater number of hair cells (**Figure 3.2** ***F-J***). By this stage of development the neuromast displayed a more complex arrangement of hair cells that no longer conformed to a plane of symmetry. In order to confirm the polarity of the hair cells, I fixed the fish after live imaging and labeled the actin-rich hair bundles with fluorescent phalloidin (**Figure 3.2** ***K***). With the consequent polarity information, I referred to the images of the living neuromast at 4.5 dpf and determined that the three largest and oldest posteriorly polarized hair cells received bulky contacts (**Figure 3.2 G,** ***H***). A young posteriorly polarized hair cell (**Figure 3.2** ***I***) and an anteriorly polarized hair cell (**Figure 3.2** ***J***) instead attracted only tenuous neurites.

These *in vivo* imaging studies suggest that each lateral-line afferent neuron forms prominent contacts selectively with hair cells of a single orientation. Furthermore, the time-lapse imaging approach revealed that afferent neurons respond continually to polarity cues as new hair cells are added to growing neuromasts.

Statistical analysis of innervation bias by afferent neurons

Although PLL afferents display a high degree of specificity in their choice of targets, they occasionally form contacts on hair cells of the opposite polarity (**Figure 3.2** ***J***). This finding suggested that the neurons have an inherent error rate in their choice of targets or that they can be caught in the act of interrogating a hair cell's polarity.

To provide a rigorous quantitative measure of the preference for hair-cell polarity, Daniel Andor-Ardó devised a statistical model of bias. For each neuromast, the number of hair cells of each polarity was noted along with the number innervated by a single labeled afferent fiber. The null hypothesis was that each neuron was strictly unbiased, with no ability to discriminate between polarities of hair cells. Because there were only a handful of cells per neuromast, the deviations from the null hypothesis for a single experiment tended not to be statistically significant. Although aggregating multiple *p*-values based on the null hypothesis alone was considered, this procedure is of controversial validity (Goodman, 1998). The issue was addressed more directly by comparing the evidence supporting the null hypothesis with that favoring the alternative hypothesis that the neurons can discriminate between polarities.

Each neuromast was assigned two probabilities that were hypothesis-dependent. The first probability, which represented the alternative hypothesis, was that the pattern reflected the choices of a neuron able to discriminate between polarities with a bias parameter ω that expresses the neuron's preference of one polarity over the other. A neuron that innervates only posteriorly polarized hair cells corresponds to $\omega = 1$, whereas a wholly anteriorly biased neuron has $\omega = 0$. As for the toss of an unfair coin, whose probability of yielding heads is given by the probability ω, any degree of bias from $\omega = 0$ to $\omega = 1$ is possible. The second probability reflected the null hypothesis that the neuron is strictly unbiased; in this instance, as for the toss of a fair coin, $\omega = 1/2$. Expressed in decibans, the logarithm W of the ratio of these probabilities

provided a quantitative measure of the evidence for bias in any neuromast (Jaynes, 2003).

Summing the scores for the entire sample of 131 neuromasts with hair bundles polarized along the anteroposterior axis yielded $W = 375$ db, which corresponds to a Bayes factor of approximately $3 \cdot 10^{37}$. This is a formidable weight of evidence in favor of the notion that lateral-line afferents are biased innervators: the same weight of evidence is obtained, for example, upon 132 successive tosses of a coin that all result in heads, in this case favoring the coin's being double-headed instead of fair.

Plotting the distribution of bias scores with respect to larval age demonstrated that the evidence for a biased model increases with neuromast development (**Figure 3.3** ***A***). It should be kept in mind, however, that the evidence for bias scales with the size of a neuromast: a neuron innervating both of two anteriorly polarized hair cells and no posteriorly polarized ones, for example, receives a lower score than a neuron innervating each of six anteriorly polarized hair cells and no posteriorly polarized ones. In order to evaluate the effect of the developmental increase in hair-cell numbers, the degree of bias at each time studied was assessed. To graphically represent neuronal bias, irrespective of whether this bias is for anteriorly or posteriorly polarized hair cells, the mean of the probability $|\omega - 0.5| + 0.5$ was plotted as a function of age and was found to be stable over time (**Figure 3.3** ***B***). The observed increase in evidence for bias thus reflects neuromast growth rather than a heightened sensitivity to hair-cell polarity.

Because neuromasts comprise two equal populations of hair cells with opposite orientations, I expected no more than half of a neuromast's hair cells to be innervated by a labeled fiber. Indeed, 50% or fewer of the hair cells within a neuromast were innervated by the labeled afferent fiber in 113 of the 131 instances (**Figure 3.3 *C***). Using a rigorous statistical test for bias in the choice of targets, Daniel Andor-Ardó and I found that afferent neurons consistently innervate many, if not all, hair cells of one orientation within each neuromast.

Receptive fields of single PLL afferents

I was intrigued to find that most of the labeled afferents innervated multiple neuromasts (**Figure 3.3 *D***). I asked whether each neuron selects hair cells of a common orientation across many neuromasts, as would be required to preserve independent channels of sensory information corresponding to distinct hair-cell orientations. In each of 56 instances of multiple innervation, the afferent neuron was consistent in its preference of hair-cell polarity. In 93% of these cases, the afferent fiber innervated spatially consecutive PLL neuromasts along the tail.

The innervation of multiple neuromasts by the same neuron might be indicative of an immature pattern of connectivity that is eventually pruned to a single neuromast. Instead I found that the receptive fields of single afferent neurons persisted over the period from 2.5 dpf to 5.5 dpf (**Figure 3.3 *E***). Although synaptic elimination may occur later in development, it is possible that the concurrent wiring of multiple sensory organs serves an essential function, such as increasing the sensitivity or signal-to-noise ratio, that is supported by a

consistent choice in hair-cell polarity and by the consecutive arrangement of the neuromasts innervated.

Because there are roughly equal numbers of anteriorly and posteriorly polarized hair cells in the PLL, I was surprised to find that posteriorly polarized hair cells were disproportionately innervated by the labeled afferents. Tallying the innervated hair cells over all ages yielded 263 innervated posteriorly polarized hair cells out of a total of 460 in comparison to 135 innervated anteriorly polarized hair cells out of 453. This discrepancy could not be attributed entirely to a greater ratio of hair cells to neurons, for the number of posteriorly biased neurons was proportionately increased (37 posteriorly biased *versus* 22 anteriorly biased). If posteriorly biased neurons more readily took up or expressed the injected DNA, the mosaic labeling method might have accounted for these disparities. Because posteriorly biased neurons were more likely to innervate multiple neuromasts (**Figure 3.3 *F***), though, the excess of posteriorly biased neurons more probably reflects the existence of neuronal subtypes with divergent receptive-field properties.

Specificity in dorsoventral neuromasts

The analysis of neuronal connectivity has thus far been limited to neuromasts containing hair cells sensitive to stimuli along the anteroposterior axis. The correlated wiring of similarly oriented hair cells might therefore reflect, not hair-cell polarity cues, but rather the anatomical arrangement of cells within the neuromast. To distinguish between these possibilities, I examined fish in which labeled single afferents innervated dorsoventral neuromasts. In all four cases,

there was a marked bias in the innervation of dorsally *versus* ventrally polarized hair cells. Owing to the more ventral location of these neuromasts (Ledent, 2002; Lopez-Schier et al., 2004), the afferent neuron veered ventrally from the PLL nerve in its approach to the neuromast (**Figure 3.4** ***A, B***). Staining with fluorescent phalloidin revealed the polarities of the constituent hair cells and confirmed that four of five ventrally oriented hair cells received boutons (**Figure 3.4** ***C-E***). The fifth and youngest ventrally polarized hair cell was contacted by only a tenuous neurite (**Figure 3.4** ***C***). Despite the afferent fiber's tortuous course beneath the neuromast, the dorsally polarized hair cells apparently received no contacts.

From the examination of neuromasts sensitive to dorsally and ventrally oriented stimuli, it is possible to conclude that neuronal preference for individual hair cells depends on their polarity or on a cue normally associated with this polarity. I never encountered a neuron that innervated both a dorsoventral and an anteroposterior neuromast.

Electron microscopy of synaptic contacts

Although the light-microscopic observations documented an orderly pattern of apposition between afferent terminals and specifically oriented hair cells, they could not unequivocally demonstrate synapses between the two. Moreover, it was unclear from the foregoing observations whether the apparent contacts are endowed with the morphological features of functional hair-cell synapses. I therefore used transmission electron microscopy to examine larval neuromasts.

Even at the earliest stage examined, 2 dpf, the hair cells contained numerous synaptic ribbons associated with synaptic vesicles and prominent pre- and postsynaptic densities. A comparison of two-day-old and five-day-old synaptic ribbons disclosed no striking differences between the two (**Figure 3.5** ***A, B***) save that the synaptic ribbons of some younger hair cells were smaller. These results confirm that hair-cell afferent synapses, or at least a substantial majority of them, are potentially competent for neurotransmitter release from as early as 2 dpf.

This descriptive study of synaptic ultrastructure does not address whether the appositions between afferent neurons and hair cells observed *in vivo* are truly synapses. To directly answer this question, I sought a genetically encoded marker that labels neuronal membranes during the imaging of living cells and in correlative electron microscopy. Existing approaches, such as labeling with HRP::CD2 (Watts et al., 2004) or tetracysteine tags (Gaietta et al., 2002), possess serious drawbacks such as the need to express a fluorescent protein in parallel or to apply intense illumination in the presence of biarsenical compounds to photoconvert diaminobenzidine. To circumvent these concerns, I created a construct that encodes a single-pass transmembrane protein, HRP-mCherry, with horseradish peroxidase (HRP) extracellularly and the fluorescent marker mCherry intracellularly (**Figure 3.5** ***C***). In the presence of diaminobenzidine and hydrogen peroxide, horseradish peroxidase generates a local osmiophilic precipitate visible both by light microscopy (**Figure 3.5** ***D***) and by electron microscopy. HRP-mCherry allows one to track the neurites of cells expressing mCherry *in vivo* by confocal fluorescence microscopy, then to examine regions of interest with the resolving power of transmission electron microscopy.

The *HuC:HRP-mCherry* plasmid was injected into larvae of the *Pou4f3:gap43-GFP* transgenic line, in which hair-cell membranes are marked with GFP (Xiao et al., 2005). By obtaining a stack of confocal images through a neuromast at 5 dpf, I observed an mCherry-expressing afferent innervating a subset of hair cells within a neuromast (**Figure 3.6** ***A, B***). Although another afferent fiber was labeled as well, it expressed the marker more weakly and did not innervate this particular neuromast. The larva was then fixed and processed to demonstrate horseradish peroxidase activity at the electron-microscopic level. After completion of the preparative protocol and embedding in plastic, the labeled neuron could be visualized under brightfield illumination (**Figure 3.5** ***D***). Although electron microscopy of the PLL nerve from a control larva confirmed that the afferent fibers displayed no labeling (**Figure 3.6** ***C***), sections from the labeled preparation revealed two afferent fibers delineated by extracellular precipitate (arrowheads, **Figure 3.6** ***D***). In keeping with the mCherry fluorescence pattern, one fiber displayed substantially greater expression than the other. At higher magnification, the strongly labeled afferent was cloaked in an electron-dense precipitate that remained extracellular and did not appear to damage the neuron itself or the surrounding tissue (**Figure 3.6** ***E***).

To ensure that regions of membrane contact identified by fluorescence were not missed, I cut serial sections through an entire neuromast. The afferent synapses of unlabeled neurons appeared normal and lacked extracellular electron density (**Figure 3.6** ***F***). In striking contrast, an afferent synapse corresponding to an mCherry-positive terminal (**Figure 3.6** ***A***) demonstrated extensive extracellular precipitate (**Figure 3.6** ***G***). Upon examining another intercellular contact (**Figure 3.6** ***B***), I found an afferent synapse apposed to a

neuron surrounded by and filled with electron-dense material (**Figure 3.6 *H*, *I***). This neuron appeared to have experienced extensive damage (**Figure 3.6 *H***), most likely a result of gas evolution during the demonstration of horseradish peroxidase activity.

These results confirm that the contacts observed by fluorescence microscopy indeed represent vesicle-loaded afferent synapses. This approach has a number of advantages over other tools for correlative electron microscopy. Most notably, HRP-mCherry consists of a proteinaceous fluorophore directly linked to a widely used enzymatic label. The result is a clearly defined fluorescence pattern that is manifested as electron density when studied at high resolution.

The preference for hair-cell polarity in regenerating neurons

The hair cells of fish, amphibians, and birds regenerate on timescales of hours to days after extirpation by ototoxic agents such as aminoglycoside antibiotics and Cu^{2+} (Williams and Holder, 2000; Hernández et al., 2007). By examining how afferent neurons re-innervate neuromasts after hair-cell ablation, I inquired about the degree to which hair-cell polarity preferences are specified through an intrinsic affinity for a particular polarity. If afferent neurons display a polarity preference prior to hair-cell ablation, do they maintain that preference after newly minted hair cells have repopulated the neuromast, or is the polarity preference reset? In the latter instance, afferents would be expected to innervate hair cells of either polarity after regeneration, with no memory of the pre-ablation preference.

I injected DNA encoding membrane-targeted mCherry driven by the *HuC* promoter (*HuC:gap43-mCherry*) into stably transgenic embryos bearing the *Pou4f3:gap43-GFP* transgene. After screening for larvae that expressed mCherry in PLL neurons, I imaged the innervated neuromasts at 3 dpf. At this stage, neuromasts are small enough to display an unambiguous axis of mirror symmetry, so that the polarities of hair cells are certain (**Figure 3.7 *A***). The afferent fiber innervated all four posteriorly polarized hair cells and none of the anteriorly polarized hair cells, indicating a marked preference for the former. Immediately after imaging, the fish were immersed in 10 μM $CuSO_4$ solution to eliminate lateral-line hair cells. Two hours after this treatment, the same neuromast was examined again and found to be devoid of hair cells (**Figure 3.7 *B***). In conjunction with the loss of hair cells, the labeled neuron underwent considerable retraction of its terminals.

As the neuromast repopulated its hair cells over the next 46 hr, the afferent neuron extended its neurites and formed synapses anew (**Figure 3.7 *C-K***). After 6 hr, a centrally positioned cell began to express GFP and probably represented a hair-cell progenitor that would give rise to two daughter hair cells (Lopez-Schier and Hudspeth, 2006). By 12 hr after treatment, the neuromast contained two mature hair cells; the posteriorly polarized hair cell received a small contact from the labeled afferent fiber, which grew more pronounced by 24 hr. At 36 hr, the neuromast had grown to encompass seven hair cells, of which the nerve appeared to contact only three (**Figure 3.7 *F*, *G***). At this stage of neuromast recovery, it was impossible to reliably infer the hair-bundle polarity without phalloidin staining. Finally, 48 hr after ablation, the neuromast contained eight mature hair cells, as well as two immature hair cells

at its rostral extreme. Phalloidin staining revealed the presence of four anteriorly polarized and four posteriorly hair cells, and I ascertained that the labeled neuron formed synapses with all four of the latter (**Figure 3.7** ***H-L***). In contrast, two of the four anteriorly polarized hair cells were contacted by thin neurites (arrowheads, **Figure 3.7** ***H, J***) that differed significantly from the larger boutons on the posteriorly polarized hair cells. Repeating this protocol in three additional animals yielded results consistent with this representative example for both anteriorly and posteriorly biased neurons.

This experimental approach has elucidated two important properties of this system. First, afferent fibers recover and re-innervate neuromasts after acute injury on a timescale that largely matches that of hair-cell regeneration. Second, afferent fibers evidently remember the polarity of the hair cells that they innervated prior to ablation. This consistency in the preference for hair-cell polarity led me to question whether the neuron passively interprets hair-cell polarity cues or plays an instructive role in determining hair-cell polarity. To distinguish between these possibilities, I determined the polarities of hair cells in *neurogenin1* mutant zebrafish, which lack the PLL nerve and possess supernumerary neuromasts (Grant et al., 2005; Lopez-Schier and Hudspeth, 2005). The neuromast hair cells of mutant larvae were polarized normally across a plane of mirror symmetry despite the complete absence of the PLL nerve (**Figure 3.8**), ruling out a scenario in which the neuron dictates hair-cell polarities.

DISCUSSION

In vivo time-lapse imaging revealed that each lateral-line afferent neuron specifically contacts hair cells of a common hair-bundle polarity within a neuromast and across multiple consecutive neuromasts. Because these studies relied on membrane propinquity alone to signal the presence of intercellular contacts, I created a reagent, HRP-mCherry, that allowed me to confirm that fluorescently marked contacts correspond at the electron-microscopic level to synapses between hair cells and afferent terminals. Finally, I examined the reestablishment of neuronal connectivity after hair-cell ablation and found that afferents promptly resume contact with regenerating hair cells of the same polarity as those innervated originally.

The findings presented in this chapter were published in the *Journal of Neuroscience* (Nagiel et al., 2008) and later confirmed by another laboratory group (Faucherre et al., 2009). Using a similar experimental approach to ours, Faucherre et al. showed that afferent neurons selectively innervate hair cells of one polarity within a neuromast and across consecutive neuromasts. Using time-lapse confocal microscopy of regenerating neuromasts, however, they additionally demonstrated that afferent neurons prefer the same hair-cell polarity even after three rounds of ablation and that afferent neurites display highly dynamic exploratory behaviors as they seek out particular hair cells.

The receptive fields of single afferent neurons

These findings provide direct anatomical evidence that each afferent fiber contacts hair cells of the same polarity and a statistical demonstration of the

consistence of this pattern. In addition, the majority of afferent neurons stably innervate several neuromasts (**Figure 3.3** ***D-E***). This represents a more extreme version of the pattern seen in amphibians, in which only a fraction of afferent fibers innervate multiple stitches of clustered neuromasts (Fritzsch, 1989; Mohr and Görner, 1996). The variability in the sizes of receptive fields in the zebrafish PLL casts doubt on whether the primary purpose of this sensory system is a fine-grained mapping of the periphery through a one-to-one allocation of afferents to neuromasts. The innervation of multiple neuromasts may represent a compromise that boosts the sensitivity of the system through the binning of adjacent inputs. It is reassuring that afferents rarely innervate non-consecutive neuromasts, for this would place a seemingly unnecessary burden on the establishment of an appropriate pattern of neural connections.

The somatotopic mapping of PLL hindbrain inputs prior to neuromast innervation suggests a marked degree of intrinsic patterning. With this in mind, I scrutinized neurons innervating multiple neuromasts to learn whether these neuromasts were co-innervated in any reproducible pattern. For example, do the fifth and sixth neuromasts of the larval PLL always wire together? Except for the terminal neuromasts located on the caudal tailfin, which often shared afferents, I found no consistent pattern of co-innervation, so it remains possible that some flexibility in neuromast choice exists and that the prepatterning of afferents guides but does not strictly determine this choice.

HRP-mCherry, a tool for correlative electron microscopy

Because specialized organelles regulate neurotransmitter release, evidence of intercellular contact is insufficient to infer the presence of a synapse. I therefore developed HRP-mCherry to provide direct evidence that sites of membrane contact between hair cells and afferent neurons represent functional synapses (**Figure 3.6 *A*, *B*, and *G-I***). Horseradish peroxidase requires glycosylation for its enzymatic activity (Veitch, 2004), so I designed a fusion protein in which the enzyme moiety is situated at the N-terminus and is directed across the membrane by a signal peptide. Linkage of the fluorescent protein mCherry to the extracellular horseradish peroxidase by the transmembrane region of N-cadherin then allows fluorescent as well as electron-microscopic labeling of specific cells.

This approach offers a significant improvement over previously available techniques for correlating neurolemmal fluorescence *in vivo* with electron-dense precipitates, such as tetracysteine tags or CD2::HRP. Tetracysteine tags require the use of potentially toxic arsenical compounds as well as sharply focused illumination, which precludes the uniform labeling of lengthy cellular processes. Unlike HRP-mCherry, CD2::HRP necessitates the co-expression of a fluorescent protein, which may be inconvenient and provides no stoichiometric relation between fluorescence intensity and electron density. The extracellular reaction product of HRP-mCherry does not interfere with the observation of organelles within a labeled cell. Although the reaction product diffuses somewhat, labeling is sufficiently circumscribed that the identity of a labeled cell is clear (**Figure 3.6 *D*, *E***).

Synaptic-target selection by developing afferent neurons

Although an obvious requirement for the proper functioning of sensory circuits is that neurons form synapses with the appropriate targets, we lack a comprehensive understanding of the factors that guide the choice of target cells (Benson et al., 2001; Waites et al., 2005). I have illustrated an experimental preparation that facilitates the study of synaptogenesis through non-invasive optical techniques in a living vertebrate. An attractive feature of this system is that an experimenter may readily determine relevant properties of both pre- and postsynaptic cells. For the hair cell, it is possible to ascertain the position on the larval surface and the axis of mechanosensitivity. For the afferent neuron, one can observe the complement of neuromasts innervated, the specific hair cells selected, and the pattern of axon projections in the hindbrain. These features permit the study of synaptogenesis at the resolution of individual contacts in a system that is amenable to experimental manipulation, properties usually associated with neuronal cultures or invertebrate organisms.

A noteworthy aspect of this experimental system is the temporal course of synaptic target selection and stabilization. The evidence for polarity bias was strong at every time examined, and there was no significant change in the degree of bias (**Figure 3.3** ***A***, ***B***). This result suggests that the neurons respond to polarity cues throughout neuromast growth and turnover. This conclusion contrasts with that for sensory circuits in which there are distinct periods of exuberant synaptogenesis and activity-dependent synaptic elimination, such as occurs in the mammalian visual system (Luo and O'Leary, 2005).

The mechanism of synaptic specificity

The wiring specificity documented here could arise if the afferent neurons instruct hair cells to assume a certain polarity. Because the hair bundles of mutant animals lacking the PLL nerve are polarized normally (**Figure 3.8**), however, this mechanism is unlikely. Another possibility is that a polarity signal within the neuromast dictates both the polarity of the hair cells and the synaptic targets of the neurons. One argument against this arrangement comes from large neuromasts with multiple planes of mirror symmetry, in which hair cells of opposing polarities are extensively intermixed. A neuron contacts all the hair cells of a specific polarity regardless of their location within such a neuromast (**Figure 3.7** ***H-L***). The consistent choice of hair-cell polarity across several neuromasts provides a second piece of evidence, for it is difficult to understand how an individual fiber would receive the same polarization instructions as it enters distinct neuromasts.

The most likely possibility—and one that is consistent with all of my observations—is that afferent neurons have a capacity to sense the polarity of the hair cells and synapse accordingly. The findings presented in this chapter provide some initial clues into the role of synaptic activity. The following chapter scrutinizes the mechanism of polarity-specificity in greater detail.

Figure 3.1

Afferent and efferent innervation of the PLL

A, Efferent synaptic endings occur in a PLL neuromast in a living *islet1:GFP* fish at 3 dpf. ***B***, Dual labeling with FM 4-64 (red) demonstrates that one immature hair cell of this neuromast failed to take up the dye but was nevertheless innervated (arrowhead). ***C***, GFP expression in the PLL nerve of a live *HuC:GFP* embryo at 2 dpf documents the afferent innervation of two neighboring neuromasts. ***D***, Labeling of the same specimen with FM 4-64 reveals the hair cells (red). ***E***, The expression of *HuC:GFP* in a single PLL afferent neuron reveals its soma in the PLL ganglion and its bifurcated axon reaching the hindbrain. An ascending fiber from the spinal cord was labeled as well (arrowheads). ***F***, The peripheral projection of this neuron at 1.5 dpf features an actively migrating growth cone. Images are maximal-intensity projections of confocal Z-stacks. Scale bars, 20 μm.

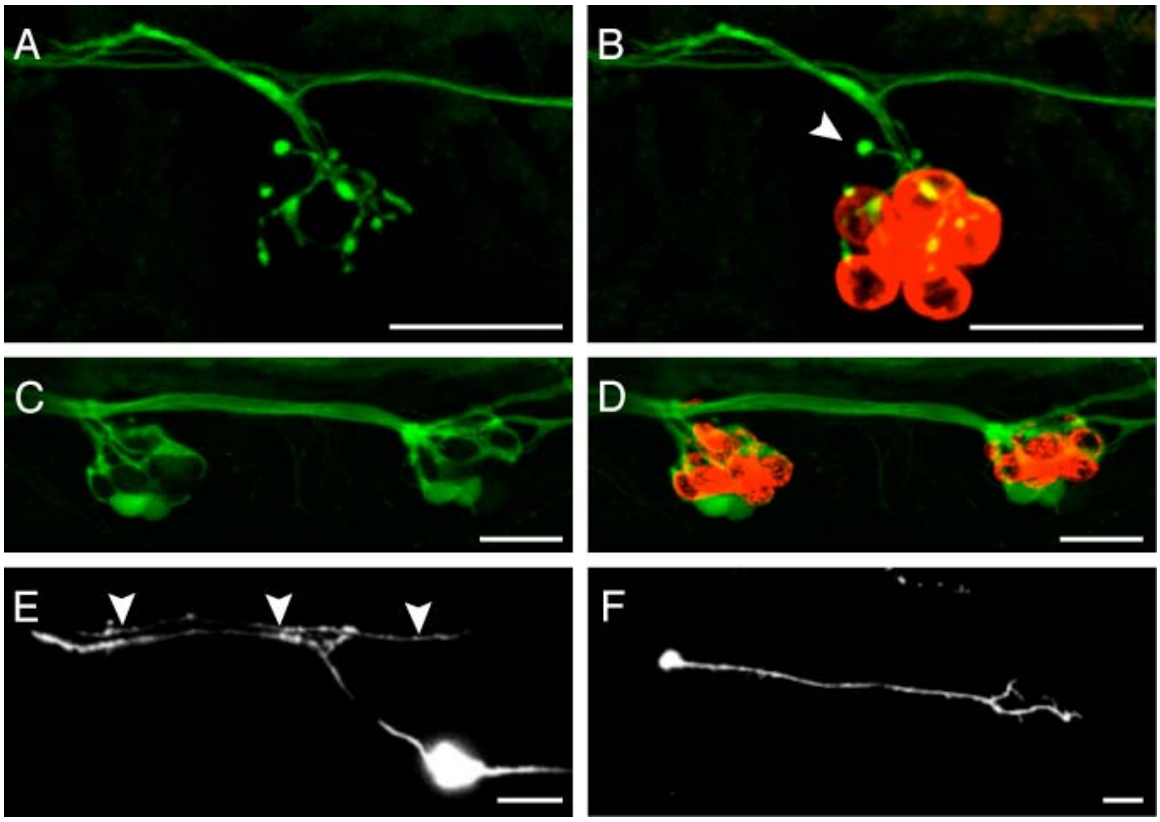
A
B
C
D
E
F

Figure 3.2

In vivo imaging of afferent synaptogenesis

A, In a maximal-intensity projection of a Z-stack of an anteroposterior neuromast at 2.5 dpf, an mCherry-labeled afferent fiber (red) forms a putative synapse with the rostral-most of the hair cells expressing GFP (green). Two immature hair cells are only dimly labeled with GFP (arrowheads). ***B***, A selected confocal section of the neuromast in ***A*** shows the extensive contact between the terminal and one hair cell as well as a substantially smaller contact with a second. ***C***, A maximal-intensity projection of the same neuromast at 3.5 dpf illustrates extensive neuronal contact with the three posteriorly polarized hair cells. ***D-E***, Selected optical sections of the neuromast depicted in ***C*** delineate the individual contacts. ***F***, A maximal-intensity projection of the same neuromast at 4.5 dpf demonstrates five putative synapses, of which four occur with posteriorly polarized hair cells. ***G-H***, Large boutons have formed on the three largest posteriorly polarized hair cells. ***I***, A newly formed hair cell has been innervated (arrowhead) just as its hair bundle has begun to polarize posteriorly (see ***K***). ***J***, One innervated hair cell of this neuromast (arrowhead) is of the opposite polarity with respect to the others (see ***K***). ***K***, Staining of hair bundles in this neuromast with fluorescent phalloidin reveals the polarities of the hair cells at 4.5 dpf. The stereocilia in each bundle display a crescentric pattern of fluorescence surrounding a dark spot at the site of the kinocilium. *A*, anterior; *P*, posterior; *D*, dorsal; *V*, ventral. Scale bars, 5 μm.

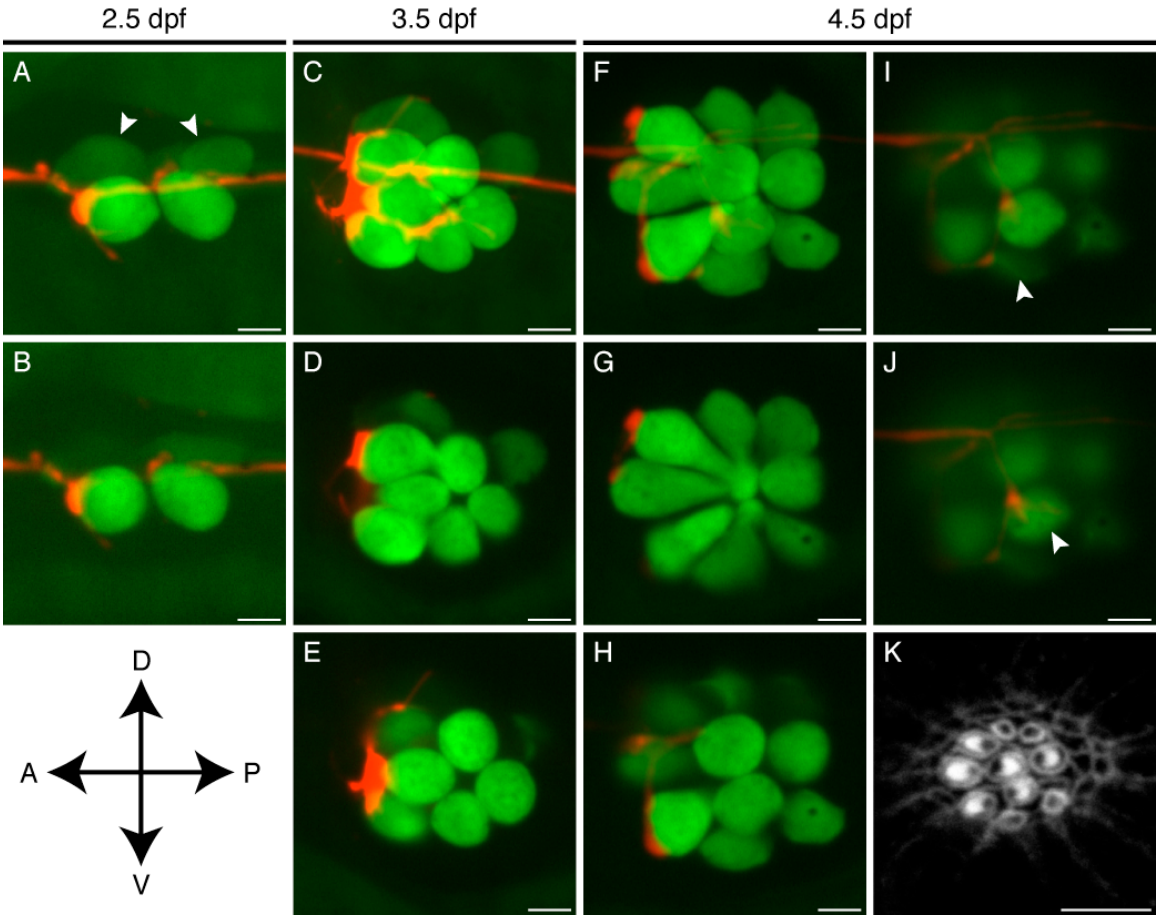
2.5 dpf
3.5 dpf
4.5 dpf
A
B
C
D
E
F
G
H
I
J
K
D
A
P
V

Figure 3.3

Statistical analysis of innervation bias and receptive fields

A, In a plot of the weight of evidence for a biased model (*W*) against larval age, the ordinate represents the average weight of evidence contributed by a single neuromast at the given time. Summing the results over the ensemble of neuromasts yields a total weight of evidence of 375 db. ***B***, Given that there is strong evidence for orientation selectivity, the parameter w reflects the degree to which the neuron's choice of hair cells is biased. To illustrate the degree of bias as a function of larval age, the results have been expressed as means of the probability of $|w-0.5|+0.5$, so that the ordinate reflects increasing bias. The error bars represent standard deviations. ***C***, A histogram illustrating the fraction of a neuromast's hair cells innervated by the labeled fiber indicates that 84% of the neuromasts studied had 50% or fewer hair cells innervated. ***D***, A plot of the number of neurons with the indicated receptive-field sizes demonstrates the preponderance of fibers innervating one or two neuromasts. ***E***, The mean number of neuromasts innervated by a single afferent is essentially constant over the range of larval ages investigated. The error bars represent standard errors of the means. ***F***, The distribution of neuromasts per neuron demonstrates an excess of posteriorly biased (black) over anteriorly biased (gray) neurons.

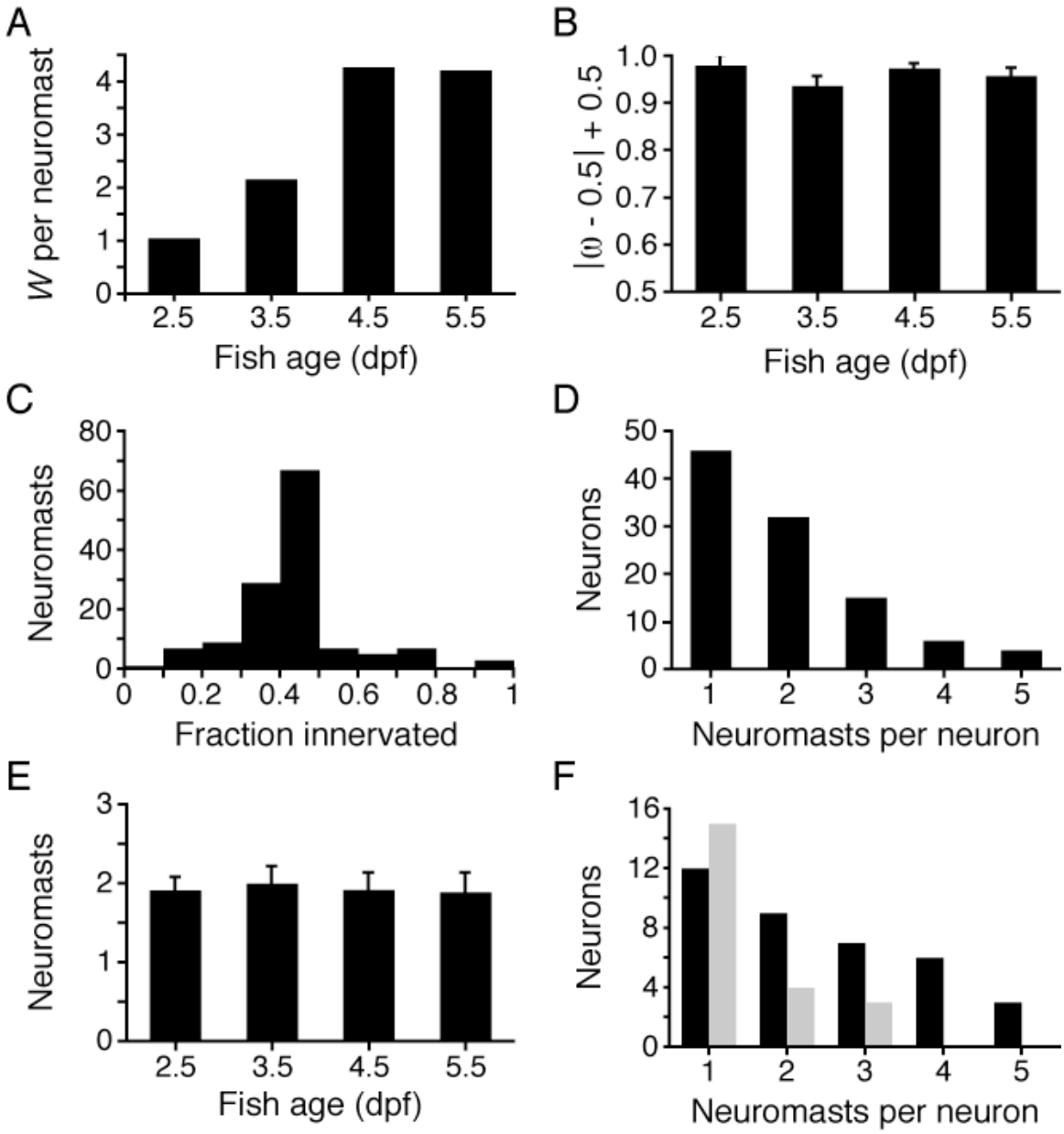
A
W per neuromast
0
1
2
3
4
2.5
3.5
4.5
5.5
Fish age (dpf)
B
|ω - 0.5| + 0.5
0.5
0.6
0.7
0.8
0.9
1.0
2.5
3.5
4.5
5.5
Fish age (dpf)
C
Neuromasts
0
20
40
60
80
0
0.2
0.4
0.6
0.8
1
Fraction innervated
D
Neurons
0
10
20
30
40
50
1
2
3
4
5
Neuromasts per neuron
E
Neuromasts
0
1
2
3
2.5
3.5
4.5
5.5
Fish age (dpf)
F
Neurons
0
4
8
12
16
1
2
3
4
5
Neuromasts per neuron

Figure 3.4

Afferent connections of dorsoventral neuromasts

A, In a maximal-intensity projection of a confocal Z-stack, the mCherry-expressing afferent fiber turns ventrally from the lateral-line nerve to reach a dorsoventral neuromast. ***B***, The hair cells in the same neuromast are labeled with GFP (green). ***C***-***D***, This neuromast contains ten hair cells, of which four receive bulbous synaptic endings. The most rostral is contacted by only a thin neurite (arrowhead). ***E***, Labeling with fluorescent phalloidin indicates that these five hair cells have ventrally polarized hair bundles. Although the dorsally polarized hair cells are embraced by a thin, circular extension of the neuron (***A***), they lack synaptic boutons. Scale bars, 5 μm.

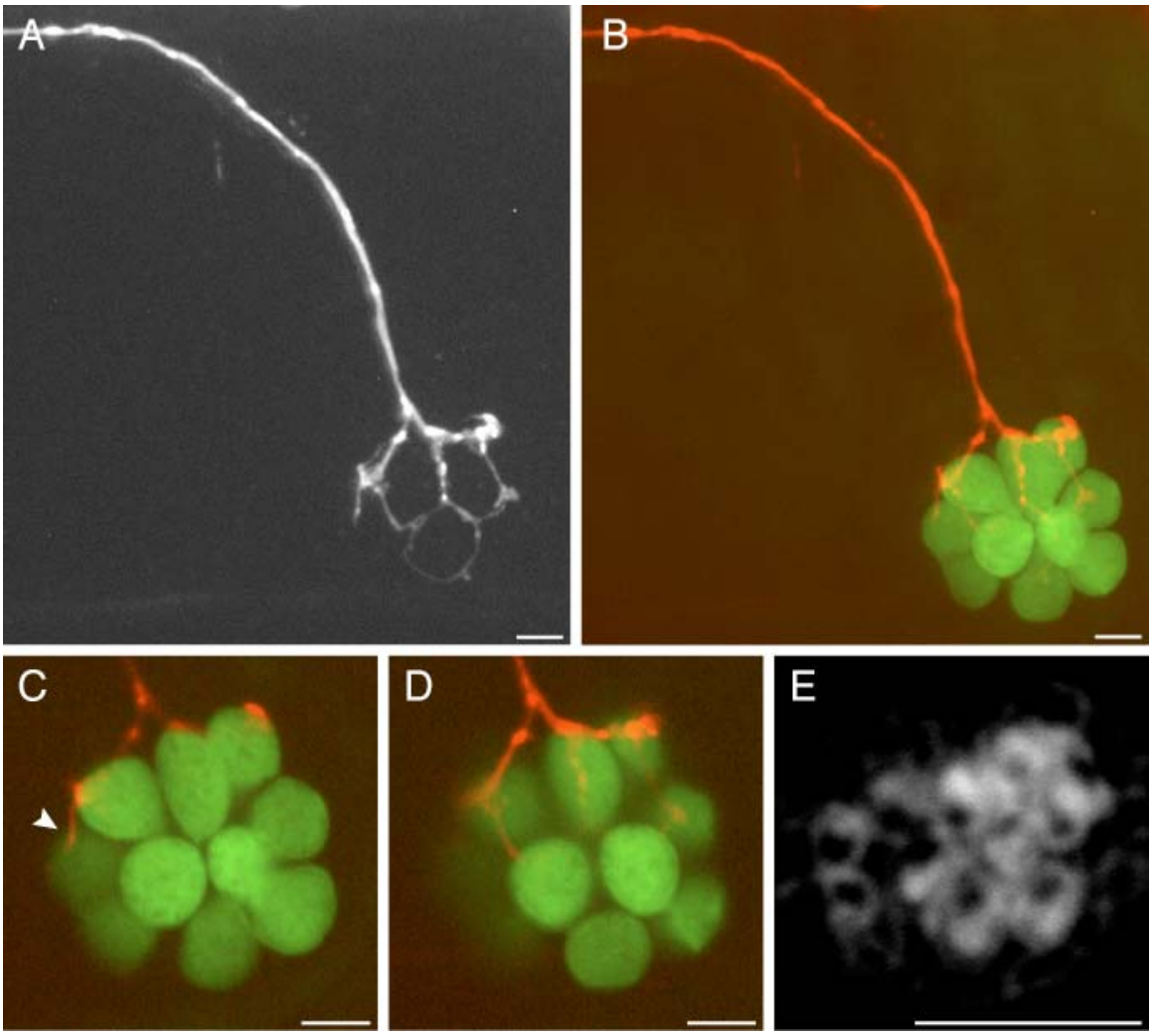
A
B
C
D
E

Figure 3.5

The ribbon synapse and the HRP-mCherry protein

A, A ribbon synapse in a 2 dpf wild-type embryo is indistinguishable from those in older animals. ***B***, The synapse in a 5 dpf wild-type larva exhibits the characteristic features of a ribbon synapse, including a presynaptic dense body or ribbon, a halo of tethered synaptic vesicles, and prominent pre- and postsynaptic densities. ***C***, Expression of the HRP-mCherry protein in the neurolemma places the fluorescent mCherry component intracellularly and the HRP moiety extracellularly. ***D***, A bright-field micrograph depicts an afferent terminal expressing HRP-mCherry within a neuromast. The densely labeled fiber, which is also depicted in **Figure 3.6**, is visible through the plastic resin in which the specimen has been embedded. Scale bars: ***A***, ***B***, 100 nm; ***D***, 5 mm.

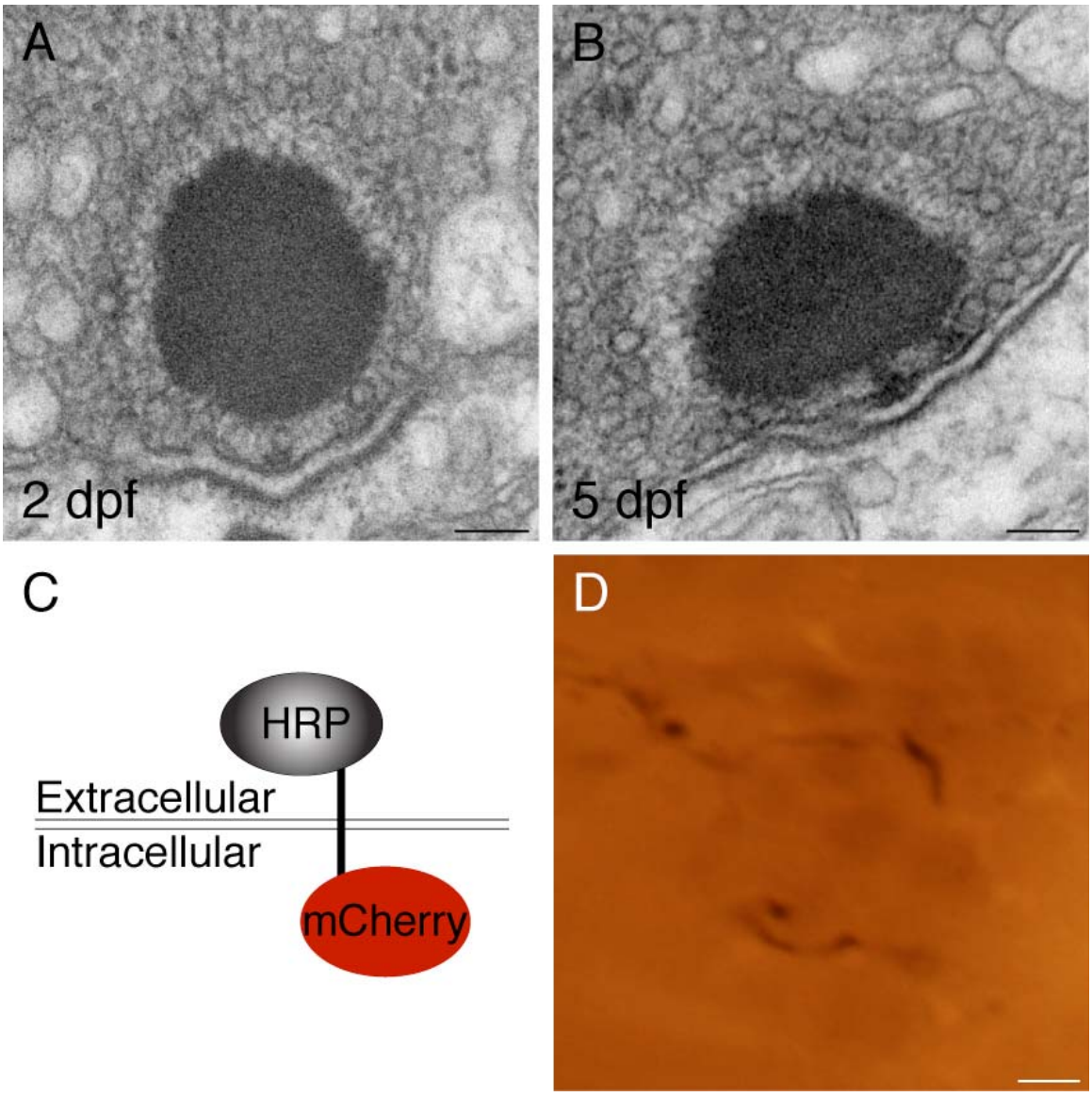
A
2 dpf
B
5 dpf
C
HRP
Extracellular
Intracellular
mCherry
D

Figure 3.6

Correlative electron microscopy with HRP-mCherry

A, An optical section through a neuromast of a living *Pou4f3:gap43-GFP* larva features hair cells expressing a membrane-localized form of GFP (green). An afferent fiber labeled with HRP-mCherry (red) innervates three of the hair cells. The region bracketed by arrowheads is examined in greater detail in ***G***. ***B***, In an optical section through the basal region of the same neuromast, arrowheads bracket a site that was later explored under the electron microscope (***H*** and ***I***). ***C***, A transverse section of the PLL nerve in a wild-type 5 dpf larva demonstrates several afferent axons. ***D***, In a transverse section through a PLL nerve, two afferent fibers that express HRP-mCherry (arrowheads) produce prominent electron density in the surrounding extracellular space. The weakly labeled fiber in the lower right did not innervate the neuromast depicted in ***A-B***, and ***D-I***. ***E***, A higher-magnification view of the labeled neuron at the upper left of ***D*** illustrates a localized precipitate that does not damage nearby cells. ***F***, An unlabeled afferent neuron lacking electron density synapses with a hair cell of the neuromast. ***G***, A synaptic ribbon (arrowhead) in the region of membrane contact denoted by arrowheads in ***A*** verifies that the membrane contact observed by light microscopy represents an afferent synapse. ***H***, This ribbon synapse occurs at the site of membrane apposition bracketed by arrowheads in ***B***. In this instance the neuron has become distorted and exhibits poor preservation of intracellular organelles. ***I***, Viewed at higher magnification, the ribbon synapse in ***H*** illustrates the typical attributes of hair-cell afferent synapses. Scale bars: ***A***, ***B***, 5 mm; ***E***-***G***, ***I***, 100 nm; ***C***-***D***, ***H***, 500 nm.

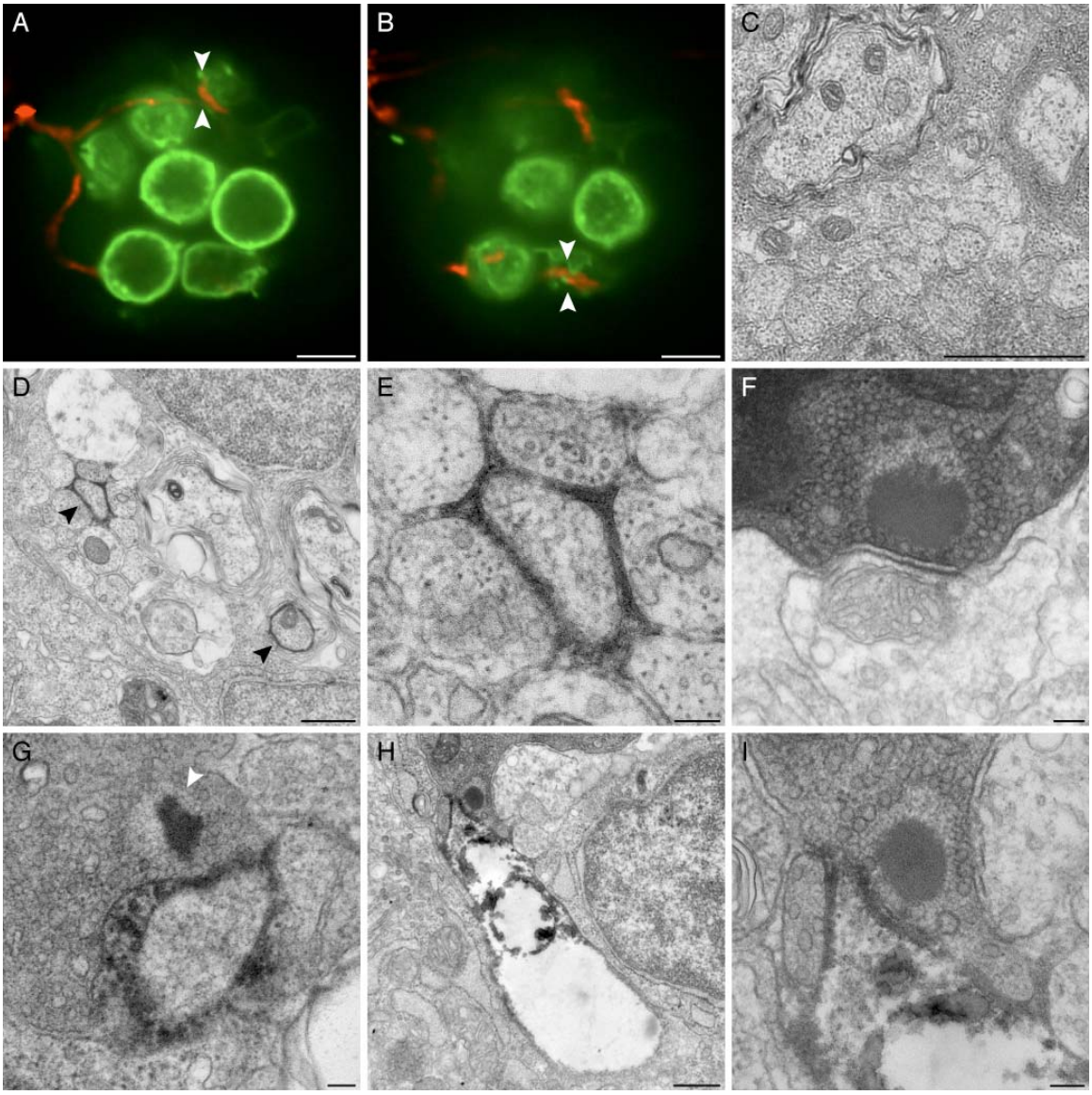
A
B
C
D
E
F
G
H
I

Figure 3.7

Reinnervation of regenerated hair cells

A, In a 3 dpf neuromast prior to hair-cell elimination, the axis of planar cellular polarity (dashed line) can be inferred from the positions of the constituent hair cells. The afferent fiber has selectively synapsed with posteriorly polarized hair cells. ***B***, In a maximal intensity projection of the same neuromast 2 hr after the application of 10 μM Cu^{2+}, the hair cells have been eliminated and the neuron has retracted its terminals. Note the presence in the lateral-line nerve of another labeled neuron that does not innervate this neuromast (arrowhead). ***C***, After 6 hr, the neuromast contains one weakly fluorescent progenitor. ***D***, After 12 hr, the newly formed posteriorly polarized hair cell receives a small synapse. ***E***, By 24 hr, the synapse depicted in ***D*** has grown in size. ***F***-***G***, At 36 hr, the neuron contacts two or three hair cells, but their polarities cannot be inferred. ***H***-***K***, By 48 hr, the neuromast has grown to encompass eight mature hair cells with polarized hair bundles (see ***L***). These four panels are ordered from the bases to the apices of the hair cells. ***H***, A thin neurite reaches an anteriorly polarized hair cell (arrowhead). ***I***, A larger bouton contacts the ventral-most of the posteriorly polarized hair cells (arrowhead). ***J***, A synaptic contact blankets the basal surface of a posteriorly polarized hair cell (arrow), whereas only a tenuous process reaches an anteriorly polarized hair cell (arrowhead). ***K***, The afferent neuron forms voluminous boutons on two posteriorly polarized hair cells. ***L***, Staining with fluorescent phalloidin 48 hr after treatment defines the polarities of the ten hair bundles. Scale bars, 5 mm.

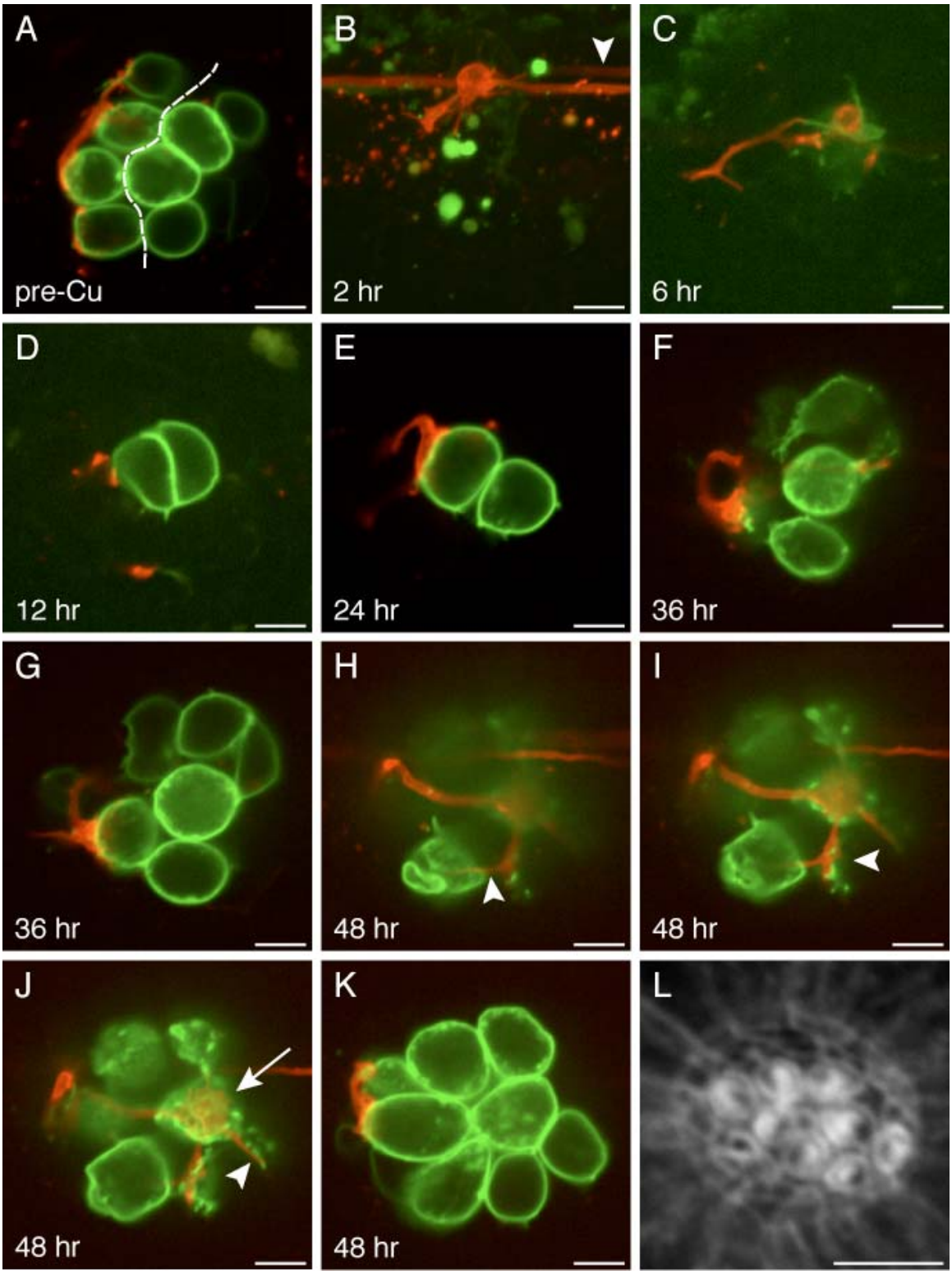
A
pre-Cu
B
2 hr
C
6 hr
D
12 hr
E
24 hr
F
36 hr
G
36 hr
H
48 hr
I
48 hr
J
48 hr
K
48 hr
L

Figure 3.8

Hair-cell polarity in the absence of innervation

A, A maximal-intensity projection of a confocal Z-stack depicts immunolabeling for acetylated α-tubulin in the lateral line of a 5 dpf wild-type larva. The PLL nerve and superficial sensory neurons are labeled, as well as microtubules in the apices of hair cells. ***B***, Immunolabeling of a *neurogenin1* mutant sibling for acetylated α-tubulin illustrates the absence of a PLL nerve. Labeling persists in the microtubules of hair cells. ***C***, Staining of a wild-type neuromast with fluorescent phalloidin (red) and immunofluorescent labeling of acetylated α-tubulin (green) reveal the polarities of the hair bundles in this anteroposterior neuromast. ***D***, The hair-bundle polarities of a *neurogenin1* mutant neuromast are unperturbed despite the lack of innervation. Scale bars: ***A***-***B***, 30 mm; ***C***-***D***, 5 mm.

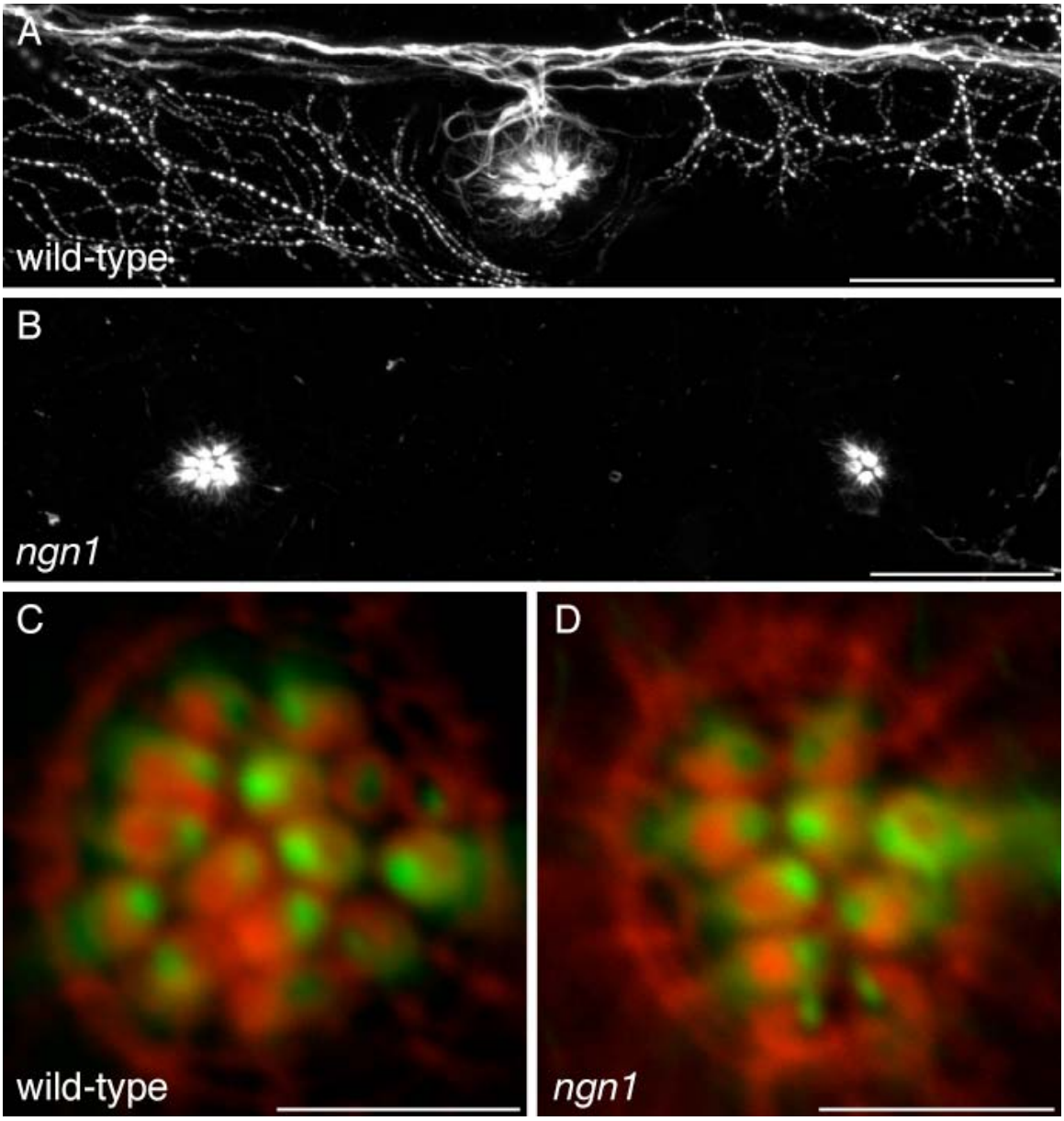
A
wild-type
B
ngn1
C
wild-type
D
ngn1

CHAPTER FOUR

Activity-independent specification of afferent synaptic targets

The results described in the previous chapter and independent evidence by Faucherre et al. (2009) illustrate a striking degree of specificity in the innervation of PLL hair cells. Afferent fibers display a consistent polarity preference throughout embryonic development, after hair-cell regeneration, and even across co-innervated neuromasts. The strength and consistency of the data point to a robust underlying mechanism that guides afferents to form the appropriate synaptic contacts. In this chapter, I begin to investigate this mechanism by asking whether synaptic activity plays a role. In one scenario, afferent neurons could distinguish hair-cell polarities by analyzing the temporal pattern of synaptic activity. This pattern of activity could be evoked by sensory experience or it could be generated intrinsically by hair cells. The other possibility is that specificity arises from an intrinsic affinity of afferent neurons for particular hair-cell polarities through direct molecular affinities.

RESULTS

We considered three models to explain polarity specificity during afferent innervation of hair cells (**Figure 4.1**). The first posits that an afferent neuron innervates hair cells randomly but then eliminates certain contacts by analyzing the temporal pattern of synaptic release elicited by sensory experience. A

unidirectional stimulus should simultaneously intensify synaptic release from hair cells of one polarity and suppress release from cells of the opposite orientation (Görner, 1963). If afferent neurites serve as coincidence detectors, they could strengthen synapses with hair cells of a particular polarity and eliminate synapses with those of the opposite polarity through a Hebbian mechanism. A second activity-dependent model requires oppositely polarized hair cells to possess different patterns of spontaneous synaptic activity. This model differs from the first in that the distinguishing quality is a spontaneous rather than an experience-evoked pattern of neurotransmitter release. The third model asserts that hair cells of opposite polarity express distinct membrane or secreted proteins that are recognized by prepatterned afferent neurons with intrinsic affinities for particular hair-cell polarities. Although this mechanism might require activity for long-term synaptic maintenance, it requires no synaptic input to achieve initial specificity. These three models were used to develop an experimental framework for deducing the mechanism at work in the lateral line.

Sensory experience is not required for synaptic specificity

I first tested whether afferent neurons can distinguish hair-cell polarity in the absence of experience-evoked patterns of synaptic release. I examined zebrafish lines bearing null mutations in two genes, *tmie* (Gleason et al., manuscript in preparation) and *protocadherin 15a* (Seiler et al., 2005). Larvae at 5 dpf displayed auditory and vestibular deficits, lacked microphonic potentials, and exhibited no uptake of fluorophores through their mechanotransduction channels (Seiler et

al., 2005). These phenotypes reflect defects in mechanotransduction that prevent sensory stimuli from eliciting membrane depolarization and synaptic-vesicle fusion.

The *tmie* gene product is a putatively single-pass transmembrane protein required for hair-cell mechanotransduction in fishes and mammals (Mitchem et al., 2002; Naz et al., 2002). In seven anteroposteriorally oriented neuromasts of *tmie* mutant larvae, each afferent fiber consistently innervated hair cells of only a single polarity (**Figure 4.2** ***A-C***). Specific innervation was also characteristic of the four *tmie* neuromasts I examined that contained dorsally and ventrally polarized hair cells (**Figure 4.2** ***D-F***).

I next examined synaptic specificity in the *protocadherin 15a* mutant, which lacks a component of the stereociliary tip link essential for transducing mechanical force into hair-cell depolarization (Seiler et al., 2005). In each of the 19 neuromasts studied, the axonal terminal formed synaptic boutons on hair cells of only one particular orientation (**Figure 4.2** ***G-I***). These results suggest that afferent neurons do not require sensory experience to distinguish hair-cell polarity.

Synaptic specificity in the absence of synaptic transmission

Because the preference of afferents for hair-cell polarity was robust in the absence of sensory input, I evaluated the possibility that an intrinsically generated pattern of synaptic release by hair cells reveals their polarity to afferents. Oppositely polarized hair cells might, for example, differ in their

frequency or pattern of spontaneous neurotransmitter release, and afferents might display complementary preferences.

I studied two mutant lines with defects in essential synaptic components and consequent loss of auditory and vestibular function. The *cav1.3a* mutant possesses a mutation in the L-type voltage-gated Ca^{2+} channel responsible for coupling membrane depolarization to transmitter release at the hair cell's afferent synapse (Sidi et al., 2004). In each of the 21 *cav1.3a* mutant neuromasts analyzed, the labeled afferent fiber made synapses onto hair cells of only a single polarity (**Figure 4.3** ***A-C***).

I additionally examined *vglut3* mutants, which lack the vesicular glutamate transporter type 3 responsible for filling synaptic vesicles with the afferent neurotransmitter glutamate (Obholzer et al., 2008). In each of fifteen *vglut3* mutant neuromasts, a labeled afferent neuron formed specific synapses onto hair cells of a common polarity (**Figure 4.3** ***D-F***). Taken together, the study of four zebrafish mutants lacking hair-bundle or synaptic function provides evidence that synaptic specificity persists in the absence of specific patterns of synaptic signaling.

Polarity preference and synapse maintenance

Although the mutants utilized for these studies displayed severe loss-of-function phenotypes, they might conceivably have retained sufficient synaptic activity to signal their polarities to afferents. If this were the case, we would nevertheless expect the afferent neurons to have exhibited a diminished capacity to distinguish between polarities. In order to rigorously detect small changes in

polarity preference, I analyzed synapse formation in many mutant and wild-type neuromasts and then Daniel Andor-Ardó applied a statistical model of polarity preference. The model contains a bias parameter ω that expresses the neuron's preference for one polarity over another. To represent neuronal bias independently of the particular polarity being preferred, he calculated the mean of the probability of $|\omega - 0.5| + 0.5$.

For all four mutant lines, afferent neurons displayed an ability to distinguish polarities to a degree commensurate with that of wild-type afferents (**Figure 4.4** ***A***). Our statistical analysis thus points to an activity-independent specification of synaptic targets, but it does not address whether afferent synapses require activity for long-term maintenance. To answer this question, I calculated the fraction of a neuromast's hair cells innervated by a single afferent fiber. Because neuromasts comprise two equal populations of oppositely polarized hair cells, one would expect no more than half of a neuromast to be innervated by a labeled fiber. The mean fraction innervated was similar for mutant and wild-type animals (**Figure 4.4** ***B***), suggesting that neurotransmitter release is not essential for synaptic maintenance.

DISCUSSION

I have assessed the role of synaptic activity in ensuring specific connectivity between afferent neurons and plane-polarized hair cells in the posterior lateral line of larval zebrafish. In two lines with defects in mechanotransduction and two with deficiencies of synaptic signaling, lateral-line afferents correctly identified and synapsed with hair cells of a common polarity. By applying a

statistical model of polarity preference to data from each mutant line, we ascertained that afferent synaptogenesis remained highly biased for one polarity over the other at levels matching those observed for wild-type animals. In addition, the fraction of each mutant neuromast innervated by the labeled afferent fiber was comparable to that in wild-type neuromasts, indicating that synaptic transmission is not essential for synaptic maintenance.

The role of synaptic signaling

These results imply that afferent neurons do not interpret a pattern of evoked or spontaneous neurotransmitter release, but instead utilize intrinsic molecular cues to identify and synapse with the appropriately polarized hair cells. This conclusion is consistent with two previous observations. First, when an afferent fiber innervates multiple neuromasts, it is consistent in its polarity preference both within each innervated neuromast and between neuromasts. It seems improbable that unbiased neurites belonging to the same fiber could consistently prefer the same polarity by analyzing experience-evoked patterns of coincident synaptic release. Second, afferent fibers retain their polarity preference following hair-cell death and regeneration. If unbiased afferents utilize patterns of coincident synaptic release to restrict themselves to a single polarity, one would expect the preference to depend on the polarity of the first hair cell innervated. This was not observed; instead, afferents synapse with hair cells of the same polarity as those innervated prior to hair-cell ablation. Both of these observations contradicted a model whereby initially unbiased afferent neurons use experience-dependent patterns of synaptic release to restrict themselves to a

single polarity. These findings were nevertheless compatible with an activity-dependent mechanism in which prepatterned afferent neurons prefer a polarity-specific pattern of spontaneous synaptic release. My present results with *cav1.3a* and *vglut3* mutant fish speak against this mechanism, however, favoring instead activity-independent specification.

Before a role for synaptic activity can be excluded altogether, three important issues need to be addressed. The first issue is the exclusive reliance on loss-of-function mutants. The unlikely possibility exists that patterned neurotransmitter release ordinarily overrides the default molecular mechanism that confers specificity in the mutants. To test this, one might express a light-gated cation channel such as channelrhodopsin-2 in hair cells and raise the fish in the presence of stroboscopic illumination. If electrical activity plays an instructive role, each afferent fiber would be expected to contact all the hair cells of a neuromast, regardless of their polarity, because they would depolarize in synchrony. The second issue is that synaptic activity could play other, more subtle roles in neuronal morphology and behavior. Despite their ability to correctly identify hair-cell polarities in the absence of synaptic signaling, afferent neurons might exhibit increased exploratory behavior manifested as a greater spread of axonal arbors or by accelerated dynamics of axonal extension and retraction. The final obstacle to rejecting a role for synaptic activity in this system is that the molecular mechanism that mediates polarity specificity remains unknown. A likely possibility is that oppositely polarized hair cells express distinct membrane or secreted proteins that attract or repel afferent neurites bearing appropriate receptors. The difficulty in identifying these molecular polarity cues stems from the fact that oppositely oriented hair cells are

commingled within neuromasts and lack distinguishing morphological characteristics after isolation.

A hard-wired molecular polarity code

Why has the PLL evolved a hard-wired approach to distinguishing between oppositely polarized hair cells? Perhaps the sheer simplicity of the system lends itself to a molecular code. Each afferent neuron faces a simple binary choice in its selection of synaptic targets. Moreover, it is a choice that the neuron must continue to make throughout life as new hair cells are produced to replace dying ones. What this system foregoes in activity-dependent refinement and plasticity, it gains in reproducibility and speed.

A question that remains to be answered is whether dorsoventral and anteroposterior neuromasts use the same code to differentiate hair-cell polarities. Single afferents ordinarily do not innervate both dorsoventral and anteroposterior neuromasts , so in theory a single code would suffice. I suspect that posteriorly and ventrally polarized hair cells bear the same polarity identity, whereas anteriorly and dorsally polarized hair cells bear the opposite polarity identity. My logic for this inference is that each of these coteries of hair cells originates respectively more proximally or more distally with respect to the migration of the primordium that deposited the neuromast. For instance, both posteriorly and ventrally polarized hair cells arise on the sides of their respective neuromasts that were proximal to the direction of primordial migration. An interesting possibility is that the planar cell polarity of a neuromast depends upon the direction of primordial movement (Lopez-Schier et al., 2004; but see

Ghysen and Dambly-Chaudiere, 2007) and that the signals responsible for this feature serve to specify neuronal connectivity as well.

Peripheral mechanisms that ensure wiring specificity do not function alone, but rather act in concert with central components in generating somatotopy and organizing sensory and behavioral circuits. An important question arising from this work is whether the degree of predetermination that we have observed peripherally also extends to the central projections (Fritzsch et al., 2005). If afferent neurons utilize a molecular code to distinguish between hair-cell polarities, does this same code function in the hindbrain to organize polarity-specific sensory pathways (Fritzsch, 1981)? If so, how are afferents encoding anteriorly and posteriorly directed stimuli distinguished from those representing dorsally and ventrally directed stimuli? Another fascinating issue is how somatotopy relates to the polarity pathway. Afferent neuronal differentiation might involve the concerted specification of polarity and target-neuromast position through a multimodal molecular code. The use of hard-wired molecular mechanisms to ensure synaptic specificity in the periphery may provide the foundation upon which to build complex yet flexible circuits in the central nervous system.

Figure 4.1

Three models for polarity specificity

Three models might explain the ability of afferent neurons to distinguish between hair-cell polarities. *Top*: A posteriorly directed stimulus depolarizes posteriorly polarized hair cells while hyperpolarizing anteriorly polarized hair cells. Afferents might form synapses diffusely but, after detecting temporal differences in synaptic release from oppositely polarized hair cells, eliminate synapses with hair cells firing out of phase with the rest of their synaptic repertoire (dashed neuronal segment). *Middle*: Oppositely polarized hair cells express distinct complements of ion channels that produce distinct patterns of spontaneous synaptic release. In this example, hair cells of the two orientations release neurotransmitter at different frequencies, allowing neurites to distinguish them. *Bottom*: Hair cells express distinct membrane or secreted proteins that attract prepatterned afferents with intrinsic affinities for particular molecular markers. The afferents then detect hair-cell polarities independently of synaptic activity.

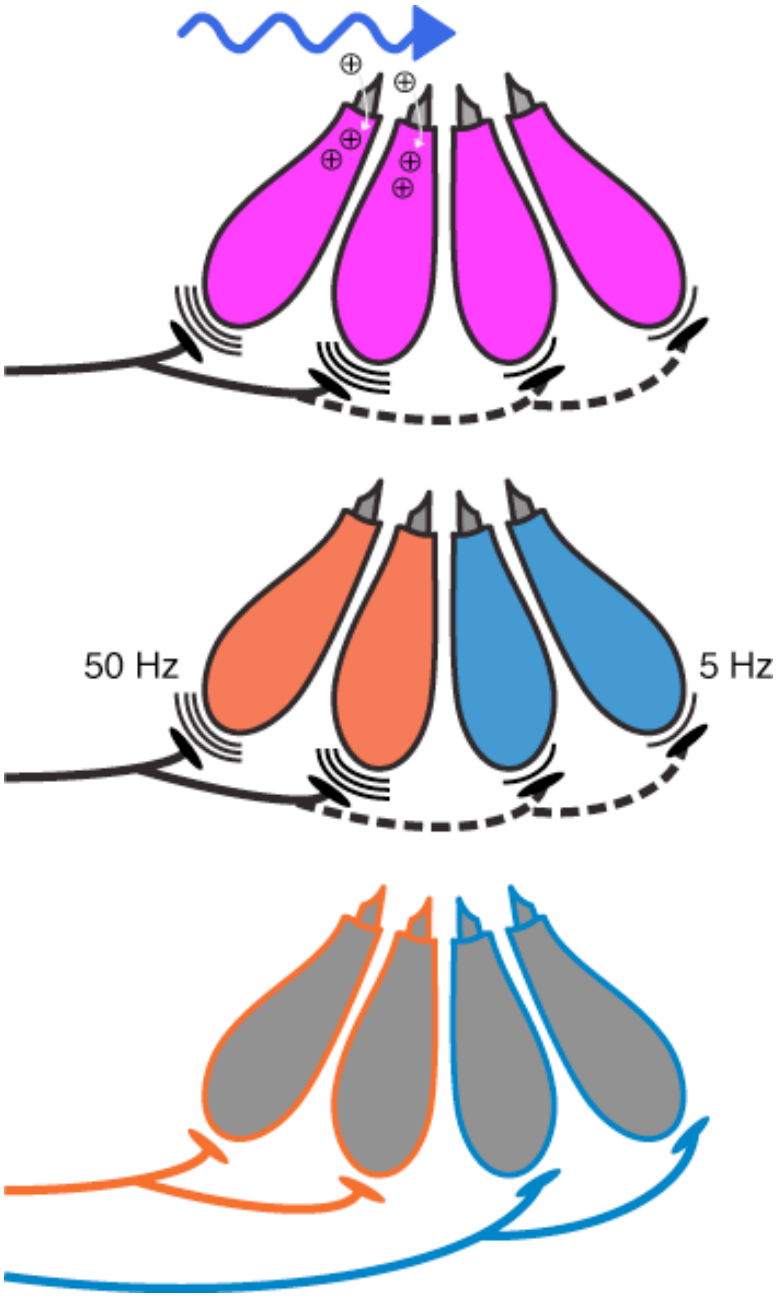
50 Hz
5 Hz

Figure 4.2

Stimulus-evoked patterns of synaptic release are not required for polarity choice

A-B, In an anteroposterior neuromast of a *tmie* mutant larva, a labeled afferent fiber synapses with five of the ten hair cells. ***C***, The hair-bundle polarities of this neuromast reveal that the neuron innervates all five posteriorly polarized hair cells and none of the opposite polarity. ***D-F***, In a dorsoventral neuromast of a *tmie* mutant, an afferent neuron innervates only the five ventrally polarized hair cells. ***G-I***, An afferent fiber in a *protocadherin 15a* mutant forms synapses with four of the five anteriorly polarized hair cells, but with none of the five cells of the opposite polarity.

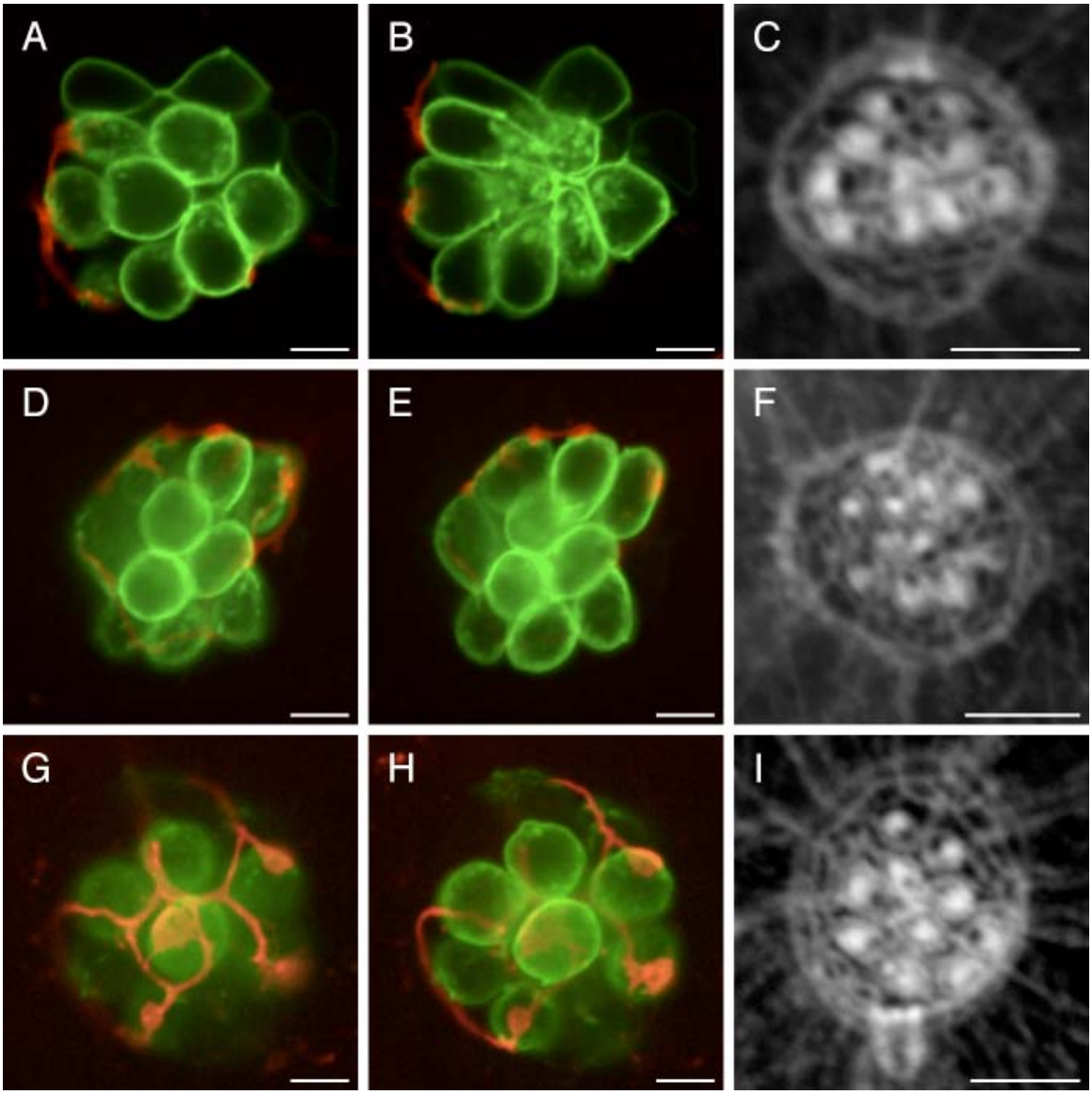
A
B
C
D
E
F
G
H
I

Figure 4.3

Synaptic transmission is dispensable for hair-cell polarity preference

A-C, In an anteroposteriorly oriented neuromast of a *cav1.3a* mutant lacking L-type voltage-gated Ca^{2+} channels, the three mature posteriorly polarized hair cells bear labeled afferent synapses whereas none of the opposite polarity do. ***D-F***, This *vglut3*-deficient neuromast contains six posteriorly polarized hair cells, all of which are innervated by the labeled afferent fiber.

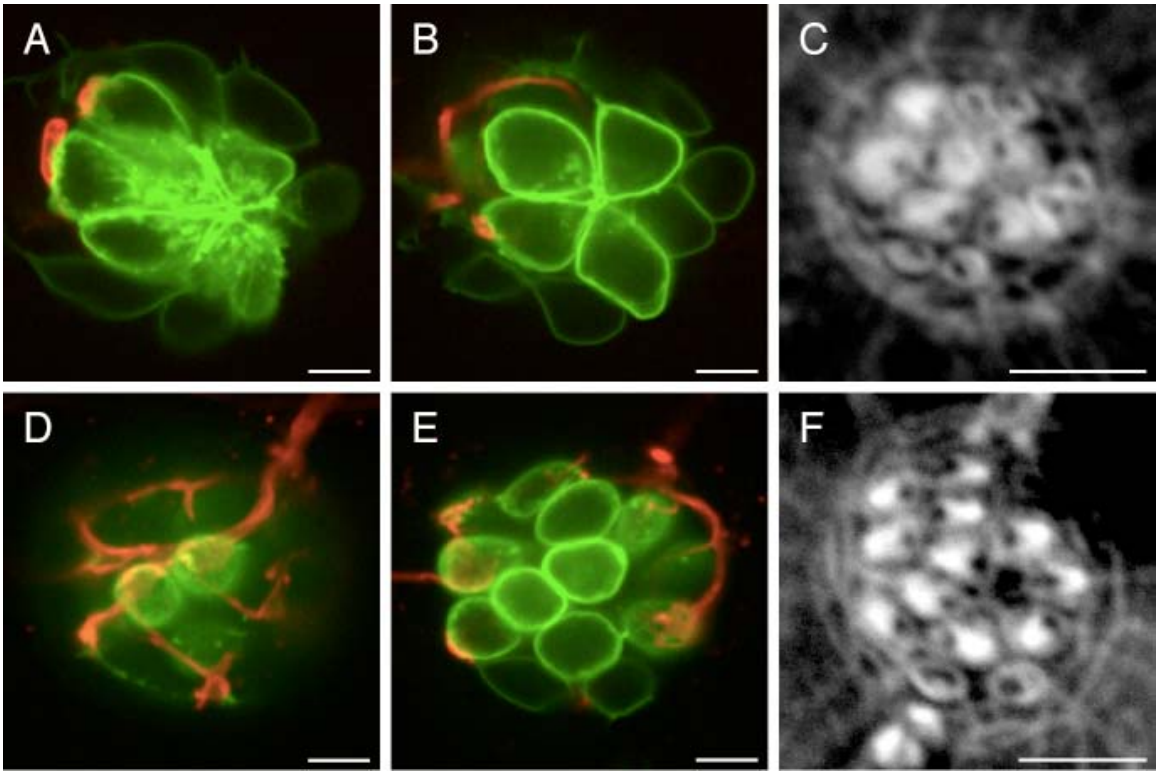
A
B
C
D
E
F

Figure 4.4

Polarity preference and synaptic maintenance

A, The parameter ω, which ranges from 0 to 1, represents the degree to which a neuron's choice of hair cells is biased toward one polarity; a value of 0.5 represents a lack of bias. The results have been expressed as the means and standard deviations of the probability distribution of $|\omega - 0.5| + 0.5$, so the ordinate reflects increasing bias. In practice, values of ω above about 0.95 represent near certainty: these populations of neurons make less than one error per three neuromasts innervated. ***B***, The mean fractions of the hair cells that were innervated by a labeled afferent fiber were similar for neuromasts of each genotype. The error bars represent standard errors of the means for the following numbers of observations: wild-type, $n=21$; *tmie*, $n=11$; *pcdh15a*, $n=19$; *cav1.3a*, $n=21$; *vglut3*, $n=15$.

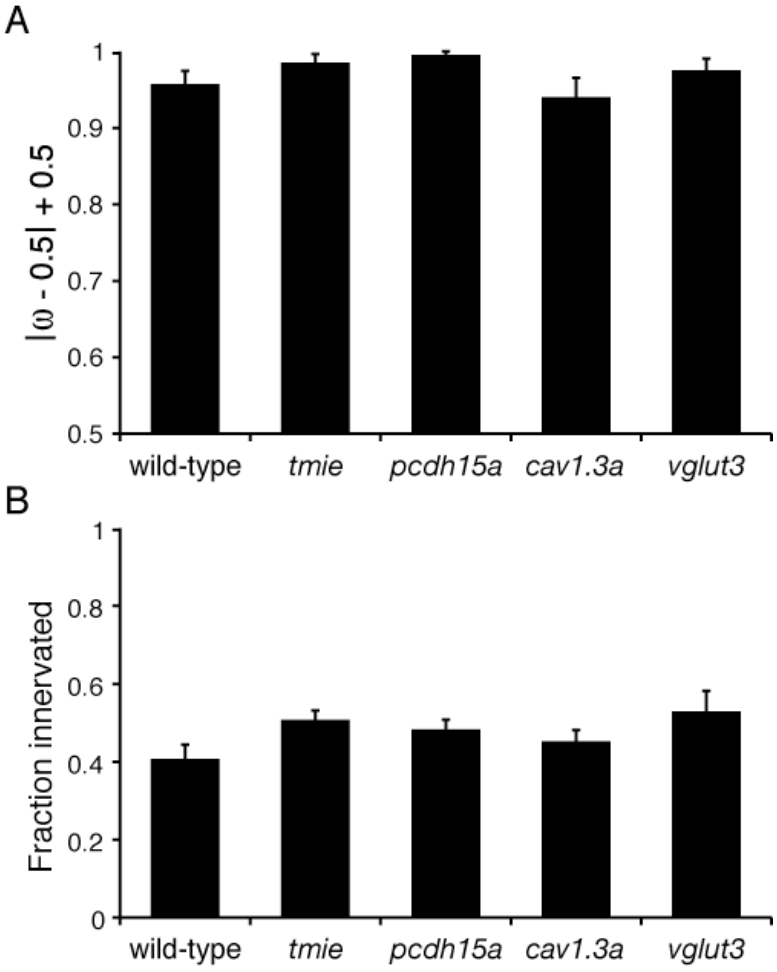
A
|ω - 0.5| + 0.5
1
0.9
0.8
0.7
0.6
0.5
wild-type
tmie
pcdh15a
cav1.3a
vglut3
B
Fraction innervated
1
0.8
0.6
0.4
0.2
0
wild-type
tmie
pcdh15a
cav1.3a
vglut3

CHAPTER FIVE

Conclusions and future directions

This work describes a novel experimental preparation for the study of synaptic target selection *in vivo*. The findings presented here represent an initial foray into the mechanism by which orientation-specific stimuli are transmitted to the brain via highly specific afferent synapses. Future work must expand on these studies to provide a molecular description of cell-polarity labels and a comprehensive reconstruction of central and peripheral connectivity in an entire PLL nerve.

A model for afferent neuronal wiring of PLL neuromasts

The previous two chapters have illustrated five salient features of this system. First, afferent neurons selectively innervate hair cells of a particular polarity from as early as 2.5 dpf. I did not observe a pattern of long-lasting non-specific synaptogenesis followed by the elimination of inappropriate contacts. Second, PLL neurons often innervate multiple consecutive neuromasts but in every case they are consistent in their polarity preference. Third, after hair-cell ablation and regeneration, afferent neurites reassume their biased innervation pattern. This bias is manifested as soon as newly minted hair-cell pairs appear. Fourth, afferent neurons do not instruct hair cells to assume a polarity. Rather, neurons interpret the polarity of the hair cells they contact. Fifth, afferents remain specific in their choice of synaptic targets even in the absence of hair-cell

mechanotransduction or synaptic transmission. This last finding bolsters the hypothesis that chemically labeled afferent neurons seek out molecular polarity labels on hair cells. Although many of the details remain sketchy, let us attempt to integrate these principal features into a functioning model. Although the emphasis will be on polarity specificity, this model will address all aspects of afferent neuronal development, including synaptic connectivity in the hindbrain, neuromast target selection, and synaptogenesis with hair cells.

The first action taken by a PLL afferent neuron appears to be the elaboration of a central axonal projection in the hindbrain, which occurs prior to neuromast innervation (Gompel et al., 2001a). Furthermore, the shape of the neuron's peripheral growth cone foreshadows the position of the neuromast that it will innervate. Although it is unknown whether the same central-before-peripheral patterning occurs with respect to polarity, there is no reason to believe it does not. Indeed, the behavior of afferent neurons in the periphery is indicative of a marked degree of intrinsic patterning. If peripheral cues do not determine central connectivity, then either the central arborization determines peripheral connectivity or the neurons bear chemical labels prior to innervating the hindbrain. In the former case, central axons compete for synaptic targets in the hindbrain. The contacts made there subsequently determine the neuron's preference for neuromast location and hair-cell polarity. In the latter case, nascent afferents are endowed with a particular cell-surface repertoire of chemical labels that guide their selection of central and peripheral targets. Either scenario fits with the results described in the work, but it is difficult to imagine how a presumably sloppy competition for hindbrain synapses could result so cleanly in specific polarity preferences. Regardless, it should be possible to

resolve this issue by ablating the hindbrain surgically or with a targeted laser beam prior to PLL afferent innervation and determining whether the peripheral projections remain specific.

While the afferents' central axons are forming contacts in the hindbrain, the peripheral growth cones trail behind the migrating primordium. As described in Chapter Three, single afferents innervate one or more neuromasts along the tail of the fish. In the case of multiple innervation, the neuromasts are spatially consecutive but they do not adhere to strict groupings; the fifth and sixth neuromasts, for example, are not obligatorily co-innervated. This is an interesting finding because it suggests that there is some flexibility in the somatotopic map. One possible explanation is that afferent neurons are predestined to innervate an ill-defined region along the tail, but once there, the axons compete for neuromasts. To test this hypothesis, one might transplant cells from early wild-type embryos into *neurogenin1* mutant embryos, which lack a PLL nerve. One could then select examples in which the PLL ganglion consists of a solitary wild-type afferent fiber and note the spatial extent of neuromast innervation. Given the high degree of prepatterning in this system, I would expect the fiber to confine its innervation to a small number of neuromasts, but it is certainly possible that this lone afferent would innervate the entire complement of neuromasts on one side of the fish. A much more basic question is how afferent neurons detect the presence of neuromasts in the first place. In my experience, I never observed a neuron sending branches into a neuromast-free area of the tail. A straightforward but unproven explanation is that neuromasts secrete a trophic signal locally onto the underlying axons, causing them to sprout neurites.

The final stage of afferent innervation consists of hair-cell synaptogenesis. The present report has described synaptic specificity with respect to hair-cell polarity, but leaves many questions unanswered. What type of molecular code is utilized by afferents and hair cells? Is it repulsive or attractive in nature? Does it involve membrane-bound or secreted proteins? Despite these towering uncertainties about the nature of the cue, it should nevertheless be possible to identify it. If a molecular polarity code exists, then hair cells of opposite polarity might well bear different transcriptional profiles. In the simplest case, hair-cell polarity A would exclusively harbor A mRNAs whereas hair-cell polarity B would harbor B mRNAs. In order to demonstrate as much, however, one must obtain pure populations of each hair-cell polarity, isolate the mRNA, and perform microarray analysis to identify differentially expressed transcripts. As mentioned in the previous chapter, obtaining pure populations of oppositely polarized hair cells is no easy task. It could be done, however, by flowing a fluorophore such as FM4-64 across the tail of the fish in a strictly unidirectional manner (e.g. posteriorly) such that hair cells of only one polarity take up the fluorophore through their transduction channels. Ideally, one could then flow a spectrally distinct fluorophore such as FM1-43 across the fish in the opposite direction (e.g. anteriorly). Following this, hair cells of each polarity will become positively labeled with distinct fluorophores that can be differentiated by a fluorescence-activated cell sorter (FACS). To ensure that only anteriorly and posteriorly polarized hair cells are included among those sorted, it would be necessary to dissociate only the terminal two-thirds of the tail into single cells. The discovery of differentially expressed transcripts, especially if they occur at low abundance, would presumably require large numbers of hair cells. In

addition, several follow-up experiments would be required to confirm the role of any differentially expressed proteins as polarity labels.

In summary, some of the most exciting questions about PLL connectivity remain unanswered. This work nevertheless establishes a solid foundation upon which to address these issues, two of which are described below.

Planar polarity signaling and asymmetric cell division

Perhaps the most intriguing issue emanating from this work is how tissue-wide planar polarity becomes rendered into hair-cell polarity labels decipherable by afferents. In the *Drosophila* wing, one of the best examples of planar polarity, a global polarity cue apparently causes protein complexes to become polarized at the apical cell membrane along the axis of planar polarity (Wu and Mlodzik, 2009). Importantly, the accumulation of polarized complexes requires cell-cell interactions, illustrating that individual cells do not simply interpret global cues cell-autonomously. These polarized signaling modules then effect the obvious manifestations of planar polarity, such as the orientation of wing hairs.

Now let us apply this same reasoning to a simple neuromast containing just two hair cells of opposite polarity along the anteroposterior axis. The posterior direction of primordium migration establishes a proximal-distal axis over which global planar polarity cues operate. Because hair cells never come in direct contact with each other, this polarity axis would be propagated through the following five cells:

supporting cell – **hair cell** – supporting cell – **hair cell** – supporting cell.

Because global polarity cues operate along a vector in the polarity axis, it is perhaps surprising that the two hair cells of a pair assume opposite hair-bundle polarities. The result suggests, however, that individual hair cells respond to the same polarity cues in different ways. This conclusion was also reached regarding the mammalian saccule and utricle, balance organs of the inner ear that bear two populations of oppositely polarized hair cells across a line of reversal. The study demonstrated that critical planar-polarity proteins accumulate asymmetrically but consistently throughout the epithelium, and the authors posit that additional regional cues specify how this uniform planar-polarity axis is differentially interpreted by individual hair cells (Deans et al., 2007). A key difference between the neuromast and the balance organs, however, lies in the mode of hair-cell generation. In the saccule and the utricle, new hair cells arise anywhere in the epithelium and assume a particular polarity depending on which side of the line of reversal they arise (Baird et al., 2000). In the neuromast, on the other hand, hair cells of opposite polarity arise from a single progenitor-cell division along the axis of planar polarity. The neuromast's line of reversal is simply a product of symmetric cell divisions across the same plane and often disappears as the hair cells become intermingled.

Rather than invoking a regional cue that interprets the uniform polarity patterning, it is possible in the neuromast that the progenitor cell itself contains planar-polarity proteins that are asymmetrically localized along the anterior-posterior axis. These proteins might then be partitioned asymmetrically to the two daughter cells, as occurs in mammalian neurogenesis (Zhong and Chia, 2008). If these protein complexes end up serving as cell-fate determinants, they could permit the daughter hair cells to undergo transcriptional changes that

result in the differential expression of molecular polarity labels interpretable by afferents. In addition, asymmetric partitioning of fate determinants could specify how the planar-polarity axis is interpreted during hair-bundle orientation. A potential objection to this line of reasoning, however, is that planar-polarity signaling typically operates at the apical surface of epithelial cells. Although it forms part of an epithelial structure, it remains unknown whether the progenitor cell is polarized in the apicobasal axis and whether it communicates directly with the apical surface exhibiting the planar polarity.

This discussion of how tissue-wide planar polarity signals become converted into a differentially expressed polarity label for afferent wiring certainly raises more questions than it answers. The model described above is replete with speculative assumptions, but perhaps it can serve as a framework to begin asking deeper questions that address the fascinating interplay between planar polarity and synaptic specificity.

In toto reconstruction of PLL nerve connectivity

Perhaps no other experiment could provide as much insight into the logic of PLL connectivity as the complete reconstruction of an entire PLL nerve, including its peripheral synapses on hair cells, cell bodies in the ganglion, and central synapses in the hindbrain. The results described herein were obtained by fluorescently labeling single afferent neurons, the advantages of which are clear. The major drawback to this approach is that we have no knowledge of the unlabeled fibers, and thus no concept of how the entire nerve transmits lateral-line stimuli in aggregate to the brain. In order to reconstruct the PLL nerve *in*

toto at single-cell resolution, I propose applying the Brainbow multi-color cell-labeling system (Livet et al., 2007). This system consists of a tissue-specific promoter driving a series of three or more distinct fluorescent proteins. Each fluorescent protein is followed by a stop codon such that in the initial state only the first fluorescent protein is expressed. However, the protein-coding sequences contain intervening lox sites which allow for Cre-mediated excision of randomly chosen fluorescent-protein sequences. By expressing Cre in *trans* using a heat-shock inducible promoter, it is possible to produce a colorful mosaic in the tissue of interest; multiple transgenic insertions of Brainbow create an even broader color palette.

Because its expression is restricted to cranial sensory ganglia, the *neuroD* promoter is ideal for driving expression of fluorescent proteins in PLL afferents. As far as is known, there is no expression in the central nervous system, thus permitting clean imaging that is unpolluted from out-of-focus fluorescence from the spinal cord and brain. With a broad enough color palette it should be possible to distinctly label each of the 20 or so afferent neurons in the PLL nerve (Metcalfe et al., 1985) and to trace their cellular contacts from hair cell to hindbrain. This would simultaneously reveal the receptive field structures of all the afferent neurons and the level of redundancy in hair-cell innervation. The axons could be traced back to the ganglion in order to look for a somatotopic organization of the cell bodies. Finally, the synaptic repertoire of the central projections could be examined in the context of their known peripheral connectivity. The labeling of the entire nerve allows for a detailed examination of the relative spatial positions of the central axons. This analysis is much harder

to perform when only single afferents are labeled, for spatial relationships must be inferred by comparing individuals.

In sum, the Brainbow experiment has great potential to illuminate the logic of sensory transmission in this vertebrate model and eventually permit a reexamination of the PLL from a systems neuroscience viewpoint. For example, one might represent afferent neuronal connectivity as a matrix that transforms patterns of hair-cell synaptic release into a different pattern that is decipherable by secondary sensory neurons in the hindbrain. When the appropriate promoters become available, it should also be possible to apply the Brainbow technology to secondary sensory neurons and beyond. Only by delineating the neural pathways involved in lateral-line perception can we begin to understand how this sensory system decomposes environmental stimuli in the periphery and then recapitulates the richness of sensory information in the brain.

APPENDIX ONE

Specificity of afferent synapses onto plane-polarized hair cells in the posterior lateral line of the zebrafish

Nagiel A, Andor-Ardo D, and Hudspeth AJ

J. Neurosci. **28:8442-8453 (2008)**

Development/Plasticity/Repair

Specificity of Afferent Synapses onto Plane-Polarized Hair Cells in the Posterior Lateral Line of the Zebrafish

Aaron Nagiel, Daniel Andor-Ardó, and A. J. Hudspeth
Howard Hughes Medical Institute and Laboratory of Sensory Neuroscience, The Rockefeller University, New York, New York 10065-6399

The proper wiring of the vertebrate brain represents an extraordinary developmental challenge, requiring billions of neurons to select their appropriate synaptic targets. In view of this complexity, simple vertebrate systems provide necessary models for understanding how synaptic specificity arises. The posterior lateral-line organ of larval zebrafish consists of polarized hair cells organized in discrete clusters known as neuromasts. Here we show that each afferent neuron of the posterior lateral line establishes specific contacts with hair cells of the same hair-bundle polarity. We quantify this specificity by modeling the neuron as a biased selector of hair-cell polarity and find evidence for bias from as early as 2.5 d after fertilization. More than half of the neurons form contacts on multiple neuromasts, but the innervated organs are spatially consecutive and the polarity preference is consistent. Using a novel reagent for correlative electron microscopy, HRP-mCherry, we show that these contacts are indeed afferent synapses bearing vesicle-loaded synaptic ribbons. Moreover, afferent neurons reassume their biased innervation pattern after hair-cell ablation and regeneration. By documenting specificity in the pattern of neuronal connectivity during development and in the context of organ regeneration, these results establish the posterior lateral-line organ as a vertebrate system for the *in vivo* study of synaptic target selection.

Key words: **acousticolateralis system; eighth nerve; fluorescent protein; hair cell; planar cell polarity; ribbon synapse**

Introduction

Our perception of environmental stimuli depends critically on the ability of developing neuronal processes to obey guidance cues, recognize appropriate targets, and synapse with particular cells (Goodman and Shatz, 1993; Benson et al., 2001). Although much progress has been made in understanding the first two steps (Dickson, 2002), how neurons decide to form stable synapses with particular target cells remains unclear.

The lateral-line organ of larval zebrafish possesses a number of qualities that facilitate the study of this question. Lateral lines enable certain aquatic vertebrates to sense water currents and thus aid in prey capture, predator avoidance, rheotaxis, and shoaling (Montgomery et al., 1997). The functional unit of the lateral line is the neuromast, which consists of superficial hair cells ensheathed by supporting cells, surrounded by mantle cells, and innervated by afferent and efferent neurons (Metcalfe et al., 1985). The cell responsible for the detection of mechanical stimuli is the hair cell, which bears on its apical surface a hair bundle that transduces mechanical deflections into electrical signals (Hudspeth, 1989). The hair bundle comprises a staircase-like arrangement of actin-filled stereocilia and a true cilium, the kinocilium, which stands at the tall edge (see Fig. 1*C*). Hair-bundle deflections toward the kinocilium depolarize the hair cell, whereas movements in the opposite direction hyperpolarize it (Shotwell et al., 1981). Membrane depolarizations trigger the release of neurotransmitter from the cell's base at presynaptic specializations known as synaptic ribbons (Keen and Hudspeth, 2006).

A striking feature of the lateral line is the planar polarization of hair cells within a neuromast (Flock and Wersäll, 1962), which is manifested in two ways. The first is the aforementioned hair-bundle polarity, which defines the vector of mechanosensitivity and is intrinsic to each hair cell. The second manifestation of polarity, which is governed by the planar-cell-polarity pathway, arises from the coordinated orientation of polarized hair bundles with respect to the bodily axes (López-Schier et al., 2004). The bilaterally symmetrical lateral-line system of a larval zebrafish has two components, each containing approximately 10 neuromasts: an anterior lateral line covering the head and a posterior lateral line (PLL) along the trunk and tail (Metcalfe et al., 1985). Each neuromast contains two sets of hair cells of opposite hair-bundle polarities disposed across a plane of mirror symmetry (López-Schier and Hudspeth, 2006). In the PLL, most neuromasts contain anteriorly polarized hair cells and posteriorly polarized hair cells, whereas a few specific neuromasts contain dorsally polarized and ventrally polarized hair cells (see Fig. 1*A*).

Although the polarization of hair cells in the PLL has been well characterized, it remains unclear how afferent neurons transmit

Received May 29, 2008; revised July 10, 2008; accepted July 11, 2008.

This work was supported by National Institutes of Health Grants DC00241 and DC07294 and Medical Scientist Training Program Grant GM07739. A.N. is the recipient of Ruth L. Kirschstein National Research Service Award Predoctoral Fellowship NS62486. A.J.H. is an Investigator of Howard Hughes Medical Institute. We thank A. Afolalu for expert fish husbandry, Dr. P. Brehm for the *6let1:GFP* fish, Dr. A. Chitnis for the *HoC:GFP* fish, Dr. H. Baier for the *Brn3c:gap43-GFP* fish, the Zebrafish International Resource Center for the *neurogenin1* mutant fish, Dr. S.-I. Higashijima for the *HoC:GFP* cDNA, Dr. P. Ortiz de Montellano for the *HRP-C* cDNA, Dr. A. North for assistance with the spinning-disk microscope, and Drs. E. Fuchs and A. Pasolli for access to the transmission electron microscope. Dr. E. Gonzalez, J. A. Robbins, Dr. M. Schober, and the members of our research group provided helpful comments on this manuscript.

Correspondence should be addressed to Dr. A. J. Hudspeth, Howard Hughes Medical Institute and Laboratory of Sensory Neuroscience, The Rockefeller University, Campus Box 314, 1230 York Avenue, New York, NY 10065-6399. E-mail: hudspaj@rockefeller.edu.

DOI:10.1523/JNEUROSCI.2425-08.2008

Copyright © 2008 Society for Neuroscience 0270-6474/08/288442-12$15.00/0

information about stimulus orientation to the brain. Electrophysiological evidence suggests that afferent neurons receive inputs from hair cells of the same polarity (Obholzer et al., 2008), but the degree of specificity has not been demonstrated at the level of single synapses. In this study, we investigated whether afferent neurons distinguish hair-cell polarities as they innervate lateral-line neuromasts during normal development and after regeneration.

Materials and Methods

Zebrafish strains and husbandry. Zebrafish were maintained under standard conditions. Naturally spawned eggs were collected, cleaned, staged (Kimmel et al., 1995), and maintained in system water at 28.5°C at a density of 50 per 100-mm-diameter Petri dish. Embryos were raised in system water with the addition of 200 μM 1-phenyl-2-thiourea at 1 d postfertilization (dpf) to inhibit pigment formation. The wild-type strain used was *Tübingen Long Fin*. The relevant transgenic strains and their respective transgenic insertions included the following: *HuC:GFP*, *Tg(elavl3:EGFP)*^{nf8}; *islet1:GFP*, *Tg(isl1:GFP)*^{rw01}; *ET4*, *Et(krt4:GFP)*^{sqet4}; *Brn3c:gap43-GFP*, *Tg(Brn3c:gap43-mGFP)*^{s356t}; and *neurogenin1*, *ngn1*^{hi1059Tg}.

Plasmid DNA construction. To create *HuC:mCherry*, *HuC:GFP* DNA (Park et al., 2000) was digested with *Xho*I and *Xba*I to remove the green fluorescent protein (GFP)-polyA sequence. The *HuC* promoter-containing backbone was then gel purified and ligated to an mCherry-polyA fragment that had been PCR-amplified (forward, 5′-TGCTCGAGTGCCACCATGGTGAGCAAGGGCGAGG-3′; reverse, 5′-GTCATTCTAGAGTCGCTTACAATTTACGCCTTAAG-3′). To create *HuC:gap43-mCherry*, the *HuC:mCherry* plasmid was digested with *Xho*I and ligated to annealed oligonucleotides containing a Kozak sequence and the first 20 codons of the *gap43* cDNA (forward, 5′-TCGACTGCCACCATGCTGTGCTGCATCAGAAGAACTAAACCGGTTGAGAAGAATGAAGAGGCCGATCAGGAG-3′; reverse, 5′-TCGACTCCTGATCGGGCCTCTTCATTCTTCTCAACGGGTTTAGTTCTTCTGATGCAGCACAGCATGGTGGCAG-3′). To create the *HuC:HRP-mCherry* plasmid, the *Not*I site of *HuC-mCherry* was destroyed by blunt-end ligation, and the *Xho*I site was changed to a *Not*I-*Age*I site with annealed oligonucleotides. The *HRP-C* cDNA was PCR-amplified with a forward primer containing a 5′ *Eco*RI site and a reverse primer containing a 5′ *Bam*HI site (forward, 5′-CTGAATTCATGCAGTTAACCCCTACATTC-3′; reverse, 5′-GAGGATCCAGAGTTGCTGTTGACCACTCTGC-3′). This amplified segment of DNA was ligated into pBluescript SK+, which was subsequently digested with *Bam*HI and *Not*I. Synthesized, annealed, 5′-phosphorylated oligonucleotides encoding the transmembrane region of cadherin2 (Cdh2) followed by an *Age*I site (forward, 5′-GATCCGCAGCCGGGCTGGGCACCGGAGCCATCATCGCCATACTTATCTGCATCATCATTCTGCTGGTGCTGGTGTTGATGTTTGTGATGTGGATGAAGAGACGGGATAAAGAGAGACAGACCGGTGC-3′; reverse, 5′-GGCCGCACCGGTCTGTCTCTCTTTATCCCGTCTCTTCATCCACATCACAAACATCAACACCAGCACCAGCAGAATGATGATGCAGATAAGTATGGCGATGATGGCTCCGGTGCCCAGCCCGGCTGCG-3′) were ligated into the *Bam*HI/*Not*I-digested Bluescript plasmid. This plasmid was subsequently digested with *Hin*dIII and *Eco*RI and ligated to annealed, 5′-phosphorylated oligonucleotides comprising the signal sequence of *cdh2* with a *Not*I site and Kozak sequence upstream (forward, 5′-AGCTTGCGGCCGCCACCATGTACCCCTCCGGAGGCGTGATGCTGGGGCTTCTCGCCGCTCTGCAGGTGGCGGTCCAGGGCACAGGGGCGG-3′; reverse, 5′-AATTCCGCCGCCTGTGCCCTGGACCGCCACCTGCAGAGCGGCGAGAAGCCCCAGCATCACGCCTCCGGAGGGGTACATGGTGGCGGCCGCA-3′). Finally, this plasmid was digested with *Not*I and *Age*I, liberating the signal sequence-horseradish peroxidase (HRP)-transmembrane domain construct, and ligated into the *Not*I-*Age*I sites created on the *HuC:mCherry* plasmid.

DNA injection and screening of transgenic fish. One- and two-cell embryos were pressure injected with supercoiled plasmid DNA at a concentration of 50 ng/μl. Animals were screened at 1.5–2 dpf for mCherry expression in the PLL nerve with a Zeiss Axioplan 2 wide-field fluorescence microscope. After selection of candidate fish with a 5× objective, definitive expression in the PLL nerve was ascertained using a 60× water-immersion objective.

Vital labeling of hair cells. Larvae were immersed in a 200 μM solution of 4-(4-(diethylamino)styryl)-*N*-methylpyridinium iodide (4-Di-2-ASP; Invitrogen) or in a 100 μM solution of *N*-(3-triethylammoniumpropyl)-4-(6-(4-(diethylamino)phenyl)hexatrienyl)pyridinium dibromide (FM4-64; Invitrogen) for 2 min at room temperature in the dark.

Live imaging of larvae. For imaging of 4-Di-2-ASP labeling, larvae were anesthetized in 625 μM 3-aminobenzoic acid ethyl ester methanesulfonate and imaged with a Zeiss Axioplan2 microscope using a 5× objective lens and a CCD camera (Olympus). For confocal imaging, specimens were embedded under anesthesia in 1% low-melting-point agarose on a glass coverslip. Images were acquired with an Ultramer Perkin-Elmer spinning-disk system on a Zeiss Axiovert 200M microscope equipped with a 63×, 1.4 numerical aperture (NA) PlanApochromat objective, a Hamamatsu Orca-ER cooled CCD camera, and MetaMorph software for acquisition and analysis (MDS Analytical Technologies). *Z*-stacks were acquired at 1 μm intervals, imaging GFP (488 nm excitation, 500–550 nm emission) and mCherry or FM4-64 (568 nm excitation, 590–650 nm emission). After imaging, the larvae were excised from the agarose and returned to individually marked dishes.

Hair-cell ablation. Three-day-old larvae were treated for 1 h with 10 μM $CuSO_4$ (Sigma) in system water, rinsed, and then returned to system water. The time course of recovery began when fish were removed from the $CuSO_4$ solution.

Immunofluorescence and phalloidin staining and imaging. Fish were fixed overnight at 4°C in PBS containing 1% Tween 20 (PBST) and 4% paraformaldehyde. Larvae were washed thrice in 1% PBST for 1 h and then incubated in primary antibody or in fluorescent phalloidin. For whole-mount immunofluorescence labeling, fish were immersed overnight at 4°C in a 1:1000 dilution of mouse anti-acetylated α-tubulin primary antibody (clone 6–11B-1; Sigma), washed several times in 0.2% PBST, and then incubated in a 1:200 dilution of Alexa Fluor 488-conjugated secondary antibody (Invitrogen) overnight at 4°C. The fish were washed twice for 4 h and stained with a 1:20 dilution of Alexa Fluor 568 phalloidin (Invitrogen) in 0.2% PBST overnight at 4°C. They were next washed twice for 4 h and mounted in Vectashield (Vector Laboratories). Samples were imaged on an Olympus FV1000 laser-scanning confocal microscope with a 60×, 1.42 NA PlanApochromat objective lens at a scan rate of 8 μs per pixel with Kalman averaging.

Transmission electron microscopy. Larvae were fixed at 4°C overnight in 400 mM formaldehyde, 200 mM glutaraldehyde, 20 mM sucrose, 1 mM $CaCl_2$, and 90 mM sodium cacodylate at pH 7.2. The specimens were then washed in the same solution lacking the fixatives. *HuC:HRP-mCherry*-expressing fish were exposed to wash solution containing 1.4 mM 3,3-diaminobenzidine (Electron Microscopy Sciences) and 1% DMSO for 5 min at room temperature, followed by the addition of 0.0042% H_2O_2 for 5 min. After a series of washes, specimens were postfixed in 50 mM OsO_4, 20 mM sucrose, 1 mM $CaCl_2$, and 90 mM sodium cacodylate at pH 7.2 for 1.5 h at 4°C. Several washes in distilled water were followed by dehydration through a series of ethanol concentrations to 95% ethanol.

Additional electron density was conferred by treatment with 0.4% uranyl acetate in 95% ethanol for 1 h at room temperature. The tissue was dehydrated by immersion for 2 h each in 100% ethanol and propylene oxide. Each specimen was impregnated with an epoxy-resin mixture (Embed-812; Electron Microscopy Sciences), placed between two nonsticking plastic coverslips (Unbreakable Cover Slips; Thermo Fisher Scientific), and heated under vacuum for 48 h at 50°C to cure the plastic.

Specimens were sectioned at a thickness of 70 nm with a diamond knife (Ultra 45°; Diatome) on an ultramicrotome (Ultracut-E; Leica). Serial sections were collected on formvar- and carbon-coated grids (Electron Microscopy Sciences) and stained for 2 min with 50% saturated aqueous uranyl acetate in 50% acetone and for 1.5 min with lead citrate. Micrographs were acquired with a transmission electron microscope (G2–12 Biotwin; Tecnai FEI) equipped with a CCD camera (Hamamatsu).

Image processing. Images were analyzed and adjusted for brightness and contrast with ImageJ (NIH). For the mosaic illustration in Figure

1*D*, individual images were merged using Adobe Photoshop. Figures were assembled with Adobe Illustrator.

Statistical analysis. To analyze innervation bias, we scored hair cells for membrane contact with labeled neurons. When possible, hair-cell polarity was inferred at 2.5 and 3.5 dpf from the arrangement of hair cells; at 4.5 and 5.5 dpf, hair-cell polarity was ascertained definitively by fluorescent-phalloidin staining. Neuromasts innervated by more than one labeled fiber were excluded from the analysis. We calculated the weight of evidence in favor of a statistical model in which neurons are biased in their innervation of hair cells. When reported in decibans, which are analogous to decibels in acoustics, $W = 10 \times \log_{10}[P(\text{data}|M_B)/P(\text{data}|M_U)]$. The ratio $P(\text{data}|M_B)/P(\text{data}|M_U)$ is the Bayes factor, which indicates the support of the data for the hypothesis in which the neuron is biased, M_B, versus unbiased, M_U. $P(\text{data}|M)$ is the marginal likelihood, or evidence, for hypothesis M. To model the data from such a biased neuron, we chose Fisher's noncentral hypergeometric distribution, with the probability of selecting one orientation of hair cell over another given by the parameter ω in the range 0–1. For the calculation of W, we marginalized over ω, that is, integrated over all possible values. We used a vague prior distributed as beta(1, 1) that is uniform and therefore convenient for computation (Fog, 2008). When we used more typically noninformative priors, such as the proper beta(1/2, 1/2), W grew by 10–20%; the persuasiveness of the result increased. We repeated our calculations using Wallenius's noncentral distribution, but the change in results was barely noticeable, and the qualitative answers were in agreement. The unbiased model (M_U) is a special case of both these biased models for $\omega = 0.5$. In this instance, no marginalization is necessary. Because we believe that it corresponds more closely to a physiological model of neuronal activity, we report the results from Fisher's distribution.

Results

Afferent and efferent innervation of lateral-line hair cells

By 5 dpf, the PLL on each side of a larval zebrafish comprises about 10 neuromasts innervated by both afferent and efferent neurons (Fig. 1*A–D*) (for review, see Dambly-Chaudière et al., 2003). Because we wished to analyze the afferent innervation in particular, we first characterized the morphology of efferent neurons so that we could reliably distinguish afferents from efferents. We examined efferent neurons labeled with GFP under the control of the *islet1* promoter (Higashijima et al., 2000) and then stained hair cells at 3 dpf with the fluorophore FM4-64 that enters them selectively through their mechanotransduction channels. The efferent axons appeared thin and featured bulbous terminals (Fig. 1*E*,*F*).

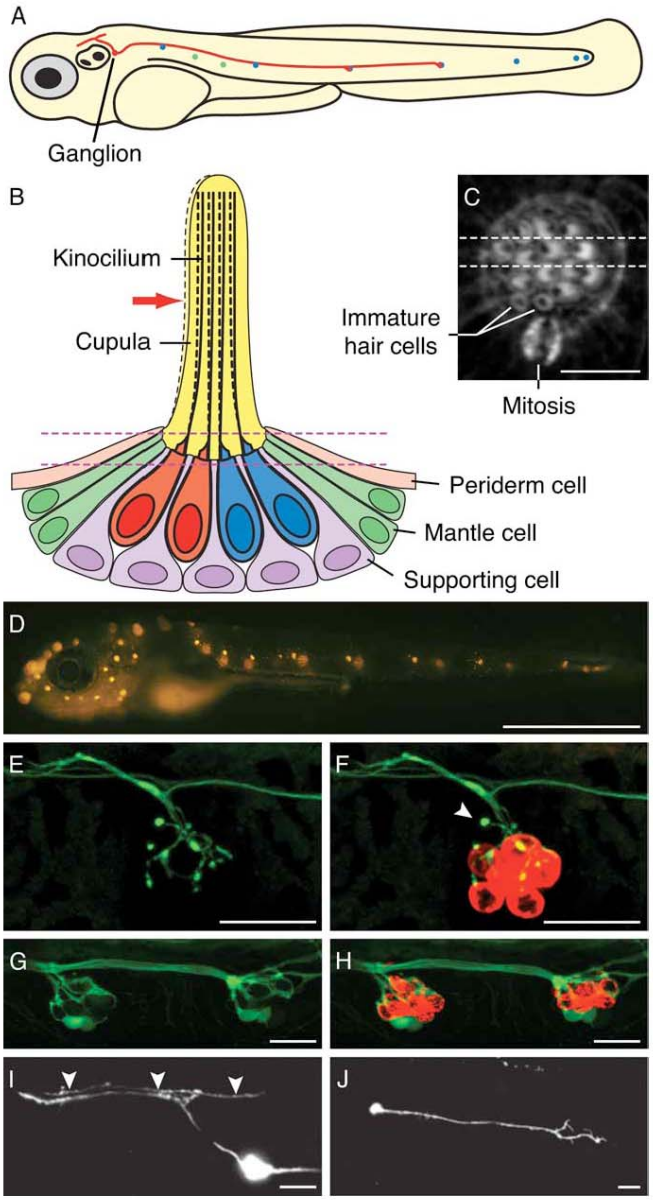

Figure 1. Structure and innervation of the lateral-line organ of a larval zebrafish. ***A***, A schematic diagram of a zebrafish larva at 4 dpf depicts seven anteroposterior neuromasts (blue) and two dorsoventral neuromasts (green) of the PLL. Additional neuromasts, which are not shown, adorn the animal's head. The soma of a single afferent neuron (red) lies in the PLL ganglion immediately caudal to the developing ear. In this example, its peripheral axon runs in the PLL nerve and contacts hair cells in two neuromasts. The central axon bifurcates and synapses in the nascent octavolateralis nucleus along the length of the hindbrain. The diameters of the neuromasts, neuronal soma, and axons are exaggerated. ***B***, Four hair cells occur at the center of a schematic depiction of a section through a single anteroposterior neuromast. Displacement of the gelatinous cupula by a hydraulic stimulus, in this instance directed toward the animal's posterior (red arrow), deflects the long kinocilia of the hair cells. (*Figure legend continues.*)

To visualize afferent neurons, we examined the most caudal neuromasts of *HuC:GFP* transgenic zebrafish, which express GFP in all neurons early in development (Park et al., 2000). By studying these terminal neuromasts before 2 dpf, we could restrict our analysis to afferents because efferent neurons do not reach this location until several hours later (Sapède et al., 2005). We found that the afferent fibers beneath each neuromast formed a dense, interlacing web that impeded the identification of fibers and of individual contacts (Fig. 1*G*,*H*).

Our inability to resolve individual afferents in a stable transgenic line necessitated the labeling of single PLL neurons by transient-expression methods, in which an arbitrary subset of neurons expressed a fluorescent protein. We injected wild-type embryos with the *HuC:GFP* plasmid and screened for larvae expressing GFP in the PLL nerve. Whereas lateral-line efferents have cell bodies in diencephalic and rhombencephalic nuclei (Metcalfe et al., 1985; Bricaud et al., 2001), GFP-labeled afferents possess somata in the PLL ganglion and send bifurcated axons into the hindbrain (Fig. 1*I*). At 1.5 dpf, the neurons also feature migratory growth cones destined to innervate a subset of PLL neuromasts (Fig. 1*J*).

Afferent and efferent PLL neurons therefore display clear morphological differences that are discernable not only by the anatomical location of cellular structures but also by their distinct contacts with hair cells. Our preliminary results also validated a technique for the labeling of single PLL afferents that requires neither surgical manipulation nor dye application.

Long-term monitoring of afferent innervation

Each PLL neuromast contains two equal populations of hair cells with their hair bundles polarized in opposite directions (López-Schier and Hudspeth, 2006). The orientation of these hair bundles is tightly linked to the larval bodily axes, such that the hair cells in certain neuromasts are directionally sensitive to anteriorly or posteriorly directed stimuli, whereas the hair cells in other neuromasts respond to dorsally or ventrally directed stimuli. We hypothesized that afferent fibers form stable synapses with hair cells of only one orientation, for such an arrangement would permit the encoding of four directions of mechanical stimulation at the first synapse of this sensory system. To test this hypothesis, we simultaneously visualized hair cells and the associated afferents *in vivo* by injecting the *HuC:mCherry* expression plasmid into embryos of the strain ET4, an enhancer-trap line in which hair cells express GFP (Parinov et al., 2004).

During early larval development or hair-cell regeneration, the highly stereotyped division of a hair-cell progenitor reliably produces a pair of hair cells of opposite polarity (López-Schier and Hudspeth, 2006). When a neuromast displays mirror symmetry, it is possible to infer each hair cell's polarity based solely on its location and relationship to the other hair cells. Taking advantage of this regular pattern, we found that a single afferent neuron preferentially contacts hair cells of only one orientation. As early as 2.5 dpf, in a neuromast containing two mature hair cells, a labeled afferent fiber displayed a prominent bouton on the posteriorly polarized hair cell and a more limited contact onto the anteriorly polarized hair cell (Fig. 2*A*,*B*). One day later, the same neuromast had grown to encompass three pairs of hair cells. The three posteriorly polarized hair cells received voluminous contacts from the labeled fiber, whereas the anteriorly polarized hair cells lay near finer neurites that lacked this robust morphology (Fig. 2*C–E*). By 4.5 dpf, when the neuromast had grown to six hair-cell pairs, the labeled neuron innervated a commensurately greater number of hair cells (Fig. 2*F–J*). By this stage of development, the neuromast displayed a more complex arrangement of hair cells that no longer conformed to a plane of symmetry. To confirm the polarity of the hair cells, we fixed the fish after live imaging and labeled the actin-rich hair bundles with fluorescent phalloidin (Fig. 2*K*). With the consequent polarity information, we referred to the images of the living neuromast at 4.5 dpf and determined that the three largest and oldest posteriorly polarized hair cells received bulky contacts (Fig. 2*G*,*H*). A young posteriorly polarized hair cell (Fig. 2*I*) and an anteriorly polarized hair cell (Fig. 2*J*) instead attracted only tenuous neurites.

These *in vivo* imaging studies suggest that each lateral-line afferent neuron forms prominent contacts selectively with hair cells of a single orientation. Furthermore, our time-lapse imaging approach revealed that afferent neurons respond continually to polarity cues as new hair cells are added to growing neuromasts.

Statistical analysis of innervation bias by afferent neurons

Although PLL afferents display a high degree of specificity in their choice of targets, they occasionally form contacts on hair cells of the opposite polarity (Fig. 2*J*). This finding suggested that the neurons have an inherent error rate in their choice of targets or that they can be caught in the act of interrogating a hair cell's polarity.

To provide a rigorous quantitative measure of the preference for hair-cell polarity, we devised a statistical model of bias. For each neuromast, the number of hair cells of each polarity was noted along with the number innervated by a single labeled afferent fiber (supplemental Table 1, available at www.jneurosci.org as supplemental material). Our null hypothesis was that each neuron was strictly unbiased, with no ability to discriminate between polarities of hair cells. Because there were only a handful of cells per neuromast, the deviations from the null hypothesis tended not to be statistically significant. Although we considered aggregating multiple p values based on the null hypothesis alone, this procedure is of controversial validity (Goodman, 1998). We therefore addressed the issue more directly by comparing the

←

(*Figure legend continued.*) When communicated to the stereocilia of the hair bundles, this movement depolarizes the posteriorly polarized hair cells (red) and hyperpolarizes the anteriorly polarized cells (blue). Supporting cells separate the hair cells; mantle cells outline the neuromast and contact the periderm cells of the larva's integument. The neuromast's innervation is not shown. The parallel dashed lines depict the plane of the parasagittal optical section shown in the following panel. ***C***, A light micrograph of a neuromast's apical surface reveals the staining of filamentous actin by fluorescent phalloidin. The 20–30 stereocilia in each hair bundle form a crescent in whose concavity stands the unlabeled kinocilium. The dashed lines delineate the horizontal plane of section depicted in the preceding panel. A mitosis at the boundary between the mantle cells and supporting cells probably represents the division of an amplifying progenitor to form a mirror-symmetrical pair of hair cells. The two hair cells produced by an earlier mitosis remain immature: their hair bundles have yet to exhibit the polarization characteristic of mature hair cells. In this and all subsequent light micrographs, the animal's anterior is located to the left, and its dorsum is oriented upward. ***D***, Labeling of hair cells in a living 6 dpf larva with 4-Di-2-ASP reveals 11 neuromasts in the PLL on the animal's left side. The neuromasts on the right side of the transparent larva appear out of focus. ***E***, Efferent synaptic endings occur in a PLL neuromast in a living *islet1:GFP* fish at 3 dpf. ***F***, Dual labeling with FM4-64 (red) demonstrates that one immature hair cell of this neuromast failed to take up the dye but was nevertheless innervated (arrowhead). ***G***, GFP expression in the PLL nerve of a live *HuC:GFP* larva at 2 dpf documents the afferent innervation of two neighboring neuromasts. ***H***, Labeling of the same specimen with FM4-64 reveals the hair cells (red). ***I***, The expression of *HuC:GFP* in a single PLL afferent neuron reveals its soma in the PLL ganglion and its bifurcated axon reaching the hindbrain. An ascending fiber from the spinal cord is labeled as well (arrowheads). ***J***, The peripheral projection of this neuron at 1.5 dpf features an actively migrating growth cone. ***D*** is a mosaic of several images; ***E–J*** are maximal-intensity projections of confocal *Z*-stacks. Scale bars: ***C***, 5 μm; ***D***, 1 mm; ***E–J***, 20 μm.

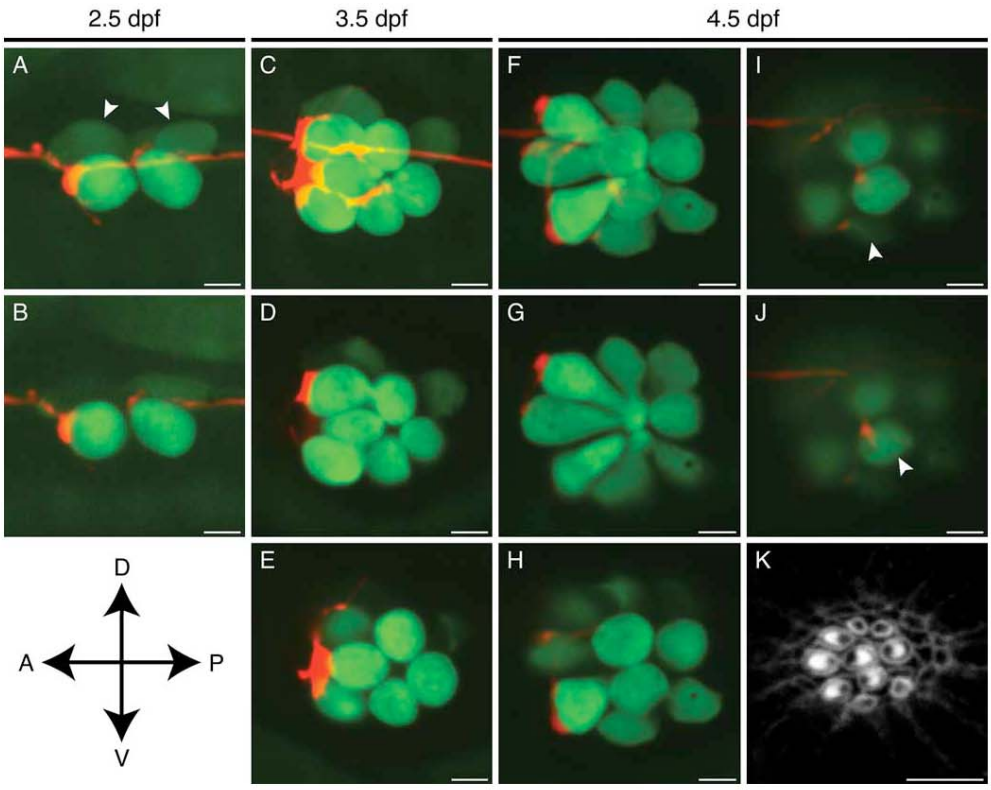

Figure 2. *In vivo* imaging of afferent synaptogenesis in a developing neuromast. ***A***, In a maximal-intensity projection of a *Z*-stack of an anteroposterior neuromast at 2.5 dpf, an mCherry-labeled afferent fiber (red) forms a putative synapse with the rostralmost of the hair cells expressing GFP (green). Two immature hair cells are only dimly labeled with GFP (arrowheads). ***B***, A selected confocal section of the neuromast in ***A*** shows the extensive contact between the terminal and one hair cell as well as a substantially smaller contact with a second. ***C***, A maximal-intensity projection of the same neuromast at 3.5 dpf illustrates extensive neuronal contact with the three posteriorly polarized hair cells. ***D***, ***E***, Selected optical sections of the neuromast depicted in ***C*** delineate the individual contacts. ***F***, A maximal-intensity projection of the same neuromast at 4.5 dpf demonstrates five putative synapses, of which four occur with posteriorly polarized hair cells. ***G***, ***H***, Large boutons have formed on the three largest posteriorly polarized hair cells. ***I***, A newly formed hair cell has been innervated (arrowhead) just as its hair bundle has begun to polarize posteriorly (see ***K***). ***J***, One innervated hair cell of this neuromast (arrowhead) is of the opposite polarity with respect to the others (see ***K***). ***K***, Staining of hair bundles in this neuromast with fluorescent phalloidin reveals the polarities of the hair cells at 4.5 dpf. The stereocilia in each bundle display a crescentic pattern of fluorescence surrounding a dark spot at the site of the kinocilium. A, Anterior; P, posterior; D, dorsal; V, ventral. Scale bars, 5 μm.

evidence supporting the null hypothesis with that favoring the alternative hypothesis that the neurons can discriminate between polarities.

Each neuromast was assigned two probabilities that were hypothesis dependent. The first probability, which represented the alternative hypothesis, was that the pattern reflected the choices of a neuron able to discriminate between polarities with a bias parameter ω that expresses the neuron's preference of one polarity over the other. A neuron that innervates only posteriorly polarized hair cells corresponds to $\omega = 1$, whereas a wholly anteriorly biased neuron has $\omega = 0$. As for the toss of an unfair coin, whose probability of yielding heads is given by the probability ω, any degree of bias between $\omega = 0$ and $\omega = 1$ is possible. The second probability reflected the null hypothesis that the neuron is strictly unbiased; in this instance, as for the toss of a fair coin, $\omega = 1/2$. Expressed in decibans, the logarithm W of the ratio of these probabilities provided a quantitative measure of the evidence for bias in any neuromast (Kass and Raftery, 1995; Jaynes, 2003).

Summing the scores for the entire sample of 131 neuromasts with hair bundles polarized along the anteroposterior axis yielded $W = 375$ db, which corresponds to a Bayes factor of $\sim 3 \times 10^{37}$. This is a formidable weight of evidence in favor of the notion that lateral-line afferents are biased innervators: the same weight of evidence is obtained, for example, after 132 successive tosses of a coin that all result in heads, in this case favoring the coin's being double-headed instead of fair.

Plotting the distribution of bias scores with respect to larval age demonstrated that the evidence for a biased model increases with neuromast development (Fig. 3*A*). It should be kept in mind, however, that the evidence for bias scales with the size of a neuromast: a neuron innervating both of two anteriorly polarized hair cells and no posteriorly polarized ones, for example,

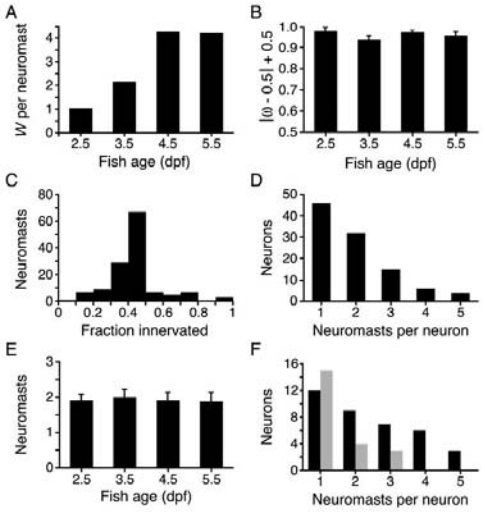

Figure 3. Statistical analysis of innervation bias and afferent neuronal receptive fields. ***A***, In a plot of the weight of evidence for a biased model (*W*) against larval age, the ordinate represents the average weight of evidence contributed by a single neuromast at the given time. Summing the results over the ensemble of neuromasts yields a total weight of evidence of 375 db. ***B***, Given that there is strong evidence for orientation selectivity, the parameter ω reflects the degree to which the neuron's choice of hair cells is biased. To illustrate the degree of bias as a function of larval age, the results have been expressed as means of the probability of $|\omega - 0.5| + 0.5$, so that the ordinate reflects increasing bias. The error bars represent SDs. ***C***, A histogram illustrating the fraction of a neuromast's hair cells innervated by the labeled fiber indicates that 84% of the neuromasts studied had 50% or fewer hair cells innervated. ***D***, A plot of the number of neurons with the indicated receptive-field sizes demonstrates the preponderance of fibers innervating one or two neuromasts. ***E***, The mean number of neuromasts innervated by a single afferent is essentially constant over the range of larval ages investigated. The error bars represent SEMs. ***F***, The distribution of neuromasts per neuron demonstrates an excess of posteriorly biased (black) over anteriorly biased (gray) neurons.

receives a lower score than a neuron innervating each of six anteriorly polarized hair cells and no posteriorly polarized ones. To evaluate the effect of the developmental increase in hair-cell numbers, we assessed the degree of bias at each time studied. To graphically represent neuronal bias, regardless of whether this bias is for anteriorly or posteriorly polarized hair cells, we plotted the mean of the probability of $|\omega - 0.5| + 0.5$ as a function of age and found this value to be stable over time (Fig. 3*B*). The observed increase in evidence for bias thus reflects neuromast growth rather than a heightened sensitivity to hair-cell polarity cues.

Because neuromasts comprise two equal populations of hair cells with opposite orientations, we expected no more than half of a neuromast's hair cells to be innervated by a labeled fiber. Indeed, 50% or fewer of the hair cells within a neuromast were innervated by the labeled afferent fiber in 113 of the 131 instances (Fig. 3*C*). Using a rigorous statistical test for bias in the choice of targets, we find that afferent neurons consistently innervate many, if not all, hair cells of one orientation within each neuromast.

Receptive fields of single PLL afferents

We were intrigued to find that most of the labeled afferents innervated multiple neuromasts (Fig. 3*D*). We asked whether each neuron selects hair cells of a common orientation across many neuromasts, as would be required to preserve independent channels of sensory information corresponding to distinct hair-cell orientations. In each of 56 instances of multiple innervation, the afferent neuron was consistent in its preference of hair-cell polarity. In 93% of these cases, the afferent fiber innervated spatially consecutive PLL neuromasts along the tail.

The innervation of multiple neuromasts by the same neuron might be indicative of an immature pattern of connectivity that is eventually pruned to a single neuromast. We found, however, that the receptive fields of single afferent neurons persisted over the period from 2.5 to 5.5 dpf (Fig. 3*E*). Although synaptic elimination may occur later in development, it is possible that the concurrent wiring of multiple sensory organs serves an essential function, such as increasing the sensitivity or signal-to-noise ratio, that is supported by a consistent choice in hair-cell polarity and by the consecutive arrangement of the neuromasts innervated.

Because there are approximately equal numbers of anteriorly and posteriorly polarized hair cells in the PLL, we were surprised to find that posteriorly polarized hair cells were disproportionately innervated by the labeled afferents. Tallying the innervated hair cells over all ages yielded 263 innervated posteriorly polarized hair cells out of a total of 460 compared with 135 innervated anteriorly polarized hair cells out of 453. This discrepancy could not be attributed entirely to a greater ratio of hair cells to neurons, for the number of posteriorly biased neurons was proportionately increased (37 posteriorly biased versus 22 anteriorly biased). If posteriorly biased neurons more readily took up or expressed the injected DNA, our mosaic labeling method might have accounted for these disparities. Because we also found that posteriorly biased neurons were more likely to innervate multiple neuromasts (Fig. 3*F*), however, the excess of posteriorly biased neurons more probably reflects the existence of neuronal subtypes with divergent receptive-field properties.

Specificity in dorsoventral neuromasts

Our analysis of neuronal connectivity has thus far been limited to neuromasts containing hair cells sensitive to stimuli along the anteroposterior axis. The correlated wiring of similarly oriented hair cells might therefore reflect, not hair-cell polarity cues, but rather the anatomical arrangement of cells within the neuromast. To distinguish between these possibilities, we examined fish in which we labeled single afferents innervating dorsoventral neuromasts. In all four cases, we found a marked bias in the innervation of dorsally versus ventrally polarized hair cells (supplemental Table 1, available at www.jneurosci.org as supplemental material). Because of the more ventral location of these neuromasts (Ledent, 2002; López-Schier et al., 2004), the afferent neuron veered ventrally from the PLL nerve in its approach to the neuromast (Fig. 4*A*,*B*). Staining with fluorescent phalloidin revealed the polarities of the constituent hair cells and confirmed that four of five ventrally oriented hair cells received boutons (Fig. 4*C*–*E*). The fifth and youngest ventrally polarized hair cell was contacted by only a tenuous neurite (Fig. 4*C*). Despite the afferent fiber's tortuous course beneath the neuromast, the dorsally polarized hair cells apparently received no contacts.

From the examination of neuromasts sensitive to dorsally and ventrally oriented stimuli, we conclude that neuronal preference for individual hair cells depends on their polarity or on a cue normally associated with this polarity. We never encountered a neuron that innervated both a dorsoventral and an anteroposterior neuromast.

Electron microscopy of synaptic contacts

Although our light-microscopic observations documented an orderly pattern of apposition between afferent terminals and specifically oriented hair cells, they could not unequivocally demonstrate synapses between the two. Moreover, it was unclear from the foregoing observations whether the apparent contacts are endowed with the morphological features of functional hair-cell synapses. We therefore used transmission electron microscopy to examine larval neuromasts.

Even at the earliest stage examined, 2 dpf, the hair cells contained numerous synaptic ribbons associated with synaptic vesicles and prominent presynaptic and postsynaptic densities. Our comparison of 2- and 5-d-old synaptic ribbons disclosed no striking differences between the two (Fig. 5*A*,*B*) save that the synaptic ribbons of some younger hair cells were smaller. These results confirm that hair-cell afferent synapses, or at least a substantial majority of them, are potentially competent for neurotransmitter release from as early as 2 dpf.

Our descriptive study of synaptic ultrastructure does not address whether the appositions between afferent neurons and hair cells observed *in vivo* are truly synapses. To directly answer this question, we sought a genetically encoded marker that labels neuronal membranes during the imaging of living cells and in correlative electron microscopy. Existing approaches, such as labeling with HRP::CD2 (Watts et al., 2004) or tetracysteine tags (Gaietta et al., 2002), possess serious drawbacks such as the need to express a fluorescent protein in parallel or to apply intense illumination in the presence of biarsenical compounds to photoconvert diaminobenzidine. To circumvent these concerns, we created a construct that encodes a single-pass transmembrane protein, HRP-mCherry, with HRP extracellularly and the fluorescent marker mCherry intracellularly (Fig. 5*C*). In the presence of diaminobenzidine and hydrogen peroxide, horseradish peroxidase generates a local osmiophilic precipitate visible both by light microscopy (Fig. 5*D*) and by electron microscopy. HRP-mCherry allows one to track the neurites of cells expressing mCherry *in vivo* by confocal fluorescence microscopy, then to examine regions of interest with the resolving power of transmission electron microscopy.

We injected the *HuC:HRP-mCherry* plasmid into larvae of the *Brn3c:gap43-GFP* transgenic line, in which hair-cell membranes are marked with GFP (Xiao et al., 2005). By obtaining a stack of confocal images through a neuromast at 5 dpf, we observed an mCherry-expressing afferent innervating a subset of hair cells within a neuromast (Fig. 5*E*,*F*). Although another afferent fiber was labeled as well, it expressed the marker more weakly and did not innervate this particular neuromast. We then fixed the larva and processed it to demonstrate horseradish peroxidase activity at the electron-microscopic level. After completion of the preparative protocol and embedding in plastic, the labeled neuron could be visualized under brightfield illumination (Fig. 5*D*). Although electron microscopy of the PLL nerve from a control larva confirmed that the afferent fibers displayed no labeling (Fig. 5*G*), sections from the labeled preparation revealed two afferent fibers delineated by extracellular precipitate (Fig. 5*H*, arrowheads). In keeping with the mCherry fluorescence pattern, one fiber displayed substantially greater expression than the other. At higher magnification, the strongly labeled afferent was cloaked in an electron-dense precipitate that remained extracellular and did not appear to damage the neuron itself or the surrounding tissue (Fig. 5*I*).

To ensure that regions of membrane contact identified by fluorescence were not missed, we cut serial sections through an entire neuromast. The afferent synapses of unlabeled neurons appeared normal and lacked extracellular electron density (Fig. 5*J*). In striking contrast, an afferent synapse corresponding to an mCherry-positive terminal (Fig. 5*E*) demonstrated extensive extracellular precipitate (Fig. 5*K*). After examining another intercellular contact (Fig. 5*F*), we found an afferent synapse apposed to a neuron surrounded by and filled with electron-dense material (Fig. 5*L*,*M*). This neuron appeared to have experienced extensive damage (Fig. 5*L*), most likely a result of gas evolution during the demonstration of horseradish peroxidase activity.

These results confirm that the contacts we observed by fluorescence microscopy indeed represent vesicle-loaded afferent synapses. Our approach has a number of advantages over other tools for correlative electron microscopy. Most notably, HRP-mCherry consists of a fluorescent protein directly conjugated to a widely used enzymatic label. The result is a clearly defined fluo-

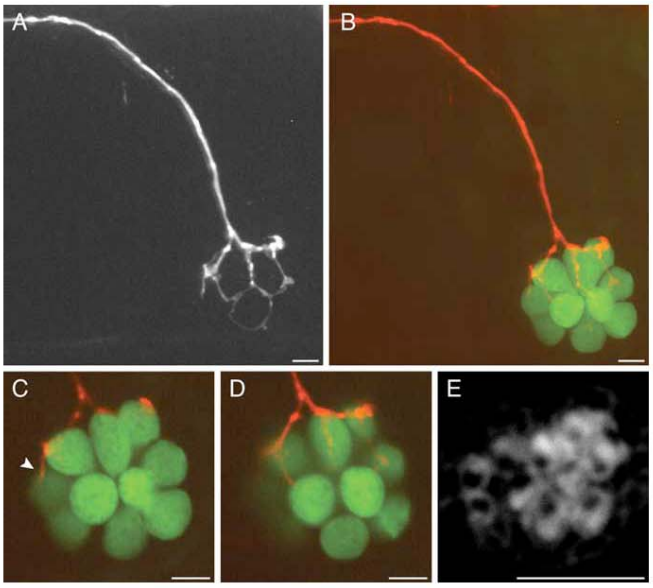

Figure 4. Afferent connections of dorsoventral neuromasts. ***A***, In a maximal-intensity projection of a confocal *Z*-stack, the mCherry-expressing afferent fiber turns ventrally from the lateral-line nerve to reach a dorsoventral neuromast. ***B***, The hair cells in the same neuromast are labeled with GFP (green). ***C***, ***D***, This neuromast contains 10 hair cells, of which four receive bulbous synaptic endings. The most rostral is contacted by only a thin neurite (arrowhead). ***E***, Labeling with fluorescent phalloidin indicates that these five hair cells have ventrally polarized hair bundles. Although the dorsally polarized hair cells are embraced by a thin, circular extension of the neuron (***A***), they lack synaptic boutons. Scale bars, 5 μm.

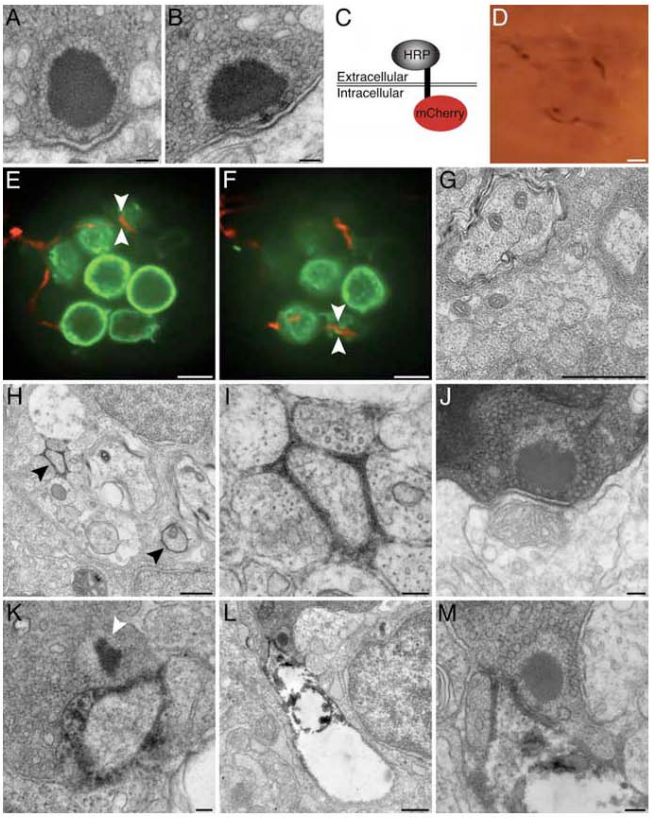

Figure 5. Correlative electron microscopy with HRP-mCherry. ***A***, A ribbon synapse in a 2 dpf wild-type larva is indistinguishable from those in older animals. ***B***, The synapse in a 5 dpf wild-type larva exhibits the characteristic features of a ribbon synapse, including a presynaptic dense body or ribbon, a halo of tethered synaptic vesicles, and prominent presynaptic and postsynaptic densities. ***C***, Expression of the HRP-mCherry protein in the neurolemma places the fluorescent mCherry component intracellularly and the HRP moiety extracellularly. ***D***, A bright-field micrograph depicts an afferent terminal expressing HRP-mCherry within a neuromast. The densely labeled fiber, which is also depicted in ***E***, ***F***, and ***H–M***, is visible through the plastic resin in which the specimen has been embedded. ***E***, An optical section through a neuromast of a living *Brn3c:gap43-GFP* larva features hair cells expressing a membrane-localized form of GFP (green). An afferent fiber labeled with HRP-mCherry (red) innervates three of the hair cells. The region bracketed by arrowheads is examined in greater detail in ***K***. ***F***, In an optical section through the basal region of the same neuromast, arrowheads bracket a site that was later explored under the electron microscope (***L***, ***M***). ***G***, A transverse section of the PLL nerve in a wild-type 5 dpf larva demonstrates several afferent axons. ***H***, In a transverse section through a PLL nerve, two afferent fibers that express HRP-mCherry (arrowheads) produce prominent electron density in the surrounding extracellular space. The weakly labeled fiber in the lower right did not innervate the neuromast depicted in ***D–F*** and ***H–M***. ***I***, A higher-magnification view of the labeled neuron at the top left of ***H*** illustrates a localized precipitate that does not damage nearby cells. ***J***, An unlabeled afferent neuron lacking electron density synapses with a hair cell of the neuromast. ***K***, A synaptic ribbon (arrowhead) in the region of membrane contact denoted by arrowheads in ***E*** verifies that the membrane contact observed by light microscopy represents an afferent synapse. ***L***, This ribbon synapse occurs at the site of membrane apposition bracketed by arrowheads in ***F***. In this instance, the neuron has become distorted and exhibits poor preservation of intracellular organelles. ***M***, Viewed at higher magnification, the ribbon synapse in ***L*** illustrates the typical attributes of hair-cell afferent synapses. Scale bars: ***A***, ***B***, ***I–K***, ***M***, 100 nm; ***D–F***, 5 μm; ***G***, ***H***, ***L***, 500 nm.

rescence pattern that is manifested as electron density when studied at high resolution.

The preference for hair-cell polarity in regenerating neurons

The hair cells of fish, amphibians, and birds regenerate on time scales of hours to days after extirpation by ototoxic agents such as aminoglycoside antibiotics and Cu^{2+} (Williams and Holder, 2000; Hernández et al., 2007). By examining how afferent neurons reinnervate neuromasts after hair-cell ablation, we inquired about the degree to which hair-cell polarity preferences are specified through an intrinsic affinity for a particular polarity. If afferent neurons display a polarity preference before hair-cell ablation, do they maintain that preference after newly minted hair cells have repopulated the neuromast, or is the polarity preference reset? In the latter instance, afferents would be expected to innervate hair cells of either polarity after regeneration, with no memory of the preablation preference.

We injected DNA encoding membrane-targeted mCherry driven by the *HuC* promoter (*HuC:gap43-mCherry*) into stably transgenic embryos bearing the *Brn3c:gap43-GFP* transgene. After screening for larvae that expressed mCherry in PLL neurons, we imaged the innervated neuromasts at 3 dpf. At this stage, neuromasts are small enough to display an unambiguous axis of mirror symmetry, so that the polarities of hair cells are certain (Fig. 6*A*). The afferent fiber innervated all four posteriorly polarized hair cells and none of the anteriorly polarized hair cells, indicating a marked preference for the former. Immediately after imaging, we immersed the fish in 10 μM $CuSO_4$ solution to eliminate lateral-line hair cells. Two hours after this treatment, we examined the same neuromast again and found it to be devoid of hair cells (Fig. 6*B*). In conjunction with the loss of hair cells, the labeled neuron underwent considerable retraction of its terminals.

As the neuromast repopulated its hair cells over the next 46 h, the afferent neuron extended its neurites and formed synapses anew (Fig. 6*C–K*). After 6 h, a centrally positioned cell began to express GFP and probably represented a hair-cell progenitor that would give rise to two daughter hair cells (López-Schier and Hudspeth, 2006). By 12 h after treatment, the neuromast contained two mature hair cells; the posteriorly polarized hair cell received a small contact from the labeled afferent fiber, which grew more pronounced by 24 h. At 36 h, the neuromast had grown to encompass seven hair cells, of which the nerve appeared to contact only three (Fig. 6*F*, *G*). At this stage of neuromast recovery, it was impossible to reliably infer the hair-bundle polarity without phalloidin staining. Finally, 48 h after ablation, the neuromast contained eight mature hair cells, as well as two immature hair cells at its rostral extreme. Phalloidin staining revealed the presence of four anteriorly polarized and four posteriorly polar-

ized hair cells, and we ascertained that the labeled neuron had formed synapses with all four of the latter (Fig. 6*H–L*). In contrast, two of the four anteriorly polarized hair cells were contacted by thin neurites (Fig. 6*H*, *J*, arrowheads) that differed significantly from the larger boutons on the posteriorly polarized hair cells. Repeating this protocol in three additional animals yielded results consistent with this representative example for both anteriorly and posteriorly biased neurons.

This experimental approach has elucidated two important properties of this system. First, afferent fibers recover and reinnervate neuromasts after acute injury on a time scale that largely matches that of hair-cell regeneration. Second, afferent fibers evidently remember the polarity of the hair cells that they innervated before ablation. This consistency in the preference for hair-cell polarity led us to question whether the neuron passively interprets hair-cell polarity cues or plays an instructive role in determining hair-cell polarity. To distinguish between these possibilities, we determined the polarities of hair cells in *neurogenin1* mutant zebrafish, which lack the PLL nerve and possess supernumerary neuromasts (Grant et al., 2005; López-Schier and Hudspeth, 2005). The neuromast hair cells of mutant larvae were polarized normally across a plane of mirror symmetry despite the complete absence of the PLL nerve (Fig. 7), ruling out a scenario in which the neuron dictates hair-cell polarities.

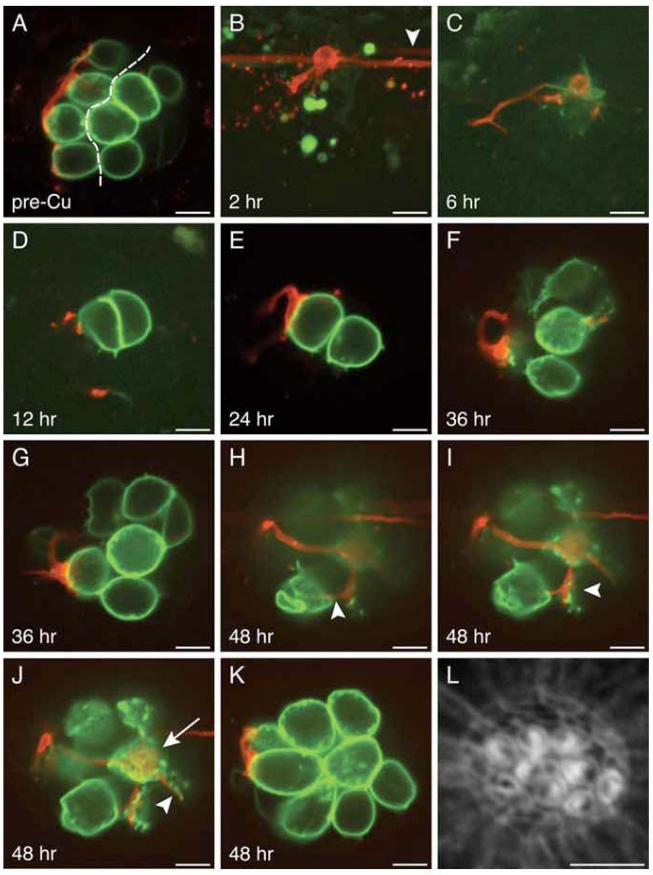

Figure 6. Reinnervation of regenerated hair cells. ***A***, In an optical section through a 3 dpf neuromast before hair-cell elimination, the axis of planar cellular polarity (dashed line) can be inferred from the positions of the constituent hair cells. The afferent fiber has selectively synapsed with posteriorly polarized hair cells. ***B***, In a maximal-intensity projection of the same neuromast 2 h after the application of 10 μM Cu^{2+}, the hair cells have been eliminated, and the neuron has retracted its terminals. Note the presence in the lateral-line nerve of another labeled neuron that does not innervate this neuromast (arrowhead). ***C***, After 6 h, the neuromast contains one weakly fluorescent progenitor that has not yet undergone mitosis to form two new hair cells. ***D***, Twelve hours after Cu^{2+} treatment, the newly formed posteriorly polarized hair cell receives a small synapse. ***E***, By 24 h, the synapse depicted in ***D*** has grown in size and in the extent of membrane contact. ***F***, ***G***, At 36 h after treatment, the neuron appears to contact two or three hair cells, but their polarities cannot be inferred because of the complex organization of the neuromast. It is likely, however, that the synapse depicted in ***G*** is identical to that in ***D*** and ***E***. ***H–K***, By 48 h, the neuromast has grown to encompass eight mature hair cells with polarized hair bundles (see ***L***). These four panels are ordered from the bases to the apices of the hair cells. ***H***, A thin neurite reaches an anteriorly polarized hair cell (arrowhead). ***I***, A larger bouton contacts the ventralmost of the posteriorly polarized hair cells (arrowhead). ***J***, A synaptic contact blankets the basal surface of a posteriorly polarized hair cell (arrow), whereas only a tenuous process reaches an anteriorly polarized hair cell (arrowhead). ***K***, The afferent neuron forms voluminous boutons on two posteriorly polarized hair cells. ***L***, Staining with fluorescent phalloidin 48 h after treatment defines the polarities of the 10 hair bundles. Scale bars, 5 μm.

Discussion

Our *in vivo* time-lapse imaging revealed that each lateral-line afferent neuron specifically contacts hair cells of a common hair-bundle polarity within a neuromast and across multiple consecutive neuromasts. Because these studies relied on membrane propinquity alone to signal the presence of intercellular contacts, we created a reagent, HRP-mCherry, that allowed us to confirm that fluorescently marked contacts correspond at the electron-microscopic level to synapses between hair cells and afferent terminals. Finally, we examined the reestablishment of neuronal connectivity after hair-cell ablation and found that afferents promptly resume contact with regenerating hair cells of the same polarity as those innervated originally.

The receptive fields of single afferent neurons

Before this study, electrophysiological evidence had suggested that lateral-line afferents synapse with hair cells of the same polarity. The bipartite pattern of action potential firings in nerve recordings from the *Xenopus* lateral line reflects the afferent wiring of two populations of hair cells with opposite polarity (Görner, 1963). Single-neuron recordings from the PLL ganglion of zebrafish have more recently demonstrated the receptive field to be confined to unidirectional mechanical stimuli (Obholzer et al., 2008). Our findings provide direct anatomical evidence that each

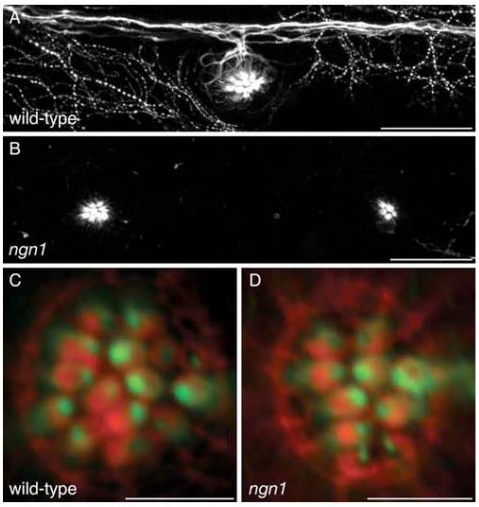

Figure 7. Hair-cell polarity in the absence of innervation. ***A***, A maximal-intensity projection of a confocal *Z*-stack depicts immunolabeling for acetylated α-tubulin in the lateral line of a 5 dpf wild-type larva. The PLL nerve and superficial sensory neurons are labeled, as well as microtubules in the apices of hair cells. ***B***, Immunolabeling of a *neurogenin1* mutant sibling for acetylated α-tubulin illustrates the absence of a PLL nerve. Labeling persists in the microtubules of hair cells. ***C***, Staining of a wild-type neuromast with fluorescent phalloidin (red) and immunofluorescent labeling of acetylated α-tubulin (green) reveal the polarities of the hair bundles in this anteroposterior neuromast. ***D***, The hair-bundle polarities of a *neurogenin1* mutant neuromast are unperturbed despite the lack of innervation. Scale bars: ***A***, ***B***, 30 μm; ***C***, ***D***, 5 μm.

afferent fiber contacts hair cells of the same polarity and a statistical demonstration of the consistence of this pattern.

We noted that the majority of afferent neurons stably innervate several neuromasts (Fig. 3*D*,*E*). This represents a more extreme version of the pattern seen in amphibians, in which only a fraction of afferent fibers innervate multiple stitches of clustered neuromasts (Fritzsch, 1989; Mohr and Görner, 1996). The variability in the sizes of receptive fields in the zebrafish PLL casts doubt on whether the primary purpose of this sensory system is a fine-grained mapping of the periphery through a one-to-one allocation of afferents to neuromasts. The innervation of multiple neuromasts may represent a compromise that boosts the sensitivity of the system through the binning of adjacent inputs. It is reassuring that afferents rarely innervate nonconsecutive neuromasts, for this would place a seemingly unnecessary burden on the establishment of an appropriate pattern of neural connections.

Somatotopy, the mapping of sensory inputs to corresponding positions in the brain, has been demonstrated in the central projection of the lateral-line nerve of larval zebrafish (Alexandre and Ghysen, 1999; Gompel et al., 2001). Compared with anterior lateral-line neurons, PLL neurons project to a more dorsomedial position in the hindbrain (Alexandre and Ghysen, 1999). A PLL neuron extends its central axon before neuromast innervation, and the position of the target neuromast can be predicted from the morphology of the growth cone (Gompel et al., 2001). These findings suggest a marked degree of intrinsic patterning before synaptic contact with hair cells. With this in mind, we scrutinized neurons innervating multiple neuromasts to learn whether these neuromasts were coinnervated in any reproducible pattern. For example, do the fifth and sixth neuromasts of the larval PLL always wire together? Except for the terminal neuromasts located on the caudal tailfin, we found no consistent pattern of coinnervation, so it remains possible that some flexibility in neuromast choice exists and that the prepatterning of afferents guides but does not strictly determine this choice.

HRP-mCherry, a tool for correlative electron microscopy

Because specialized organelles regulate neurotransmitter release, evidence of intercellular contact is insufficient to infer the presence of a synapse. We therefore developed HRP-mCherry to provide direct evidence that sites of membrane contact between hair cells and afferent neurons represent functional synapses (Fig. 5*E*,*F*,*K*–*M*). Horseradish peroxidase requires glycosylation for its enzymatic activity (Veitch, 2004), so we designed a fusion protein in which the enzyme moiety is situated at the N terminus and is directed across the membrane by a signal peptide. Linkage of the fluorescent protein mCherry to the extracellular horseradish peroxidase by the transmembrane region of N-cadherin then allows fluorescent as well as electron-microscopic labeling of specific cells.

This approach offers a significant improvement over previously available techniques for correlating neurolemmal fluorescence *in vivo* with electron-dense precipitates, such as tetracysteine tags or CD2::HRP. Tetracysteine tags require the use of potentially toxic arsenical compounds as well as sharply focused illumination, which precludes the uniform labeling of lengthy cellular processes. Unlike HRP-mCherry, CD2::HRP necessitates the coexpression of a fluorescent protein, which may be inconvenient and provides no stoichiometric relation between fluorescence intensity and electron density. The extracellular reaction product of HRP-mCherry does not interfere with the observation of organelles within a labeled cell. Although the reaction product diffuses somewhat, labeling is sufficiently circumscribed that the identity of a labeled cell is clear (Fig. 5*H*,*I*).

Synaptic-target selection by developing afferent neurons

Although an obvious requirement for the proper functioning of sensory circuits is that neurons form synapses with the appropriate targets, we lack a comprehensive understanding of the factors that guide the choice of target cells (Benson et al., 2001; Waites et al., 2005). We have illustrated an experimental preparation that facilitates the study of synaptogenesis through noninvasive optical techniques in a living vertebrate. An attractive feature of this system is that an experimenter may readily determine relevant properties of both presynaptic and postsynaptic cells. For the hair cell, it is possible to ascertain the position on the larval surface and the axis of mechanosensitivity. For the afferent neuron, one can observe the complement of neuromasts innervated, the specific hair cells selected, and the pattern of axon projections in the hindbrain. These features permit the study of synaptogenesis at the resolution of individual contacts in a system that is amenable to experimental manipulation, properties usually associated with neuronal cultures or invertebrate organisms.

A noteworthy aspect of this experimental system is the temporal course of synaptic target selection and stabilization. The evidence for polarity bias was strong at every time examined, and we detected no significant change in the degree of bias (Fig. 3*A*,*B*). This result suggests that the neurons respond to polarity cues throughout neuromast growth and turnover. This conclusion contrasts with that for sensory circuits in which there are

distinct periods of exuberant synaptogenesis and activity-dependent synaptic elimination, such as occurs in the mammalian visual system (Luo and O'Leary, 2005).

The mechanism of synaptic specificity

The wiring specificity documented here could arise if the afferent neurons instruct hair cells to assume a certain polarity. Because the hair bundles of mutant animals lacking the PLL nerve are polarized normally (Fig. 7), however, this mechanism is unlikely. Another possibility is that a polarity signal within the neuromast dictates both the polarity of the hair cells and the synaptic targets of the neurons. One argument against this arrangement comes from large neuromasts with multiple planes of mirror symmetry, in which hair cells of opposing polarities are extensively intermixed. A neuron contacts all the hair cells of a specific polarity regardless of their location within such a neuromast (Fig. 6*I*,*J*). The consistent choice of hair-cell polarity across several neuromasts provides a second piece of evidence, for it is difficult to understand how an individual fiber would receive the same polarization instructions as it entered distinct neuromasts.

The most likely possibility, and one that is consistent with all of our observations, is that afferent neurons have a capacity to sense the polarity of the hair cells and synapse accordingly. Mechanisms of this sort can be divided into two broad and potentially overlapping categories (Cline, 2003): those that require synaptic activity and those that do not. Although we cannot rule out either possibility, our data provide some initial clues and permit us to outline future studies to determine the underlying mechanism. The consistent polarity preference of afferent fibers before and after hair-cell elimination (Fig. 6) is interesting in this regard. If afferents behave as detectors of coincident synaptic release, then the choice of hair-cell polarity after reinnervation should be determined by the polarity of the first hair cell encountered. Because this was not observed, it is likely that afferents are specified to prefer a certain polarity or that, once a preference has been established, afferents remain committed to this polarity even after hair-cell ablation.

The availability of tools to manipulate electrical activity in selected cell types *in vivo* will permit further investigation into the processes involved. Using hair cell-specific promoters, one may constitutively silence synaptic activity by expressing the inwardly rectifying potassium channel Kir2.1 (Burrone et al., 2002) or temporally modulate synaptic release with *Chlamydomonas* channelrhodopsin-2 or *Natronomonas* halorhodopsin (Nagel et al., 2003; Zhang et al., 2007). The same approaches could also be used to investigate how afferent receptive fields are established. For example, afferent fibers might compete for neuromasts and hair cells in an activity-dependent manner similar to that observed for retinal ganglion cells in the optic tectum (Hua et al., 2005). By delineating the molecular processes responsible for the establishment of synaptic specificity, this approach should shed light on the mechanism by which sensory systems decompose environmental stimuli in the periphery and then recapitulate the richness of sensory information in the brain.

References

Alexandre D, Ghysen A (1999) Somatotopy of the lateral line projection in larval zebrafish. Proc Natl Acad Sci U S A 96:7558–7562.

Benson DL, Colman DR, Huntley GW (2001) Molecules, maps and synapse specificity. Nat Rev Neurosci 2:899–909.

Bricaud O, Chaar V, Dambly-Chaudière C, Ghysen A (2001) Early efferent innervation of the zebrafish lateral line. J Comp Neurol 434:253–261.

Burrone J, O'Byrne M, Murthy VN (2002) Multiple forms of synaptic plasticity triggered by selective suppression of activity in individual neurons. Nature 420:414–418.

Cline H (2003) Sperry and Hebb: oil and vinegar? Trends Neurosci 26:655–661.

Dambly-Chaudière C, Sapède D, Soubiran F, Decorde K, Gompel N, Ghysen A (2003) The lateral line of zebrafish: a model system for the analysis of morphogenesis and neural development in vertebrates. Biol Cell 95:579–587.

Dickson BJ (2002) Molecular mechanisms of axon guidance. Science 298:1959–1964.

Flock Å, Wersäll J (1962) A study of the orientation of the sensory hairs of the receptor cells in the lateral line organ of fish, with special reference to the function of the receptors. J Cell Biol 15:19–27.

Fog A (2008) Calculation methods for Wallenius' noncentral hypergeometric distribution. Comm Stat Simul Comp 37:258–273.

Fritzsch B (1989) Diversity and regression in the amphibian lateral line and electrosensory system. In: The mechanosensory lateral line: neurobiology and evolution (Coombs S, Görner P, Münz H, eds). New York: Springer.

Gaietta G, Deerinck TJ, Adams SR, Bouwer J, Tour O, Laird DW, Sosinsky GE, Tsien RY, Ellisman MH (2002) Multicolor and electron microscopic imaging of connexin trafficking. Science 296:503–507.

Gompel N, Dambly-Chaudière C, Ghysen A (2001) Neuronal differences prefigure somatotopy in the zebrafish lateral line. Development 128:387–393.

Goodman CS, Shatz CJ (1993) Developmental mechanisms that generate precise patterns of neuronal connectivity. Cell 72 [Suppl]:77–98.

Goodman SN (1998) Multiple comparisons, explained. Am J Epidemiol 147:807–812.

Görner P (1963) Untersuchungen zur Morphologie und Elektrophysiologie des Seitenlinienorgans vom Krallenfrosch (*Xenopus laevis* Daudin). Z Vergl Physiol 47:316–338.

Grant KA, Raible DW, Piotrowski T (2005) Regulation of latent sensory hair cell precursors by glia in the zebrafish lateral line. Neuron 45:69–80.

Hernández PP, Olivari FA, Sarrazin AF, Sandoval PC, Allende ML (2007) Regeneration in zebrafish lateral line neuromasts: expression of the neural progenitor cell marker sox2 and proliferation-dependent and-independent mechanisms of hair cell renewal. Dev Neurobiol 67:637–654.

Higashijima S, Hotta Y, Okamoto H (2000) Visualization of cranial motor neurons in live transgenic zebrafish expressing green fluorescent protein under the control of the islet-1 promoter/enhancer. J Neurosci 20:206–218.

Hua JY, Smear MC, Baier H, Smith SJ (2005) Regulation of axon growth in vivo by activity-based competition. Nature 434:1022–1026.

Hudspeth AJ (1989) How the ear's works work. Nature 341:397–404.

Jaynes ET (2003) Probability theory: the logic of science. Cambridge, UK: Cambridge UP.

Kass RE, Raftery AE (1995) Bayes factors. J Am Stat Assoc 90:773–795.

Keen EC, Hudspeth AJ (2006) Transfer characteristics of the hair cell's afferent synapse. Proc Natl Acad Sci U S A 103:5537–5542.

Kimmel CB, Ballard WW, Kimmel SR, Ullmann B, Schilling TF (1995) Stages of embryonic development of the zebrafish. Dev Dyn 203:253–310.

Ledent V (2002) Postembryonic development of the posterior lateral line in zebrafish. Development 129:597–604.

López-Schier H, Hudspeth AJ (2005) Supernumerary neuromasts in the posterior lateral line of zebrafish lacking peripheral glia. Proc Natl Acad Sci U S A 102:1496–1501.

López-Schier H, Hudspeth AJ (2006) A two-step mechanism underlies the planar polarization of regenerating sensory hair cells. Proc Natl Acad Sci U S A 103:18615–18620.

López-Schier H, Starr CJ, Kappler JA, Kollmar R, Hudspeth AJ (2004) Directional cell migration establishes the axes of planar polarity in the posterior lateral-line organ of the zebrafish. Dev Cell 7:401–412.

Luo L, O'Leary DD (2005) Axon retraction and degeneration in development and disease. Annu Rev Neurosci 28:127–156.

Metcalfe WK, Kimmel CB, Schabtach E (1985) Anatomy of the posterior lateral line system in young larvae of the zebrafish. J Comp Neurol 233:377–389.

Mohr C, Görner P (1996) Innervation patterns of the lateral line stitches of

the clawed frog, *Xenopus laevis*, and their reorganization during metamorphosis. Brain Behav Evol 48:55–69.
Montgomery JC, Baker CF, Carton AG (1997) The lateral line can mediate rheotaxis in fish. Nature 389:960–963.
Nagel G, Szellas T, Huhn W, Kateriya S, Adeishvili N, Berthold P, Ollig D, Hegemann P, Bamberg E (2003) Channelrhodopsin-2, a directly light-gated cation-selective membrane channel. Proc Natl Acad Sci U S A 100:13940–13945.
Obholzer N, Wolfson S, Trapani JG, Mo W, Nechiporuk A, Busch-Nentwich E, Seiler C, Sidi S, Söllner C, Duncan RN, Boehland A, Nicolson T (2008) Vesicular glutamate transporter 3 is required for synaptic transmission in zebrafish hair cells. J Neurosci 28:2110–2118.
Parinov S, Kondrichin I, Korzh V, Emelyanov A (2004) Tol2 transposon-mediated enhancer trap to identify developmentally regulated zebrafish genes in vivo. Dev Dyn 231:449–459.
Park HC, Kim CH, Bae YK, Yeo SY, Kim SH, Hong SK, Shin J, Yoo KW, Hibi M, Hirano T, Miki N, Chitnis AB, Huh TL (2000) Analysis of upstream elements in the HuC promoter leads to the establishment of transgenic zebrafish with fluorescent neurons. Dev Biol 227:279–293.
Sapède D, Rossel M, Dambly-Chaudière C, Ghysen A (2005) Role of SDF1 chemokine in the development of lateral line efferent and facial motor neurons. Proc Natl Acad Sci U S A 102:1714–1718.
Shotwell SL, Jacobs R, Hudspeth AJ (1981) Directional sensitivity of individual vertebrate hair cells to controlled deflection of their hair bundles. Ann N Y Acad Sci 374:1–10.
Veitch NC (2004) Horseradish peroxidase: a modern view of a classic enzyme. Phytochemistry 65:249–259.
Waites CL, Craig AM, Garner CC (2005) Mechanisms of vertebrate synaptogenesis. Annu Rev Neurosci 28:251–274.
Watts RJ, Schuldiner O, Perrino J, Larsen C, Luo L (2004) Glia engulf degenerating axons during developmental axon pruning. Curr Biol 14:678–684.
Williams JA, Holder N (2000) Cell turnover in neuromasts of zebrafish larvae. Hear Res 143:171–181.
Xiao T, Roeser T, Staub W, Baier H (2005) A GFP-based genetic screen reveals mutations that disrupt the architecture of the zebrafish retinotectal projection. Development 132:2955–2967.
Zhang F, Wang LP, Brauner M, Liewald JF, Kay K, Watzke N, Wood PG, Bamberg E, Nagel G, Gottschalk A, Deisseroth K (2007) Multimodal fast optical interrogation of neural circuitry. Nature 446:633–639.

APPENDIX TWO

Activity-independent specification of synaptic targets in the posterior lateral line of the zebrafish

Nagiel A, Andor-Ardo D, and Hudspeth AJ

(Manuscript in preparation)

Activity-independent specification of synaptic targets in the posterior lateral line of the zebrafish

Aaron Nagiel, Daniel Ando-Ardó, and A. J. Hudspeth

Howard Hughes Medical Institute and Laboratory of Sensory Neuroscience, The Rockefeller University, 1230 York Avenue, New York, NY 10065-6399

lateral-line | neuromast | hair cell | planar cell polarity | vglut3 | tmie | cav1.3a | pcdh15a |

Abstract

The development of functional neural circuits requires that connections between neurons be established in a precise manner. Although patterned synaptic activity has been shown to promote synaptic specificity, the mechanisms by which complex nervous systems perform this daunting task remain largely unknown. In the posterior lateral line of larval zebrafish, each afferent neuron forms synaptic contacts with hair cells of a common hair-bundle polarity. In this study, we investigated whether afferent neurons distinguish hair-cell polarities by analyzing differences in the synaptic signaling between oppositely polarized hair cells. By examining two mutant zebrafish lines with defects in mechanoelectrical transduction, we found that afferent neurons could form specific synapses in the absence of stimulus-evoked patterns of synaptic release. Asking next whether this specificity could arise through intrinsically generated patterns of synaptic release, we found that the polarity preference persisted in two mutant lines lacking essential synaptic proteins. These results indicate that lateral-line afferent neurons do not utilize synaptic activity to distinguish hair-cell polarities and suggest that molecular markers of hair-cell polarity guide prepatterned afferents to form the appropriate synapses.

Introduction

An essential feature of neural development is the establishment of specific synaptic connections. In order to form the appropriate contacts, each growing axon must respond to guidance cues, find its target region, and then establish synapses with specific target cells (1, 2). The first two of these steps—axonal guidance and target recognition—rely predominantly on molecular signposts that attract or repulse growth cones in a manner independent of neuronal activity (3, 4). How neurons decide to form stable synapses with particular target cells, however, remains unclear. Activity serves an important role in regulating the growth of axonal arbors and in selectively stabilizing synapses (5-8). In several vertebrate systems, axons form synapses diffusely within the target region and then undergo activity-dependent pruning to eliminate inappropriate synapses (9-14). Hebb's postulate, by which correlated activity between synaptic partners strengthens synapses (15, 16), offers an attractive model to explain this phenomenon (17). Nevertheless, the evidence for an activity-dependent process must be reconciled with data suggesting that normal brain architecture can form in the absence of synaptic transmission (18-20). In this case, synaptic specificity could derive from a combinatorial code of cell-surface molecules such as cadherins (21) or members of the immunoglobulin superfamily (22). These fundamental uncertainties highlight the need for *in vivo* studies in an experimentally tractable vertebrate system.

The posterior lateral line (PLL) of zebrafish permits a detailed analysis of the role of activity in establishing synaptic specificity. The larval PLL consists of superficial clusters of hair cells, the neuromasts, that respond to water-borne mechanical stimuli (23). To transduce water motions into electrical signals, each

hair cell bears an apical hair bundle comprising a staircase-like array of stereocilia with the kinocilium, a true cilium, at the tall edge (24). The planar-cell-polarity pathway (25) controls the polarization of the hair bundle and determines its axis of mechanical sensitivity, such that bundle deflection toward the kinocilium causes depolarization whereas deflection in the opposite direction hyperpolarizes the hair cell (26). Each neuromast contains two groups of hair cells of opposite hair-bundle polarity arranged across a plane of mirror symmetry (27). In the PLL, most neuromasts contain anteriorly and posteriorly polarized hair cells, whereas a particular few neuromasts contain dorsally and ventrally polarized cells (28).

Upon innervating a neuromast, each afferent neuron forms synapses almost exclusively with hair cells of one and the same orientation (29, 30). One possible explanation for this result is that afferent neurons distinguish hair-cell polarities by analyzing the temporal pattern of synaptic activity. Another possibility is that the specificity arises from an intrinsic affinity of afferent neurons for particular hair-cell polarities through direct molecular interactions. In this study, we have investigated the role of synaptic activity in target cell choice and in doing so shed light on the mechanisms by which neurons form the appropriate connections.

Results

Afferent neurons selectively innervate hair cells of a common polarity. Using a line of zebrafish that expresses membrane-targeted GFP in hair cells (*Pou4f3:gap43-GFP*, formerly *Brn3c:gap43-GFP*; 33) we labeled individual afferent neurons *in vivo* with a membrane-targeted form of the fluorescent protein mCherry (*HuC:gap43-mCherry*). Upon innervating a neuromast containing two groups of oppositely polarized hair cells, a fluorescently labeled afferent fiber

reliably contacts hair cells of a common polarity revealed by staining with fluorescent phalloidin (Fig. 1*A*, *B*). This specificity in target choice is remarkably robust and likely occurs through direct sensing of hair-cell polarity by the afferent neurons (29).

We considered three models to explain the observed specificity (Fig. 1*C*). The first posits that an afferent neuron innervates hair cells randomly but then eliminates certain contacts by analyzing the temporal pattern of synaptic release elicited by sensory experience. A unidirectional stimulus should simultaneously intensify synaptic release from hair cells of one polarity and suppress release from cells of the opposite orientation (31). If afferent neurites serve as coincidence detectors, they could strengthen synapses with hair cells of a particular polarity and eliminate synapses with those of the opposite polarity through a Hebbian mechanism. A second activity-dependent model requires oppositely polarized hair cells to possess different patterns of spontaneous synaptic activity. This model differs from the first in that the distinguishing quality is a spontaneous rather than an experience-evoked pattern of neurotransmitter release. The third model asserts that hair cells of opposite polarity express distinct membrane or secreted proteins that are recognized by prepatterned afferent neurons with intrinsic affinities for particular hair-cell polarities. Although this mechanism might require activity for long-term synaptic maintenance, it requires no synaptic input to achieve initial specificity. We used these three models to develop an experimental framework for deducing the mechanism at work in the lateral line.

Sensory experience is not required for synaptic specificity. We first tested whether afferent neurons can distinguish hair-cell polarity in the absence of experience-evoked patterns of synaptic release. We examined zebrafish lines

bearing null mutations in two genes, *tmie* (M. Gleason, personal communication) and *protocadherin 15a* (32). Larvae at 5 dpf displayed auditory and vestibular deficits, lacked microphonic potentials, and exhibited no uptake of fluorophores through their mechanotransduction channels (32). These phenotypes reflect defects in mechanotransduction that prevent sensory stimuli from eliciting membrane depolarization and synaptic-vesicle fusion.

The *tmie* gene product is a putatively single-pass transmembrane protein required for hair-cell mechanotransduction in fishes and mammals (33, 34). In seven anteroposteriorally oriented neuromasts of *tmie* mutant larvae, each afferent fiber consistently innervated hair cells of only a single polarity (Fig. 2*A*-*C*). Specific innervation was also characteristic of the four *tmie* neuromasts we examined that contained dorsally and ventrally polarized hair cells (Fig. 2*D*-*F*).

We next examined synaptic specificity in the *protocadherin 15a* mutant, which lacks a component of the stereociliary tip link essential for transducing mechanical force into hair-cell depolarization (32). In each of the 19 neuromasts studied, the axonal terminal formed synaptic boutons on hair cells of only one particular orientation (Fig. 2*G*-*I*). These results suggest that afferent neurons do not require sensory experience to distinguish hair-cell polarity.

Synaptic specificity is preserved in the absence of synaptic transmission. Because the preference of afferents for hair-cell polarity was robust in the absence of sensory input, we evaluated the possibility that an intrinsically generated pattern of synaptic release by hair cells reveals their polarity to afferents. Oppositely polarized hair cells might, for example, differ in their frequency or pattern of spontaneous neurotransmitter release, and afferents might display complementary preferences.

We studied two mutant lines with defects in essential synaptic components and consequent loss of auditory and vestibular function. The *cav1.3a* mutant possesses a mutation in the L-type voltage-gated Ca^{2+} channel responsible for coupling membrane depolarization to transmitter release at the hair cell's afferent synapse (35). In each of the 21 *cav1.3a* mutant neuromasts that we analyzed, the labeled afferent fiber made synapses onto hair cells of only a single polarity (Fig. 3*A-C*).

We additionally examined *vglut3* mutants, which lack the vesicular glutamate transporter type 3 responsible for filling synaptic vesicles with the afferent neurotransmitter glutamate (36). In each of fifteen *vglut3* mutant neuromasts, a labeled afferent neuron formed specific synapses onto hair cells of a common polarity (Fig. 3*D-F*). Taken together, our study of four zebrafish mutants lacking hair-bundle or synaptic function provides evidence that synaptic specificity persists in the absence of specific patterns of synaptic signaling.

Polarity preference and synapse maintenance are activity-independent. Although the mutants we utilized for these studies displayed severe loss-of-function phenotypes, they might conceivably have retained sufficient synaptic activity to signal their polarities to afferents. If this were the case, we would nevertheless expect the afferent neurons to have exhibited a diminished capacity to distinguish between polarities. In order to rigorously detect small changes in polarity preference, we analyzed synapse formation in many mutant and wild-type neuromasts and then applied a statistical model of polarity preference (29). The model contains a bias parameter ω that expresses the neuron's preference for one polarity over another. To represent neuronal bias independently of the

particular polarity being preferred, we calculated the mean of the probability of $|\omega - 0.5| + 0.5$.

For all four mutant lines, afferent neurons displayed an ability to distinguish polarities to a degree commensurate with that of wild-type afferents (Fig. 4*A*). Our statistical analysis thus points to an activity-independent specification of synaptic targets, but it does not address whether afferent synapses require activity for long-term maintenance. To answer this question, we calculated the fraction of a neuromast's hair cells innervated by a single afferent fiber. Because neuromasts comprise two equal populations of oppositely polarized hair cells, we expected no more than half of a neuromast to be innervated by a labeled fiber. The mean fraction innervated was similar for mutant and wild-type animals (Fig. 4*B*), suggesting that neurotransmitter release is not essential for synaptic maintenance.

Discussion

We have assessed the role of synaptic activity in ensuring specific connectivity between afferent neurons and plane-polarized hair cells in the posterior lateral line of larval zebrafish. In two lines with defects in mechanotransduction and two with deficiencies of synaptic signaling, lateral-line afferents correctly identified and synapsed with hair cells of a common polarity. By applying a statistical model of polarity preference to data from each mutant line, we ascertained that afferent synaptogenesis remained highly biased for one polarity over the other at levels matching those observed for wild-type animals. In addition, the fraction of each mutant neuromast innervated by the labeled afferent fiber was comparable to that in wild-type neuromasts, indicating that synaptic transmission is not essential for synaptic maintenance. These results imply that afferent neurons do not interpret a pattern of evoked or spontaneous

neurotransmitter release, but instead utilize intrinsic molecular cues to identify and synapse with the appropriately polarized hair cells.

This conclusion is consistent with two previous observations (29). First, when an afferent fiber innervates multiple neuromasts, it is consistent in its polarity preference both within each innervated neuromast and between neuromasts. It seems improbable that unbiased neurites belonging to the same fiber could consistently prefer the same polarity by analyzing experience-evoked patterns of coincident synaptic release. Second, afferent fibers retain their polarity preference following hair-cell death and regeneration. If unbiased afferents utilize patterns of coincident synaptic release to restrict themselves to a single polarity, one would expect the preference to depend on the polarity of the first hair cell innervated. This was not observed; instead, afferents synapse with hair cells of the same polarity as those innervated prior to hair-cell ablation. Both of these observations contradicted a model whereby initially unbiased afferent neurons use experience-dependent patterns of synaptic release to restrict themselves to a single polarity. These findings were nevertheless compatible with an activity-dependent mechanism in which prepatterned afferent neurons prefer a polarity-specific pattern of spontaneous synaptic release. Our present results with *cav1.3a* and *vglut3* mutant fish speak against this mechanism, however, favoring instead activity-independent specification.

Before a role for synaptic activity can be excluded altogether, three important issues should be addressed in future studies. The first is that our experimental approach involved loss-of-function mutants. The unlikely possibility exists that patterned neurotransmitter release ordinarily overrides the default molecular mechanism that confers specificity in the mutants. To test this, one might express a light-gated cation channel such as channelrhodopsin-2 in hair cells and raise the fish in the presence of stroboscopic illumination. If

electrical activity plays an instructive role, each afferent fiber would be expected to contact all the hair cells of a neuromast, regardless of their polarity, because they would depolarize in synchrony. The second issue is that synaptic activity could play other, more subtle roles in neuronal morphology and behavior. Despite their ability to correctly identify hair-cell polarities in the absence of synaptic signaling, afferent neurons might, for example, exhibit increased exploratory behavior. This could be manifested through a larger spatial spread of axonal arbors or through accelerated dynamics of axonal extension and retraction. Although we have not investigated these possibilities in detail, we believe that any changes in axonal morphology or dynamics are minor. The third and final obstacle to rejecting a role for synaptic activity in this system is that the molecular mechanism that mediates polarity-specificity remains unknown. A likely possibility is that oppositely polarized hair cells express distinct membrane or secreted proteins that attract or repel afferent neurites bearing appropriate receptors. The difficulty in identifying these molecular polarity cues stems from the fact that oppositely oriented hair cells are commingled within neuromasts and lack distinguishing morphological characteristics after isolation.

It is interesting to speculate why the PLL has evolved a hard-wired approach to distinguishing between oppositely polarized hair cells. Perhaps the sheer simplicity of the system lends itself to a molecular code. Each afferent neuron faces a simple binary choice in its selection of synaptic targets. Moreover, it is a choice that the neuron must continue to make throughout life as new hair cells are produced to replace dying ones. What this system foregoes in activity-dependent refinement and plasticity, it gains in reproducibility and speed.

A question that remains to be answered is whether dorsoventral and anteroposterior neuromasts use the same code to differentiate hair-cell polarities.

Single afferents ordinarily do not innervate both dorsoventral and anteroposterior neuromasts (29), so in theory a single code would suffice. We suspect that posteriorly and ventrally polarized hair cells bear the same polarity identity, whereas anteriorly and dorsally polarized hair cells bear the opposite polarity identity. Our logic for this inference is that each of these coteries of hair cells originates respectively more proximally or more distally with respect to the migration of the primordium that deposited the neuromast. For instance, both posteriorly and ventrally polarized hair cells arise on the sides of their respective neuromasts that were proximal to the direction of primordial migration. An interesting possibility is that the planar cell polarity of a neuromast depends upon the direction of primordial movement (28, but see 37) and that the signals responsible for this feature serve to specify neuronal connectivity as well.

Peripheral mechanisms that ensure wiring specificity do not function alone, but rather act in concert with central components in generating somatotopy and organizing sensory and behavioral circuits. An important question arising from this work is whether the degree of predetermination that we have observed peripherally also extends to the central projections (38). If afferent neurons utilize a molecular code to distinguish between hair-cell polarities, does this same code function in the hindbrain to organize polarity-specific sensory pathways (39)? If so, how are afferents encoding anteriorly and posteriorly directed stimuli distinguished from those representing dorsally and ventrally directed stimuli? Another fascinating issue is how somatotopy, the mapping of neuromast position along the body to the corresponding projection zone in the brain, relates to the polarity pathway. Because an afferent's choice of neuromast can be predicted from its hindbrain projection and from the morphology of its growth cone (40, 41), afferent neuronal differentiation might involve the concerted specification of polarity and target-neuromast position

through a multimodal molecular code. The use of hard-wired molecular mechanisms to ensure synaptic specificity in the periphery may provide the foundation upon which to build complex yet flexible circuits in the central nervous system.

Materials and Methods

Zebrafish strains and husbandry. Zebrafish were maintained under standard conditions. Naturally spawned eggs were collected, cleaned, staged (42), and maintained in system water at 28.5°C at a density of 50 per 100-mm-diameter Petri dish. Embryos were raised in system water with the addition of 200 μM 1-phenyl-2-thiourea at 1 day post-fertilization (dpf) to inhibit pigment formation.

The wild-type strain used was *Tübingen Long Fin* (TL). The relevant transgenic and mutant strains include *Pou4f3:gap43-GFP*, *Tg(Pou4f3:gap43-mGFP)*^{356t}; *tmie*, *tmie*^{ru1000}; *protocadherin 15a, pcdh15a*^{th263b}; *vlgut3*, *slc17a8*^{vo1}; *cav1.3a*, *cacna1d*^{tc323d}.

DNA injection and screening of transgenic and mutant fish. The *HuC:gap43-mCherry* plasmid was created as described (29). One- and two-cell embryos were pressure-injected with supercoiled plasmid DNA at a concentration of 50 ng/μl. Deaf mutant larvae were identified at 5 dpf by the startle-response assay (43) and screened for mCherry expression in the PLL nerve with a Zeiss Axioplan 2 wide-field fluorescence microscope.

Live imaging of larvae. For confocal imaging, specimens were embedded under anesthesia in 1% low-melting-point agarose on a glass coverslip. Images were acquired with an Ultramer Perkin-Elmer spinning-disk system on a Zeiss

Axiovert 200M microscope equipped with a 63x, 1.4 NA objective lens, a Hamamatsu Orca-ER cooled CCD camera, and MetaMorph software (Molecular Devices/MDS). Z-stacks were acquired at 1 μm intervals, imaging GFP (488 nm excitation, 500-550 nm emission) and mCherry (568 nm excitation, 590-650 nm emission). After each examination, the larvae were excised from the agarose and returned to individually marked dishes. At the conclusion of live imaging, larvae were genotyped to confirm their status as mutants.

Phalloidin staining and imaging. Fish were fixed overnight at 4°C in phosphate-buffered saline containing 1% Tween-20 (PBST) and 4% paraformaldehyde, then were washed thrice in 1% PBST for 1 hr and stained overnight at 4°C with a 1:20 dilution of Alexa Fluor 568 phalloidin (Invitrogen) in 0.2% PBST. They were next washed twice for 4 hr and mounted in Vectashield (Vector Laboratories). Samples were imaged at a scan rate of 8 μs per pixel with Kalman averaging on an Olympus FV1000 laser-scanning confocal microscope with a 60x, 1.42 NA objective lens.

Statistical modeling of polarity preference. We modeled a neuron's ability to distinguish between opposing polarities by Fisher's noncentral hypergeometric distribution (29). Using a beta(1,1) prior, we calculated $P(\omega \mid D)$, the posterior of the parameter ω for an observed distribution D of synaptic contacts. A neuron innervating only anteriorly polarized hair cells is assigned the parameter value $\omega = 0$ whereas a posteriorly selective neuron has $\omega = 1$. A neuron with no ability to distinguish polarization has $\omega = 0.5$. Since we sought to quantify each neuron's ability to distinguish polarity in a way that was independent of its specific polarization preference, we made a change of variables to $|\omega - 0.5| + 0.5$. The new distribution, $0.5\left[P(\omega \mid D) + P(1-\omega \mid D)\right]$, which we characterized by its mean and standard deviation, satisfies the symmetry requirement.

ACKNOWLEDGMENTS. The authors thank Mr. A. Afolalu for expert fish husbandry, Dr. M. Gleason for providing the *tmie* mutant fish, Dr. A. North for assistance with the spinning-disk microscope, and Dr. T. Nicolson for providing *cav1.3a*, *pcdh15a*, and *vglut3* mutant fish. This project was supported by National Institutes of Health grants DC00241 and GM07739. A. N. is the recipient of Ruth L. Kirschstein National Research Service Award Predoctoral Fellowship NS62486; A. J. H. is an Investigator of Howard Hughes Medical Institute.

1. Benson DL, Colman DR, Huntley GW (2001) Molecules, maps and synapse specificity. *Nat Rev Neurosci* 2:899-909.
2. Goodman CS, Shatz CJ (1993) Developmental mechanisms that generate precise patterns of neuronal connectivity. *Cell* 72 Suppl:77-98.
3. Dickson BJ (2002) Molecular mechanisms of axon guidance. *Science* 298:1959-1964.
4. Tessier-Lavigne M, Goodman CS (1996) The molecular biology of axon guidance. *Science* 274:1123-1133.
5. Trachtenberg JT, *et al.* (2002) Long-term in vivo imaging of experience-dependent synaptic plasticity in adult cortex. *Nature* 420:788-794.
6. Waites CL, Craig AM, Garner CC (2005) Mechanisms of vertebrate synaptogenesis. *Annu Rev Neurosci* 28:251-274.
7. Holtmaat A, Wilbrecht L, Knott GW, Welker E, Svoboda K (2006) Experience-dependent and cell-type-specific spine growth in the neocortex. *Nature* 441:979-983.
8. Hua JY, Smear MC, Baier H, Smith SJ (2005) Regulation of axon growth in vivo by activity-based competition. *Nature* 434:1022-1026.
9. Luo L, O'Leary DD (2005) Axon retraction and degeneration in development and disease. *Annu Rev Neurosci* 28:127-156.
10. Tian N, Copenhagen DR (2003) Visual stimulation is required for refinement of ON and OFF pathways in postnatal retina. *Neuron* 39:85-96.
11. Wong RO, Ghosh A (2002) Activity-dependent regulation of dendritic growth and patterning. *Nat Rev Neurosci* 3:803-812.
12. Hubel DH, Wiesel TN (1964) Effects of Monocular Deprivation in Kittens. *Naunyn Schmiedebergs Arch Exp Pathol Pharmakol* 248:492-497.
13. Shatz CJ, Stryker MP (1978) Ocular dominance in layer IV of the cat's visual cortex and the effects of monocular deprivation. *J Physiol* 281:267-283.
14. Eisele LE, Schmidt JT (1988) Activity sharpens the regenerating retinotectal projection in goldfish: sensitive period for strobe illumination and lack of effect on synaptogenesis and on ganglion cell receptive field properties. *J Neurobiol* 19:395-411.

15. Hebb DO (1949) *The Organization of Behavior* (Wiley, New York).
16. Stent GS (1973) A Physiological Mechanism for Hebb's Postulate of Learning. *Proc Natl Acad Sci U S A* 70:997-1001.
17. Bi G, Poo M (2001) Synaptic modification by correlated activity: Hebb's postulate revisited. *Annu Rev Neurosci* 24:139-166.
18. Varoqueaux F, *et al.* (2002) Total arrest of spontaneous and evoked synaptic transmission but normal synaptogenesis in the absence of Munc13-mediated vesicle priming. *Proc Natl Acad Sci U S A* 99:9037-9042.
19. Verhage M, *et al.* (2000) Synaptic assembly of the brain in the absence of neurotransmitter secretion. *Science* 287:864-869.
20. Nevin LM, Taylor MR, Baier H (2008) Hardwiring of fine synaptic layers in the zebrafish visual pathway. *Neural Dev* 3:36.
21. Shapiro L, Colman DR (1999) The diversity of cadherins and implications for a synaptic adhesive code in the CNS. *Neuron* 23:427-430.
22. Yamagata M, Sanes JR (2008) Dscam and Sidekick proteins direct lamina-specific synaptic connections in vertebrate retina. *Nature* 451:465-469.
23. Montgomery JC, Baker CF, Carton AG (1997) The lateral line can mediate rheotaxis in fish. *Nature* 389:960-963.
24. Hudspeth AJ (1989) How the ear's works work. *Nature* 341:397-404.
25. Lopez-Schier H, Hudspeth AJ (2006) A two-step mechanism underlies the planar polarization of regenerating sensory hair cells. *Proc Natl Acad Sci U S A* 103:18615-18620.
26. Shotwell SL, Jacobs R, Hudspeth AJ (1981) Directional sensitivity of individual vertebrate hair cells to controlled deflection of their hair bundles. *Ann N Y Acad Sci* 374:1-10.
27. Flock Å, Wersäll J (1962) A study of the orientation of the sensory hairs of the receptor cells in the lateral line organ of fish, with special reference to the function of the receptors. *J Cell Biol* 15:19-27.
28. Lopez-Schier H, Starr CJ, Kappler JA, Kollmar R, Hudspeth AJ (2004) Directional cell migration establishes the axes of planar polarity in the posterior lateral-line organ of the zebrafish. *Dev Cell* 7:401-412.
29. Nagiel A, Andor-Ardo D, Hudspeth AJ (2008) Specificity of afferent synapses onto plane-polarized hair cells in the posterior lateral line of the zebrafish. *J Neurosci* 28:8442-8453.
30. Faucherre A, Pujol-Marti J, Kawakami K, Lopez-Schier H (2009) Afferent neurons of the zebrafish lateral line are strict selectors of hair-cell orientation. *PLoS ONE* 4:e4477.
31. Görner P (1963) Untersuchungen zur Morphologie und Elektrophysiologie des Seitenlinienorgans vom Krallenfrosch (Xenopus laevis Daudin). *Zeitschrift für vergleichende Physiologie* 47:316-338.
32. Seiler C, *et al.* (2005) Duplicated genes with split functions: independent roles of protocadherin15 orthologues in zebrafish hearing and vision. *Development* 132:615-623.
33. Mitchem KL, *et al.* (2002) Mutation of the novel gene Tmie results in sensory cell defects in the inner ear of spinner, a mouse model of human hearing loss DFNB6. *Hum Mol Genet* 11:1887-1898.
34. Naz S, *et al.* (2002) Mutations in a novel gene, TMIE, are associated with hearing loss linked to the DFNB6 locus. *Am J Hum Genet* 71:632-636.

35. Sidi S, Busch-Nentwich E, Friedrich R, Schoenberger U, Nicolson T (2004) gemini encodes a zebrafish L-type calcium channel that localizes at sensory hair cell ribbon synapses. *J Neurosci* 24:4213-4223.
36. Obholzer N, *et al.* (2008) Vesicular glutamate transporter 3 is required for synaptic transmission in zebrafish hair cells. *J Neurosci* 28:2110-2118.
37. Ghysen A, Dambly-Chaudiere C (2007) The lateral line microcosmos. *Genes Dev* 21:2118-2130.
38. Fritzsch B, Gregory D, Rosa-Molinar E (2005) The development of the hindbrain afferent projections in the axolotl: evidence for timing as a specific mechanism of afferent fiber sorting. *Zoology (Jena)* 108:297-306.
39. Fritzsch B (1981) The pattern of lateral-line afferents in urodeles. A horseradish-peroxidase study. *Cell Tissue Res* 218:581-594.
40. Alexandre D, Ghysen A (1999) Somatotopy of the lateral line projection in larval zebrafish. *Proc Natl Acad Sci U S A* 96:7558-7562.
41. Gompel N, Dambly-Chaudière C, Ghysen A (2001) Neuronal differences prefigure somatotopy in the zebrafish lateral line. *Development* 128:387-393.
42. Kimmel CB, Ballard WW, Kimmel SR, Ullmann B, Schilling TF (1995) Stages of embryonic development of the zebrafish. *Dev Dyn* 203:253-310.
43. Nicolson T, *et al.* (1998) Genetic analysis of vertebrate sensory hair cell mechanosensation: the zebrafish circler mutants. *Neuron* 20:271-283.

Figure Legends

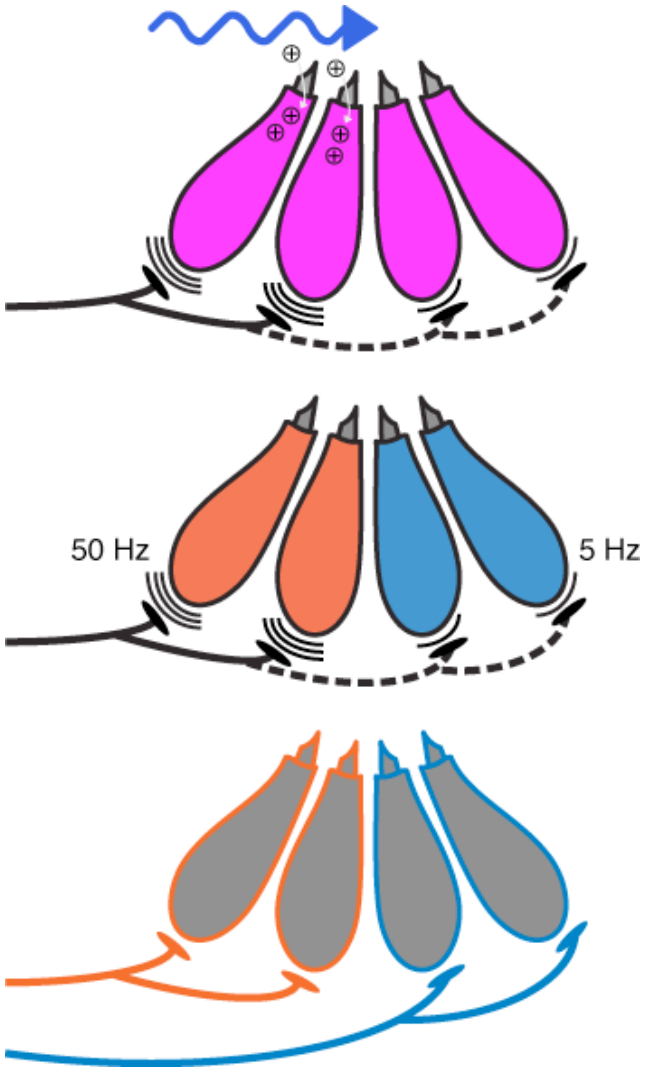

Figure 1. Synaptic specificity in the posterior lateral line of zebrafish larvae. (*A*) In this anteroposterior neuromast, the axonal terminal of an mCherry-labeled afferent neuron (red) contacts two of the six hair cells marked by GFP (green). (*B*) Staining of the same neuromast with fluorescent phalloidin reveals the hair-bundle polarities: the kinocilia appear as dark defects in the actin-rich cuticular plates. The two labeled terminals contact hair cells sensitive to anteriorly directed stimuli. In this and all subsequent morphological illustrations, anterior

is to the left and dorsal to the top. The same labeling reagents are used in Figures 2 and 3; the scale bars all represent 5 mm. (*C*) Three models might explain the ability of afferent neurons to distinguish between hair-cell polarities. *Top*: A posteriorly directed stimulus depolarizes posteriorly polarized hair cells while hyperpolarizing anteriorly polarized hair cells. Afferents might form synapses diffusely but, after detecting temporal differences in synaptic release from oppositely polarized hair cells, eliminate synapses with hair cells firing out of phase with the rest of their synaptic repertoire (dashed neuronal segment). *Middle*: Oppositely polarized hair cells express distinct complements of ion channels that produce distinct patterns of spontaneous synaptic release. In this example, hair cells of the two orientations release neurotransmitter at different frequencies, allowing neurites to distinguish them. *Bottom*: Hair cells express distinct membrane or secreted proteins that attract prepatterned afferents with intrinsic affinities for particular molecular markers. The afferents then detect hair-cell polarities independently of synaptic activity.

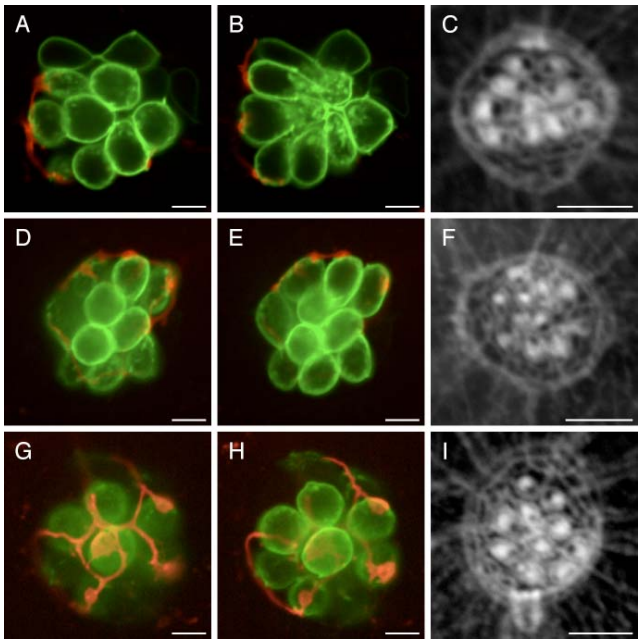

Figure 2. Stimulus-evoked patterns of synaptic release are not required for polarity choice. (*A*, *B*) In an anteroposterior neuromast of a *tmie* mutant larva, a labeled afferent fiber synapses with five of the ten hair cells. (*C*) The hair-bundle polarities of this neuromast reveal that the neuron innervates all five posteriorly polarized hair cells and none of the opposite polarity. (*D-F*) In a dorsoventral neuromast of a *tmie* mutant, an afferent neuron innervates only the five ventrally polarized hair cells. (*G-I*) An afferent fiber in a *protocadherin 15a* mutant forms synapses with four of the five anteriorly polarized hair cells, but with none of the five cells of the opposite polarity.

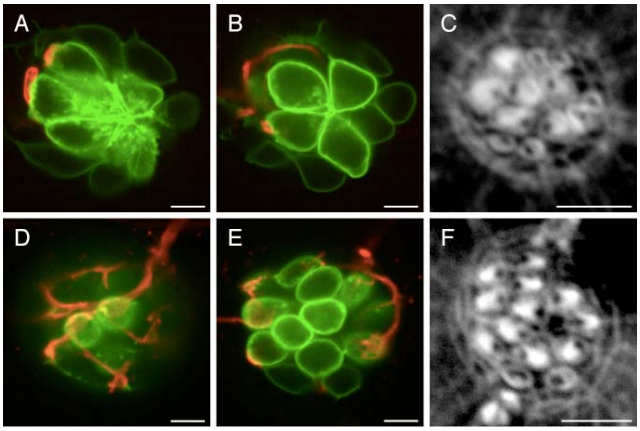

Figure 3. Synaptic transmission is dispensible for hair-cell polarity preference. (*A-C*) In an anteroposteriorly oriented neuromast of a *cav1.3a* mutant lacking L-type voltage-gated Ca^{2+} channels, the three mature posteriorly polarized hair cells bear labeled afferent synapses whereas none of the opposite polarity do. (*D-F*) This *vglut3*-deficient neuromast contains six posteriorly polarized hair cells, all of which are innervated by the labeled afferent fiber.

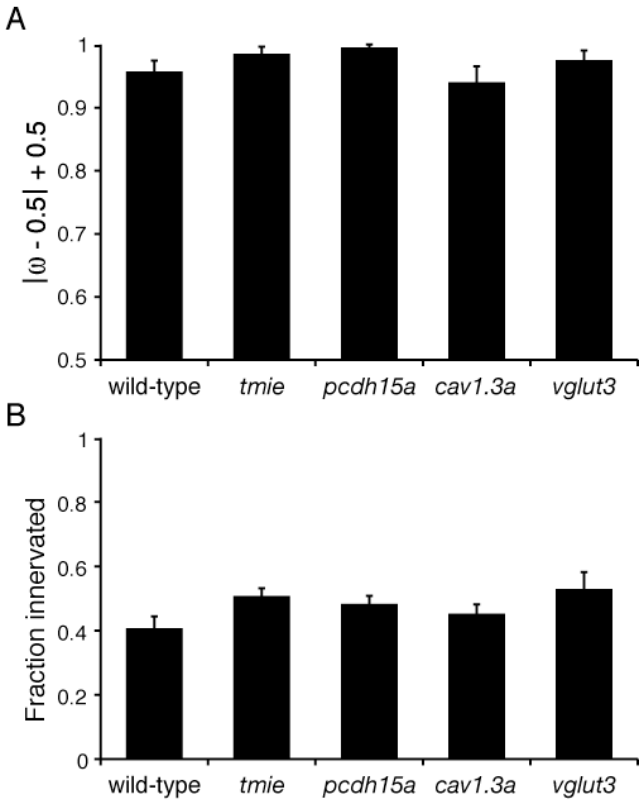

Figure 4. Statistical analysis confirms the polarity preference of afferent terminals. (*A*) The parameter ω, which ranges from 0 to 1, represents the degree to which a neuron's choice of hair cells is biased toward one polarity; a value of 0.5 represents a lack of bias. The results have been expressed as the means and standard deviations of the probability distribution of $|\omega - 0.5| + 0.5$, so the ordinate reflects increasing bias. In practice, values of ω above about 0.95 represent near certainty: these populations of neurons make less than one error per three neuromasts innervated. (*B*) The mean fractions of the hair cells that were innervated by a labeled afferent fiber were similar for neuromasts of each genotype. The error bars represent standard errors of the means for the following numbers of observations: wild-type, n=21; *tmie*, n=11; *pcdh15a*, n=19; *cav1.3a*, n=21; *vglut3*, n=15.

REFERENCES

Alexandre D, Ghysen A (1999) Somatotopy of the lateral line projection in larval zebrafish. Proceedings of the National Academy of Sciences of the United States of America 96:7558-7562.

Baier H, Bonhoeffer F (1992) Axon guidance by gradients of a target-derived component. Science 255:472-475.

Baird RA, Burton MD, Lysakowski A, Fashena DS, Naeger RA (2000) Hair cell recovery in mitotically blocked cultures of the bullfrog saccule. Proc Natl Acad Sci U S A 97:11722-11729.

Balkowiec A, Katz DM (2000) Activity-dependent release of endogenous brain-derived neurotrophic factor from primary sensory neurons detected by ELISA in situ. J Neurosci 20:7417-7423.

Benson DL, Colman DR, Huntley GW (2001) Molecules, maps and synapse specificity. Nature reviews 2:899-909.

Bi G, Poo M (2001) Synaptic modification by correlated activity: Hebb's postulate revisited. Annual review of neuroscience 24:139-166.

Biederer T, Sara Y, Mozhayeva M, Atasoy D, Liu X, Kavalali ET, Sudhof TC (2002) SynCAM, a synaptic adhesion molecule that drives synapse assembly. Science 297:1525-1531.

Brandt A, Khimich D, Moser T (2005) Few CaV1.3 channels regulate the exocytosis of a synaptic vesicle at the hair cell ribbon synapse. J Neurosci 25:11577-11585.

Bricaud O, Chaar V, Dambly-Chaudière C, Ghysen A (2001) Early efferent innervation of the zebrafish lateral line. The Journal of comparative neurology 434:253-261.

Cang J, Wang L, Stryker MP, Feldheim DA (2008) Roles of ephrin-as and structured activity in the development of functional maps in the superior colliculus. J Neurosci 28:11015-11023.

Cline H (2003) Sperry and Hebb: oil and vinegar? Trends in neurosciences 26:655-661.

Dambly-Chaudière C, Sapède D, Soubiran F, Decorde K, Gompel N, Ghysen A (2003) The lateral line of zebrafish: a model system for the analysis of morphogenesis and neural development in vertebrates. Biol Cell 95:579-587.

David NB, Sapede D, Saint-Etienne L, Thisse C, Thisse B, Dambly-Chaudiere C, Rosa FM, Ghysen A (2002) Molecular basis of cell migration in the fish lateral line: role of the chemokine receptor CXCR4 and of its ligand, SDF1. Proceedings of the National Academy of Sciences of the United States of America 99:16297-16302.

Deans MR, Antic D, Suyama K, Scott MP, Axelrod JD, Goodrich LV (2007) Asymmetric distribution of prickle-like 2 reveals an early underlying polarization of vestibular sensory epithelia in the inner ear. J Neurosci 27:3139-3147.

Dhawale A, Bhalla US (2008) The network and the synapse: 100 years after Cajal. HFSP J 2:12-16.

Dickson BJ (2002) Molecular mechanisms of axon guidance. Science 298:1959-1964.

Eisele LE, Schmidt JT (1988) Activity sharpens the regenerating retinotectal projection in goldfish: sensitive period for strobe illumination and lack of effect on synaptogenesis and on ganglion cell receptive field properties. Journal of neurobiology 19:395-411.

Engelmann J, Hanke W, Mogdans J, Bleckmann H (2000) Hydrodynamic stimuli and the fish lateral line. Nature 408:51-52.

Fame RM, Brajon C, Ghysen A (2006) Second-order projection from the posterior lateral line in the early zebrafish brain. Neural development 1:4.

Faucherre A, Pujol-Marti J, Kawakami K, Lopez-Schier H (2009) Afferent neurons of the zebrafish lateral line are strict selectors of hair-cell orientation. PLoS ONE 4:e4477.

Feldheim DA, Kim YI, Bergemann AD, Frisen J, Barbacid M, Flanagan JG (2000) Genetic analysis of ephrin-A2 and ephrin-A5 shows their requirement in multiple aspects of retinocollicular mapping. Neuron 25:563-574.

Fetcho JR, Liu KS (1998) Zebrafish as a model system for studying neuronal circuits and behavior. Ann N Y Acad Sci 860:333-345.

Flavell SW, Greenberg ME (2008) Signaling mechanisms linking neuronal activity to gene expression and plasticity of the nervous system. Annual review of neuroscience 31:563-590.

Flavell SW, Cowan CW, Kim TK, Greer PL, Lin Y, Paradis S, Griffith EC, Hu LS, Chen C, Greenberg ME (2006) Activity-dependent regulation of MEF2 transcription factors suppresses excitatory synapse number. Science 311:1008-1012.

Flock Å, Wersäll J (1962) A study of the orientation of the sensory hairs of the receptor cells in the lateral line organ of fish, with special reference to the function of the receptors. The Journal of cell biology 15:19-27.

Fog A (2008) Calculation methods for Wallenius' noncentral hypergeometric distribution. Comm Stat Simul Comp 37:241-257.

Fritzsch B (1981) The pattern of lateral-line afferents in urodeles. A horseradish-peroxidase study. Cell Tissue Res 218:581-594.

Fritzsch B (1989) Diversity and regression in the amphibian lateral line and electrosensory system. In: The Mechanosensory Lateral Line: Neurobiology and Evolution (Coombs S, Görner, P., and Münz, H., ed). New York: Springer-Verlag.

Fritzsch B, Gregory D, Rosa-Molinar E (2005) The development of the hindbrain afferent projections in the axolotl: evidence for timing as a specific mechanism of afferent fiber sorting. Zoology (Jena) 108:297-306.

Gaietta G, Deerinck TJ, Adams SR, Bouwer J, Tour O, Laird DW, Sosinsky GE, Tsien RY, Ellisman MH (2002) Multicolor and electron microscopic imaging of connexin trafficking. Science 296:503-507.

Ghysen A, Dambly-Chaudière C (2004) Development of the zebrafish lateral line. Current opinion in neurobiology 14:67-73.

Ghysen A, Dambly-Chaudiere C (2007) The lateral line microcosmos. Genes Dev 21:2118-2130.

Gilmour D, Knaut H, Maischein HM, Nüsslein-Volhard C (2004) Towing of sensory axons by their migrating target cells in vivo. Nature neuroscience 7:491-492.

Gleason M, Nagiel A, Lopez-Schier H, Hudspeth AJ (n.d.) The transmembrane inner ear (Tmie) protein is essential for normal hearing and balance in the zebrafish. Manuscript in preparation.

Gompel N, Dambly-Chaudière C, Ghysen A (2001a) Neuronal differences prefigure somatotopy in the zebrafish lateral line. Development (Cambridge, England) 128:387-393.

Gompel N, Cubedo N, Thisse C, Thisse B, Dambly-Chaudière C, Ghysen A (2001b) Pattern formation in the lateral line of zebrafish. Mechanisms of development 105:69-77.

Goodman CS, Shatz CJ (1993) Developmental mechanisms that generate precise patterns of neuronal connectivity. Cell 72 Suppl:77-98.

Goodman SN (1998) Multiple comparisons, explained. Am J Epidemiol 147:807-812.

Goodrich LV (2008) The plane facts of PCP in the CNS. Neuron 60:9-16.

Görner P (1963) Untersuchungen zur Morphologie und Elektrophysiologie des Seitenlinienorgans vom Krallenfrosch (Xenopus laevis Daudin). Zeitschrift für vergleichende Physiologie 47:316-338.

Grant KA, Raible DW, Piotrowski T (2005) Regulation of latent sensory hair cell precursors by glia in the zebrafish lateral line. Neuron 45:69-80.

Hanson MG, Landmesser LT (2004) Normal patterns of spontaneous activity are required for correct motor axon guidance and the expression of specific guidance molecules. Neuron 43:687-701.

Hebb DO (1949) The Organization of Behavior. New York: Wiley.

Hernández PP, Olivari FA, Sarrazin AF, Sandoval PC, Allende ML (2007) Regeneration in zebrafish lateral line neuromasts: expression of the neural progenitor cell marker sox2 and proliferation-dependent and-independent mechanisms of hair cell renewal. Developmental neurobiology 67:637-654.

Higashijima S, Hotta Y, Okamoto H (2000) Visualization of cranial motor neurons in live transgenic zebrafish expressing green fluorescent protein under the control of the islet-1 promoter/enhancer. J Neurosci 20:206-218.

Hong EJ, McCord AE, Greenberg ME (2008) A biological function for the neuronal activity-dependent component of Bdnf transcription in the development of cortical inhibition. Neuron 60:610-624.

Huberman AD, Feller MB, Chapman B (2008) Mechanisms underlying development of visual maps and receptive fields. Annual review of neuroscience 31:479-509.

Hudspeth AJ (1989) How the ear's works work. Nature 341:397-404.

Ibanez CF, Ernfors P, Timmusk T, Ip NY, Arenas E, Yancopoulos GD, Persson H (1993) Neurotrophin-4 is a target-derived neurotrophic factor for neurons of the trigeminal ganglion. Development (Cambridge, England) 117:1345-1353.

Jaynes ET (2003) Probability Theory: The Logic of Science: Cambridge University Press.

Jessell TM, Kandel ER (1993) Synaptic transmission: a bidirectional and self-modifiable form of cell-cell communication. Cell 72 Suppl:1-30.

Jontes JD, Phillips GR (2006) Selective stabilization and synaptic specificity: a new cell-biological model. Trends in neurosciences 29:186-191.

Katz LC, Shatz CJ (1996) Synaptic activity and the construction of cortical circuits. Science 274:1133-1138.

Keen EC, Hudspeth AJ (2006) Transfer characteristics of the hair cell's afferent synapse. Proc Natl Acad Sci U S A 103:5537-5542.

Kelly M, Chen P (2007) Shaping the mammalian auditory sensory organ by the planar cell polarity pathway. Int J Dev Biol 51:535-547.

Kennedy TE, Serafini T, de la Torre JR, Tessier-Lavigne M (1994) Netrins are diffusible chemotropic factors for commissural axons in the embryonic spinal cord. Cell 78:425-435.

Kimmel CB, Ballard WW, Kimmel SR, Ullmann B, Schilling TF (1995) Stages of embryonic development of the zebrafish. Dev Dyn 203:253-310.

Koundakjian EJ, Appler JL, Goodrich LV (2007) Auditory neurons make stereotyped wiring decisions before maturation of their targets. J Neurosci 27:14078-14088.

Ledent V (2002) Postembryonic development of the posterior lateral line in zebrafish. Development (Cambridge, England) 129:597-604.

Li Q, Shirabe K, Kuwada JY (2004) Chemokine signaling regulates sensory cell migration in zebrafish. Developmental biology 269:123-136.

Lin Y, Bloodgood BL, Hauser JL, Lapan AD, Koon AC, Kim TK, Hu LS, Malik AN, Greenberg ME (2008) Activity-dependent regulation of inhibitory synapse development by Npas4. Nature 455:1198-1204.

Livet J, Weissman TA, Kang H, Draft RW, Lu J, Bennis RA, Sanes JR, Lichtman JW (2007) Transgenic strategies for combinatorial expression of fluorescent proteins in the nervous system. Nature 450:56-62.

Lopez-Schier H, Hudspeth AJ (2005) Supernumerary neuromasts in the posterior lateral line of zebrafish lacking peripheral glia. Proceedings of the National Academy of Sciences of the United States of America 102:1496-1501.

Lopez-Schier H, Hudspeth AJ (2006) A two-step mechanism underlies the planar polarization of regenerating sensory hair cells. Proceedings of the National Academy of Sciences of the United States of America 103:18615-18620.

Lopez-Schier H, Starr CJ, Kappler JA, Kollmar R, Hudspeth AJ (2004) Directional cell migration establishes the axes of planar polarity in the posterior lateral-line organ of the zebrafish. Developmental cell 7:401-412.

Luo L, O'Leary DD (2005) Axon retraction and degeneration in development and disease. Annual review of neuroscience 28:127-156.

Maffei L, Galli-Resta L (1990) Correlation in the discharges of neighboring rat retinal ganglion cells during prenatal life. Proc Natl Acad Sci U S A 87:2861-2864.

Mann F, Ray S, Harris W, Holt C (2002) Topographic mapping in dorsoventral axis of the Xenopus retinotectal system depends on signaling through ephrin-B ligands. Neuron 35:461-473.

Mazzarello P (2007) Net without nodes and vice versa, the paradoxical Golgi-Cajal story: a reconciliation? Brain Res Bull 71:344-346.

Meister M, Wong RO, Baylor DA, Shatz CJ (1991) Synchronous bursts of action potentials in ganglion cells of the developing mammalian retina. Science 252:939-943.

Metcalfe WK (1985) Sensory neuron growth cones comigrate with posterior lateral line primordial cells in zebrafish. The Journal of comparative neurology 238:218-224.

Metcalfe WK, Kimmel CB, Schabtach E (1985) Anatomy of the posterior lateral line system in young larvae of the zebrafish. The Journal of comparative neurology 233:377-389.

Meyer RL (1983) Tetrodotoxin inhibits the formation of refined retinotopography in goldfish. Brain research 282:293-298.

Mitchem KL, Hibbard E, Beyer LA, Bosom K, Dootz GA, Dolan DF, Johnson KR, Raphael Y, Kohrman DC (2002) Mutation of the novel gene Tmie results in sensory cell defects in the inner ear of spinner, a mouse model of human hearing loss DFNB6. Human molecular genetics 11:1887-1898.

Mohr C, Görner P (1996) Innervation patterns of the lateral line stitches of the clawed frog, Xenopus laevis, and their reorganization during metamorphosis. Brain, behavior and evolution 48:55-69.

Montcouquiol M, Rachel RA, Lanford PJ, Copeland NG, Jenkins NA, Kelley MW (2003) Identification of Vangl2 and Scrb1 as planar polarity genes in mammals. Nature 423:173-177.

Montcouquiol M, Sans N, Huss D, Kach J, Dickman JD, Forge A, Rachel RA, Copeland NG, Jenkins NA, Bogani D, Murdoch J, Warchol ME, Wenthold RJ, Kelley MW (2006) Asymmetric localization of Vangl2 and Fz3 indicate novel mechanisms for planar cell polarity in mammals. J Neurosci 26:5265-5275.

Montgomery JC, Baker CF, Carton AG (1997) The lateral line can mediate rheotaxis in fish. Nature 389:960-963.

Nagiel A, Andor-Ardo D, Hudspeth AJ (2008) Specificity of afferent synapses onto plane-polarized hair cells in the posterior lateral line of the zebrafish. J Neurosci 28:8442-8453.

Nakamoto M, Cheng HJ, Friedman GC, McLaughlin T, Hansen MJ, Yoon CH, O'Leary DD, Flanagan JG (1996) Topographically specific effects of ELF-1 on retinal axon guidance in vitro and retinal axon mapping in vivo. Cell 86:755-766.

Naz S, Giguere CM, Kohrman DC, Mitchem KL, Riazuddin S, Morell RJ, Ramesh A, Srisailpathy S, Deshmukh D, Riazuddin S, Griffith AJ, Friedman TB, Smith RJ, Wilcox ER (2002) Mutations in a novel gene, TMIE, are associated with hearing loss linked to the DFNB6 locus. American journal of human genetics 71:632-636.

Nevin LM, Taylor MR, Baier H (2008) Hardwiring of fine synaptic layers in the zebrafish visual pathway. Neural Dev 3:36.

Nicol X, Voyatzis S, Muzerelle A, Narboux-Neme N, Sudhof TC, Miles R, Gaspar P (2007) cAMP oscillations and retinal activity are permissive for ephrin signaling during the establishment of the retinotopic map. Nature neuroscience 10:340-347.

Obholzer N, Wolfson S, Trapani JG, Mo W, Nechiporuk A, Busch-Nentwich E, Seiler C, Sidi S, Sollner C, Duncan RN, Boehland A, Nicolson T (2008) Vesicular glutamate transporter 3 is required for synaptic transmission in zebrafish hair cells. J Neurosci 28:2110-2118.

Palay SL (1956) Synapses in the central nervous system. J Biophys Biochem Cytol 2:193-202.

Parinov S, Kondrichin I, Korzh V, Emelyanov A (2004) Tol2 transposon-mediated enhancer trap to identify developmentally regulated zebrafish genes in vivo. Dev Dyn 231:449-459.

Park HC, Kim CH, Bae YK, Yeo SY, Kim SH, Hong SK, Shin J, Yoo KW, Hibi M, Hirano T, Miki N, Chitnis AB, Huh TL (2000) Analysis of upstream elements in the HuC promoter leads to the establishment of transgenic zebrafish with fluorescent neurons. Developmental biology 227:279-293.

Raible DW, Kruse GJ (2000) Organization of the lateral line system in embryonic zebrafish. The Journal of comparative neurology 421:189-198.

Ramón y Cajal SR (1911) Histologie du Systéme Nerveux de l'Homme et des Vertébrés. Paris: Maloine.

Sanes JR (2009) Synaptic Specificity. Annu Rev Cell Dev Biol.

Sapède D, Rossel M, Dambly-Chaudiere C, Ghysen A (2005) Role of SDF1 chemokine in the development of lateral line efferent and facial motor neurons. Proceedings of the National Academy of Sciences of the United States of America 102:1714-1718.

Schmidt JT, Edwards DL (1983) Activity sharpens the map during the regeneration of the retinotectal projection in goldfish. Brain research 269:29-39.

Schmidt JT, Eisele LE (1985) Stroboscopic illumination and dark rearing block the sharpening of the regenerated retinotectal map in goldfish. Neuroscience 14:535-546.

Seiler C, Finger-Baier KC, Rinner O, Makhankov YV, Schwarz H, Neuhauss SC, Nicolson T (2005) Duplicated genes with split functions: independent

roles of protocadherin15 orthologues in zebrafish hearing and vision. Development (Cambridge, England) 132:615-623.

Serafini T, Kennedy TE, Galko MJ, Mirzayan C, Jessell TM, Tessier-Lavigne M (1994) The netrins define a family of axon outgrowth-promoting proteins homologous to C. elegans UNC-6. Cell 78:409-424.

Shapiro L, Colman DR (1999) The diversity of cadherins and implications for a synaptic adhesive code in the CNS. Neuron 23:427-430.

Shirasaki R, Katsumata R, Murakami F (1998) Change in chemoattractant responsiveness of developing axons at an intermediate target. Science 279:105-107.

Shotwell SL, Jacobs R, Hudspeth AJ (1981) Directional sensitivity of individual vertebrate hair cells to controlled deflection of their hair bundles. Ann N Y Acad Sci 374:1-10.

Sidi S, Busch-Nentwich E, Friedrich R, Schoenberger U, Nicolson T (2004) gemini encodes a zebrafish L-type calcium channel that localizes at sensory hair cell ribbon synapses. J Neurosci 24:4213-4223.

Sperry RW (1963) Chemoaffinity in the Orderly Growth of Nerve Fiber Patterns and Connections. Proc Natl Acad Sci U S A 50:703-710.

Stent GS (1973) A Physiological Mechanism for Hebb's Postulate of Learning. Proc Natl Acad Sci U S A 70:997-1001.

Südhof TC (2008) Neuroligins and neurexins link synaptic function to cognitive disease. Nature 455:903-911.

Sugiyama S, Di Nardo AA, Aizawa S, Matsuo I, Volovitch M, Prochiantz A, Hensch TK (2008) Experience-dependent transfer of Otx2 homeoprotein into the visual cortex activates postnatal plasticity. Cell 134:508-520.

Tessarollo L, Coppola V, Fritzsch B (2004) NT-3 replacement with brain-derived neurotrophic factor redirects vestibular nerve fibers to the cochlea. J Neurosci 24:2575-2584.

Tessier-Lavigne M, Goodman CS (1996) The molecular biology of axon guidance. Science 274:1123-1133.

Twitty VC, Johson HH (1934) Motor inhibition in amblystoma produced by Trituris transplants. Science 80:78-79.

Unwin N (1993) Neurotransmitter action: opening of ligand-gated ion channels. Cell 72 Suppl:31-41.

Varoqueaux F, Sigler A, Rhee JS, Brose N, Enk C, Reim K, Rosenmund C (2002) Total arrest of spontaneous and evoked synaptic transmission but normal synaptogenesis in the absence of Munc13-mediated vesicle priming. Proc Natl Acad Sci U S A 99:9037-9042.

Veitch NC (2004) Horseradish peroxidase: a modern view of a classic enzyme. Phytochemistry 65:249-259.

Verhage M, Maia AS, Plomp JJ, Brussaard AB, Heeroma JH, Vermeer H, Toonen RF, Hammer RE, van den Berg TK, Missler M, Geuze HJ, Sudhof TC (2000) Synaptic assembly of the brain in the absence of neurotransmitter secretion. Science 287:864-869.

Waites CL, Craig AM, Garner CC (2005) Mechanisms of vertebrate synaptogenesis. Annual review of neuroscience 28:251-274.

Walter J, Henke-Fahle S, Bonhoeffer F (1987) Avoidance of posterior tectal membranes by temporal retinal axons. Development (Cambridge, England) 101:909-913.

Watts RJ, Schuldiner O, Perrino J, Larsen C, Luo L (2004) Glia engulf degenerating axons during developmental axon pruning. Curr Biol 14:678-684.

Williams JA, Holder N (2000) Cell turnover in neuromasts of zebrafish larvae. Hearing research 143:171-181.

Wu J, Mlodzik M (2009) A quest for the mechanism regulating global planar cell polarity of tissues. Trends Cell Biol 19:295-305.

Xiao T, Roeser T, Staub W, Baier H (2005) A GFP-based genetic screen reveals mutations that disrupt the architecture of the zebrafish retinotectal projection. Development (Cambridge, England) 132:2955-2967.

Yamagata M, Sanes JR (2008) Dscam and Sidekick proteins direct lamina-specific synaptic connections in vertebrate retina. Nature 451:465-469.

Yamagata M, Weiner JA, Sanes JR (2002) Sidekicks: synaptic adhesion molecules that promote lamina-specific connectivity in the retina. Cell 110:649-660.

Zallen JA (2007) Planar polarity and tissue morphogenesis. Cell 129:1051-1063.

Zhong W, Chia W (2008) Neurogenesis and asymmetric cell division. Curr Opin Neurobiol 18:4-11.

Zou Y, Stoeckli E, Chen H, Tessier-Lavigne M (2000) Squeezing axons out of the gray matter: a role for slit and semaphorin proteins from midline and ventral spinal cord. Cell 102:363-375.